Finite Volume and Semi-Analytical Studies for Partial-Integro Differential Equations

THESIS

Submitted in partial fulfillment of the requirements

for the degree of

DOCTOR OF PHILOSOPHY

by

Sanjiv Kumar Bariwal

ID No. 2019PHXF0043P

Under the Supervision of

Prof. Rajesh Kumar

BITS Pilani

Pilani | Dubai | Goa | Hyderabad | Mumbai

BIRLA INSTITUTE OF TECHNOLOGY & SCIENCE

PILANI-333031 (RAJASTHAN) INDIA

2024

BIRLA INSTITUTE OF TECHNOLOGY & SCIENCE, PILANI

CERTIFICATE

This is to certify that the thesis entitled, **"Finite Volume and Semi-Analytical Studies for Partial-Integro Differential Equations"** and submitted by **Mr. Sanjiv Kumar Bariwal** ID No. **2019PHXF0043P** for the award of Ph.D. Degree of the institute embodies original work done by him under my supervision.

Signature of the Supervisor

Name : **Prof. Rajesh Kumar**

Designation : **Associate Professor,**

Department of Mathematics, BITS Pilani, Pilani Campus,

India

Date: **24 May 2024**

Dedicated to

My Beloved Parents

ACKNOWLEDGEMENTS

I would like to thank my thesis advisor, Prof. Rajesh Kumar, from the bottom of my heart for all of his help and support during my Ph.D. I consider myself exceptionally fortunate to have had an advisor who granted me the autonomy to embark on my explorations while offering steadfast guidance whenever I encountered stumbling blocks. Under his mentorship, I honed my ability to scrutinize concepts and articulate my thoughts effectively. His unwavering patience and support proved invaluable in navigating various challenges, ultimately culminating in the successful completion of this dissertation.

I wish to express my sincere appreciation to the esteemed members of my Dissertation Advisory Committee (DAC), specifically Prof. Sangita Yadav and Prof. Anirudh Singh Rana. Their invaluable insights and discerning recommendations have notably enhanced the caliber of my research.

I'm also deeply grateful to Prof. Devendra Kumar, Head of the Department of Mathematics, and Prof. Aashish Tiwari, Convenor of the Doctoral Research Committee (DRC), for their provision of indispensable resources and the creation of a supportive research environment essential for the successful execution of this study.

I want to extend my heartfelt gratitude to my parents, Mrs. Lalta Devi and Mr. Rohitash Bariwal, for their unwavering support in realizing my aspirations. In particular, my father's influence as a disciplined and knowledgeable individual has consistently motivated me to strive for personal growth and excellence. My brothers, Ashish and Vijay, and sister-in-law Anita and Meena are my backbone for guiding and encouraging me during this period. My little nieces Shanvi and Ayanshi came into our family and fulfilled this journey with happiness.

I extend my deepest gratitude to my seniors, Dr. Kapil Kumar Chaudhary and Dr. Sonali Kaushik, for their invaluable guidance and encouragement. My junior colleagues, Gourav Arora, Saddam Hussain, and Shweta Yadav, have infused our discussions and research endeavors with fresh perspectives and positive energy.

I am incredibly fortunate to have the friendship of Dr. Riya Jain, whose unwavering support and affection have been a source of strength throughout this challenging journey. I thank one of my Master's degree friends, Sandeep Sulakh, for always motivating me in diverse situations. Additionally, I cherish the camaraderie of my research fellow friends: Dr. Deepak Bhaishahab, Dr. Pallav Bhaishahab, Dr. Swati, Dr. Chandan Kumawat, Dr. Sajan, Rishu Gandhi, Dr. Umesh Khundari, Raveena Chahar, Dr. Komal, Meghna, Amit Saini, Shipra Gupta, Dr. Ashwini Gupta, Anshu Mor, Himanshu, Yogesh Kuntal, Ankit Yadav, and Mohit Yadav. Together, we have shared many wonderful moments on this journey. In the end, I thankfully acknowledge everyone who contributed directly or indirectly to the completion of this thesis work.

Place: BITS Pilani, Pilani Campus, India
Date: **24 May 2024**

Sanjiv Kumar Bariwal
(Department of Mathematics)

ABSTRACT

The focus of the thesis is on partial-integro differential equations such as coagulation-multiple breakage and non-linear collision-induced breakage equations. These models have significant applications in chemical engineering, cloud formation, astrophysics, etc.

This thesis is dedicated to analyzing a finite volume scheme (FVS) for solving the coagulation-multiple fragmentation equation by taking two different forms of the model: the first one is the weighted discretized form, and the second one is the divergence form. The rates of coagulation and fragmentation are chosen locally bounded and unbounded (singularity near the origin), respectively. It is shown that using the weak L^1 compactness method, the numerically approximated solution tends to the weak solution of the continuous problem under a stability condition on the time step for non-uniform mesh. Further, considering a uniform mesh, first-order error approximation is demonstrated when kernels are in $W^{1,\infty}_{loc}$ space. It is authenticated numerically by taking several test problems.

Further, the weak convergence studies of FVS is exhibited for the non-linear collision-induced breakage equation having the locally bounded kernels. In this case, the first-order error estimation is theoretically and numerically validated by taking three test cases.

Proceeding further, semi-analytical techniques such as variational iteration method (VIM), optimized decomposition method (ODM), homotopy analysis method (HAM) and accelerated homotopy perturbation method (AHPM) are introduced for solving the collision-induced breakage equation for various collisional kernels. The existence of the solution (using Banach fixed point theorem) and convergence analysis of the series solution obtained through these methods are exhibited for the model. The worst upper bounds of the error are acquired for particular kernels. The approximated solutions of the model are compared with the exact ones and are observed to be in excellent agreement. In addition to this, in the absence of analytical solutions, the finite volume method is also used to resemble the semi-analytic results. Finally, the possible extensions with scope for future investigations are discussed in the concluding chapter.

Contents

List of Tables

List of Figures

Chapter 1

Introduction

The structure of particles in the particulate system can vary widely depending on their size, composition, and origin. When analyzing the dynamics of a particulate system, particles play a crucial role in population balance equations which are used to characterize the behaviour and evolution of a particle population as a function of time, i.e., how particles interact, grow and change over time. It is frequently used in various disciplines, including chemical engineering [1, 2], environmental science [3, 4], and pharmaceuticals [5, 6], to comprehend particle formation, growth, aggregation (coagulation), and breakage (fragmentation) processes. The PBE takes into account the distribution of particles based on their size, shape, or other pertinent characteristics and monitors how these distributions change over time as a result of various processes. The equation can be written in different forms, depending on the specific procedure being studied and the attributes used to characterize the particles. In a particulate system, the growth of particles signifies an increase in their size or mass over time. Particle growth can occur through various physical and chemical processes, and comprehension of these mechanisms is essential for numerous scientific and engineering applications. Coagulation is a process in which two or more particles come into contact and stick together to form larger aggregates or clusters. Coagulation is a dynamic process that continuously changes the size distribution and

structure of the particle population in the system. The coagulation rate is influenced by the concentration of particles, the collision kernels, and the particles' properties, such as their size or mass. During coagulation, the total number of particles is reduced, whereas the total mass of the particles is conserved based on the coagulation rate. During the breakage process, large size particle fragments into smaller fragments, thereby increasing the total number of particles; the total mass depends on the breakage rate. Further, breakage process is classified into two categories: linear and non-linear. In linear breakage, the distribution of fragment sizes or the breakage rate is directly proportional to the size of the original particle. However, in a non-linear, this proportionality does not hold, and the breakage behaviour is more complex.

In this thesis, we mainly focus on two PBEs such as coagulation-multiple breakage equation (CMBE) and collision-induced breakage equation (CBE). CMBE provides the insight of the particulate process due to coupled coagulation and linear multiple breakage events. CMBE has numerous applications in the pure and applied sciences to design the dynamics of particulate processes like high shear granulation, condensation of water vapor in the atmosphere, depolymerization, astrophysics, etc [7–10]. The CBE which is non-linear in nature, is used in the modeling of planet formation, aerosol, miling and crushing processes [11–13] to explain the mechanics of a massive number of particles splitting apart as a consequence of collisions.

1.0.1 Population Balance Equations (PBE)

In this thesis, we are motivated to explore the coagulation and multiple breakage equation, but we have to study the coagulation and breakage equation first. Then, a mathematical model for the collision-induced breakage equation will be reviewed, followed by existing results of these models and issues which should be discussed in the previous work. The thesis will provide ideas for the new results. Further, the objectives of the thesis are written according to the literature's gaps. Finally, the structure of the thesis is formulated at the end.

1.0.1.1 Coagulation equation

In the discrete case, particles are characterized by positive integers, where the mass ratio between the fundamental unit (monomer) and a typical cluster is a positive integer, and the cluster's size is a finite multiple of the monomer's mass. The density function with size $i \geq 0$ at time $t \geq 0$ is expressed as $c_i(t)$. The coagulation process involves particles of size i and j, where the coagulation kernel $K_{i,j}$, assumed to be non-negative and symmetric ($K_{i,j} \geq 0$ and $K_{i,j} = K_{j,i}$ for $i, j \geq 1$), represents the rate at which these particles merge. Now, let's examine how the density $c_i(t)$ evolves when particles $c_j(t)$ and $c_{i-j}(t)$ collide at the rate $k_{i-j,j}$. This coalescence process results in the generation of new particles of size i, and the density $c_i(t)$ experiences an increase due to this coalescence phenomenon as

$$\frac{1}{2}\sum_{j=1}^{i-1} k_{i-j,j} c_{i-j}(t) c_j(t).$$

Similarly, disappearance of particle $c_i(t)$ of size i occurs after colliding with any particle $c_j(t)$ of size j at rate $K_{i,j}$. So, the number density $c_i(t)$ decreases by

$$\sum_{j=1}^{\infty} K_{i,j} c_i(t) c_j(t).$$

Now, the general coagulation equation may be expressed as follows:

$$\frac{\partial c_i(t)}{\partial t} = \frac{1}{2}\sum_{j=1}^{i-1} K_{i-j,j} c_{i-j}(t) c_j(t) - \sum_{j=1}^{\infty} K_{i,j} c_i(t) c_j(t), \tag{1.1}$$

where the initial term is referred to as the birth term, while the subsequent term is termed the death term, initially, in 1917, Smoluchowski [14] introduced a set of non-linear differential equations to describe coagulation. The continuous form of the Smoluchowski's coagulation equation was given by Müller [15] in 1928 as

$$\frac{\partial c(t,x)}{\partial t} = \frac{1}{2}\int_0^x K(x-y,y) c(t,x-y) c(t,y) dy - c(t,x)\int_0^{\infty} K(x,y) c(t,y) dy, \tag{1.2}$$

where $c(t,x) \geq 0$ is the particle number density function of having particles of volume $x \in \mathbb{R}^+ :=]0,\infty[$ and at time $t \in [0,\infty[$ in a homogeneous physical system. The term

$K(x, y)$ known as coagulation kernel and expresses the rate of aggregation of particles of sizes x and y, producing new particles with size $x + y$. The term $K(x, y)$ is non-negative and satisfies $K(x, y) = K(y, x)$. In equation (1.2), the initial term on the right-hand side depicts the generation of particles with size x through the collision of particles sized $x - y$ and y. The subsequent integral characterizes the diminishment of particles of size x following collisions with particles of size y. These two components are denoted as birth and death, respectively. Including the term $\frac{1}{2}$ in the equation is intended to prevent double counting.

1.0.1.2 Linear breakage equation

The phenomenon known as fragmentation occurs when a particle breaks up into many smaller-sized particles. It is naturally found in various physical systems, ranging from comminution, separation of grains, bubbles, droplets, polymer degradation, disintegration of atomic nuclei, etc. Fragmentation may occur through external forces, spontaneously, or through interactions/collisions between particles. Spontaneous collisions (linear breakage) between the particles cause changes in their mass, shape, size, volume, etc.

In 1957, Melzak [16] extended the binary aggregation model (1.2) together with multiple fragmentation, where the separate fragmentation equation is

$$\frac{\partial c(t,x)}{\partial t} = \int_x^\infty M(y,x)c(t,y)dy - \frac{c(t,x)}{x}\int_0^x yM(x,y)dy, \tag{1.3}$$

where $M(y, x) \geq 0$ is the multiple breakage rate of particles of size y into a range of size x. If $M(y, x) = M(y, y - x)$ holds, then multiple breakage equation converted into binary breakage equation, where only two smaller particles are obtained due to breakage of the parent particles.

Friedlander [17] in 1960 gave the following form of binary breakage equation

$$\frac{\partial c(t,x)}{\partial t} = \left(\int_0^\infty V(x,y)c(t,x+y)dy\right) - \frac{c(t,x)}{2}\int_0^x V(x-y,y)dy, \tag{1.4}$$

where $V(x, y)$ represents the symmetric binary breakage kernel, and it is linked to the multiple breakage kernel through the relationship $V(x - y, y) = M(x, y)$. Finally, in 1991, Ziff [18] presented an alternative formulation for the multiple breakage equation

by using

$$M(y,x) = B(x,y)S(y) \quad \text{and} \quad S(x) = \int_0^x \frac{y}{x} M(x,y)dy.$$

To study the change of the particle number density $c(t,x) \geq 0$, for particles of volume $x \in \mathbb{R}^+$ at time $t \geq 0$ in a physical system undergoing fragmentation process, the following mathematical model known as the pure multiple breakage PBE is developed

$$\frac{\partial c(t,x)}{\partial t} = \int_x^\infty B(x,y)S(y)c(t,y)dy - S(x)c(t,x). \tag{1.5}$$

The first integral of 1.5 represents the generation of particles with size x as a result of the breakage of particles sized y where $x \leq y < \infty$. The second term portrays the reduction of particles with size x originating from their fragmentation into smaller particles. The fragmentation kernels are defined by the breakage function $B(x,y)$ and the selection rate $S(y)$ as follows:

- $B(x,y)$ indicates the breakage rate of y size particles to form x size particles. Also, $B(x,y) \neq 0$ only when $x < y$.
- $S(y)$ defines the selection rate of y size particles, selected to split.

The term $B(x,y)$ exhibits the characteristic as,

$$\int_0^y B(x,y)dx = \zeta(y) \tag{1.6a}$$

and

$$\int_0^y xB(x,y)dx = y \tag{1.6b}$$

for $\zeta(y)$ being the total number of daughter fragments due to splitting of y size particle and second relation (1.6b) is the necessary condition for the mass conservation.

1.0.1.3 Coagulation and multiple breakage equation

Describing a system of particles engaged in coagulation and fragmentation is more practical when utilizing a continuous particle size. The initial explicit form of this system in the literature can be traced back to [19], where the focus was on processes involving

polymerization and de-polymerization within the realm of chemistry. The authors specifically examined the discrete version of the equations, encompassing binary fragmentation and coagulation kernels that remain unrelated to the sizes of clusters. The mathematical formulation of CMBE [20] due to the coupling of aggregation and multiple breakage processes, is guided by the population balance equations (PBEs) as,

$$\begin{aligned}\frac{\partial c(t,x)}{\partial t} &= \frac{1}{2}\int_0^x K(y,x-y)c(t,y)c(t,x-y)dy - \int_0^\infty K(x,y)c(t,x)c(t,y)dy \\ &\quad + \int_x^\infty B(x,y)S(y)c(t,y)dy - S(x)c(t,x). \end{aligned} \tag{1.7}$$

The interpretation of the coefficients of the model such as K, B and S are already discussed in (1.0.1.1) and (1.0.1.2).

1.0.1.4 Non-linear collision-induced breakage equation

The non-linear nature of the breakage process is occurred due to the collision between the parent particles. It is also referred as non-linear collision-induced breakage equation (CBE). Due to the nonlinearity, such process has significant applications in the chemical engineering, cloud formation and planet formation etc. When a cluster breaks apart on its own (spontaneous) (1.0.1.2), it only creates smaller clusters; however, when two clusters collide, some of the matter in one cluster can be transferred to the other cluster, resulting in the formation of larger clusters, i.e., non-linear collision between them.

Cheng and Redner [21] used the following partial integro-differential equation to derive the CBE,

$$\frac{\partial c(t,x)}{\partial t} = \int_0^\infty \int_x^\infty K(y,z)b(x,y,z)c(t,y)c(t,z)\,dy\,dz - \int_0^\infty K(x,y)c(t,x)c(t,y)\,dy, \tag{1.8}$$

associated with the initial condition

$$c(0,x) = c^{in}(x) \geq 0, \quad x \in \mathbb{R}^+. \tag{1.9}$$

The variables x and t are regarded as dimensionless quantities without losing any generality. In Eq.(1.8), the symmetric collision kernel $K(x,y)$ depicts the rate of collision for breakage event between x and y volume particles. The breakage distribution function

$b(x, y, z)$ defines the rate for production of x volume particles by splitting of y volume particle due to interaction with particles of volume z . The function b holds

$$\int_0^y xb(x, y, z)dx = y, \;\; b(x, y, z) \neq 0 \;\; \text{for} \quad x \in (0, y) \;\; \text{and} \quad b(x, y, z) = 0 \;\; \text{for} \quad x > y. \tag{1.10}$$

The first term in Eq.(1.8) explains gaining x volume particles due to collisional breakage between y and z volume particles, known as the birth term. The second term is the death term, which defines the disappearance of x volume particles, resulting in a collision with particles of volume y.

Moreover, the discrete collision model is presented to enhance our comprehension of the behaviour of non-linearly colliding particles. In the linear, the rate of fragmentation of clusters made up of i particles, is thus assumed to be proportional to the quantity of i-clusters per unit volume. while, the rate of non-linear collision is directly proportional to the number of two colliding clusters per unit volume.

Furthermore, the discrete collision-induced breakage equation is also explored in the articles [22, 23].

1.0.2 Existing Literature

In this segment, we provide an overview of the general outcomes and concisely emphasize our novel discoveries within numerical solutions for PBE. Our focus will center on the numerical examination of the finite volume scheme (FVS) applied to CMBE and non-linear CBE. Additionally, several semi-analytical methods were also used on these models. Here, the details of these models and methodologies are written systematically.

1.0.2.1 Coagulation-multiple breakage equation

In 1953, Melzak [24] derived the solution of the coagulation equation (CE) (1.2) using the Laplace transforms for $K(x, y) = c$ with two initial conditions $c(0, x) = A\delta(x - 1), Ax^n e^{\alpha x}$. Further, Melzak extended the existence and uniqueness work in [16] for coupled coagulation (1.2) and fragmentation equation (1.3) having the assumptions on $0 \leq$

$K(x,y) \leq A < \infty$ and $0 \leq M(x,y) \leq C < \infty$ as well as $c(0,x) \geq 0$ is bounded and integrable. Menon et al. [25] approached the existence of self-similar solution (dynamical scaling) of coagulation equation for the solvable kernels $K(x,y) = 2, x+y, xy$ using Laplace transform. After that, the uniqueness of self-similar solutions (mass-conserving) to CE (1.2) is demonstrated in [26] when $K(x,y) = 2(xy)^{-\alpha}$, where α is a positive value. Further, Laurençot extended the mass conserving self-similar solution of the CMBE (1.7) using the compactness method having $K(x,y) = K_0(x^\alpha y^{\lambda-\alpha} + x^{\lambda-\alpha}y^\alpha)$, $S(x) = s_0 x^{\lambda-1}$ and $B(x,y) = (\nu+2)x^\nu y^{-\nu-1}, 0 < x < y$, where $\lambda \in (1,2]$ and $\nu \in (-2,0]$. In coagulation and breakage processes, two noteworthy phenomena emerge: gelation [27–29], where larger particles swiftly develop through the coagulation kernels, and shattering [30, 31], where the formation of dust particles arises from breakage rates. These processes uphold the conservation of the total particle volume in the system. However, for the coagulation and fragmentation coefficients are given by

$$K(x,y) = K_0\left(x^\alpha y^{\lambda-\alpha} + x^{\lambda-\alpha}y^\alpha\right), \quad K_0 > 0, \quad (x,y) \in (0,\infty)^2, \tag{1.11}$$

with $\alpha \in [0,1], \lambda \in [2\alpha, 1+\alpha]$, and

$$S(x) = a_0 x^\gamma, \quad B(x,y) = B_\nu(x,y) := (\nu+2)x^\nu y^{-\nu-1}, \quad 0 < x < y, \tag{1.12}$$

with $\gamma \in \mathbb{R}, \nu \in (-2,\infty)$, and $a_0 > 0$, gelation after a finite time occurs when $\alpha > 1/2$ in (1.11) and $\gamma \in (0, \lambda-1)$ in (1.12) [27–29], while shattering is observed when $\gamma < 0$ in (1.12) and there is no coagulation $(K_0 = 0)$ [30, 31]. In contrast, mass-conserving solutions to (1.7) exist for all $t \geq 0$ when, either $\lambda \in [0,1]$ and $\gamma \geq 0$, or $\lambda \in (1,2]$ and $\gamma > \lambda - 1$ [32–36]. The previous discussion reveals that the value $\gamma = \lambda - 1 > 0$ is a borderline case concerning the gelation concept. Indeed, on the one hand, when $\lambda \in (1,2], \gamma = \lambda - 1$, and $\alpha > -\nu - 1$ in (1.11-1.12), mass-conserving solutions to (1.7) on $[0,\infty)$ exist when initial volume is sufficiently small [37], which is in accordance with numerical simulations performed in [38] for the particular choice $\alpha = 1, \quad \lambda = 2, \quad \gamma = 1, \quad \nu = 0$. On the other hand, gelation (in finite time) takes place when $\alpha = 1, \lambda = 2, \gamma = 1, \nu > -1$, and the initial volume is large enough [33, 38].

The existence of weak solutions for equation (1.7) hinges on employing L^1 compactness methods applied to appropriately selected approximating equations. This methodology traces its origins to the work of Stewart [36], who examined scenarios where both K and binary B adhere to growth conditions that approach linearity. Notably, Laurençot [39] extended this approach to demonstrate existence results for the continuous CMBE, though with a distinct class of kernels, yet sharing a non-empty intersection. Furthermore, a more comprehensive outcome is presented in [40] concerning the discrete CMBE. In [41], authors demonstrated the existence of the weak solution of the truncated CMBE (1.7) using the L^1 compactness method under the assumptions on $K(x,y) = \phi(x)\phi(y)$, where $\phi(x) \leq k_1(1+x)^{\mu}, \quad 0 \leq \mu \leq 1$, $S(x) = k_2(1+x)^{\gamma}$ and $B(x,y) = (\nu+2)x^{\nu}y^{-\nu-1}, \quad 0 < x < y$ with $1 > \gamma \geq 0$ and $\nu \geq 0$. Further, for the uniqueness of the solution (inspired by the Stewart [42]), more restrictive kernels chosen. The extended results [43] of the weak solution for a class of unbounded coagulation and fragmentation kernels, the fragmentation kernel having possibly a singularity at the origin.

Typically, deriving solutions for aggregation and breakage problems involving physical kernels present a formidable challenge. Consequently, numerical and semi-analytical techniques are commonly employed to obtain solutions, either numerically approximated or in the form of analytical expressions. Within existing literature, diverse approaches exist for approximating continuous aggregation-breakage equation. These methods encompass method of successive approximation [44], method of moments [45, 46], finite element method (FVM) [47, 48], finite volume method [49–51] as well as the Monte Carlo method [52, 53]. According to the literature, finite volume scheme (FVS) [54, 55] is an appropriate choice for solving pure coagulation, breakage and combined models due to automatic mass conservation. In 2004, Filbet and Laurençot [49] pioneered the development of a numerical scheme to address coagulation problem (1.2). Specifically, the numerical investigation delves into the gelation phenomenon and the solution's behaviour over extended time periods. Further, Bourgade and Filbet [50] employed a finite

volume approximation to address the binary aggregation-breakage equation involving binary aggregation and breakage fluxes. They concentrated their efforts on demonstrating how the numerical solutions progressively align with the weak solution of the continuous equation. This was achieved through the consideration of locally bounded kernels within the space $L^{1,\infty}_{\text{loc}}(]0,\infty[\times]0,\infty[)$. Moreover, they supplied the first-order error estimation, showing the disparity between numerical approximations and weak solutions of the continuous problem. These estimates were derived under the assumption of kernels within the space $W^{1,\infty}_{\text{loc}}(]0,\infty[\times]0,\infty[)$ on uniform meshes. Next, Rajesh et al. [56] extended the convergence result only for multiple breakage equation (1.5) under the same assumptions on breakage kernel as in [50].

Articles [57, 58] provide the new FVS for multiple breakage and coagulation equations for better predicting the total mass and total particles by introducing the weight functions. Moreover, the consistency and convergence were shown by studying the Lipschitz continuity of the numerical fluxes. The scheme in [58] was systematically compared against the outcomes of existing studies [49, 59], focusing on density and moment results. The benchmarking encompassed six aggregation kernels, including standard kernels (constant, sum, and multiplicative) and more complex kernels.

Nonetheless, numerical techniques have become a common method for analyzing and addressing a wide range of difficult non-linear issues. Such schemes necessitate physical assumptions such as variable discretization, a set of basis functions, linearization, etc. in order to numerically approximate the solution. Nowadays, a lot of authors have suggested alternate strategies based on iterative methodologies to obtain the solution in series forms in order to avoid these restrictions. The so-called semi-analytical procedures enable us to obtain the results analytically. Some of the well known semi-analytical method are Taylor polynomials and radial basis functions [60], Laplace decomposition method (LDM) [61], Laplace variation iteration [62], Laplace optimized decomposition method (LODM) [63], Laplace Adomian decomposition method (LADM) [63], tensor decomposition method [64], Homotopy perturbation method (HPM) [65, 66], Varia-

tional iteration method (VIM) [67–69], Homotopy analysis method (HAM) [70], Adomian decomposition method (ADM) [69, 71], Optimized decomposition method (ODM) [72], and Accelerated homotopy perturbation method (AHPM) [73]. Article [60] discussed Taylor polynomials and radial basis functions together to solve the CE (1.2) with constant kernel. In [61], modified LDM is employed on CE (1.2) for two test cases $K(x,y) = 1, c(0,x) = e^{-x}$ and $K(x,y) = xy, c(0,x) = e^{-x}/x$ and revealed the results same as the HAM [65].

Next, LODM is applied to coagulation equation (1.2) for three examples $K(x,y) = 1, x+y, xy$ with $c(0,x) = e^{-x}$ and LADM is established to breakage equation (1.5) for various kernels $B(x,y) = 2/y, S(x) = x, x^2$ and Austin kernels $B(x,y) = 3x/y^2, S(x) = x^3$ with the initial function $c(0,x) = e^{-x}, \delta(x-a)$, see [72]. In addition, convergence analysis of the series solutions for both methods is shown for some assumptions on aggregation and breakage kernels. ADM and HPM were implemented for aggregation and breakage equations to achieve more detailed results for $K(x,y) = 1, x+y, xy, x^{2/3}+y^{2/3}$ with exponential initial conditions $c(0,x) = e^{-x}, e^{-x}/x$, and breakage kernels $B(x,y) = \frac{\alpha}{y}(\frac{x}{y})^{\alpha-2}$ having the exponential and mono disperse initial conditions, see [66, 71]. To obtain the series solution, [67] described the framework of ADM and VIM for the linear breakage equation (1.5) in batch and continuous flow systems with assumed functional forms of breakage frequencies and daughter particle distributions. In [68], ADM, HPM, and VIM are applied to aggregation (1.2) and breakage equations (1.5) to compare the analytical results for aggregation kernel xy, initial condition e^{-x} in aggregation equation and selection rate x^k, breakage kernel $\frac{kx^{k-2}}{y}$, initial condition e^{-x} in breakage equation. Additionally, it has been discovered that VIM delivers more accurate approximation results than ADM.

The PBEs like aggregation and breakage equations are solved using HAM for various benchmark kernels $K(x,y) = 1,\ x+y,\ xy,\ x^{2/3}+y^{2/3}$, breakage kernel $B(x,y) = 2/y$ with initial data $c(0,x) = e^{-x},\ \delta(x-a)$. Interestingly, for some cases, the closed form so-

lutions are obtained which are actually the exact solutions, see [70]. The authors demonstrated convergence analysis for a particular case of aggregation and breakage kernels and discussed the implementations of ADM technique on the aggregation and breakage equations, see [71]. The authors observed that the ODM solutions [72] for aggregation equation with constant, sum and product aggregation kernels, are far superior to the ADM results [71] and exhibit fast convergence. Next, the idea of AHPM is based on HPM in which accelerated polynomials are introduced by the author to compute the approximated series solutions with high rate of convergence, see [73]. The improvement in the results are justified considering several non-linear differential equations.

1.0.2.2 Collision-induced breakage equation

The pioneering research conducted by Cheng and Redner [21] delved into scaling solutions of the rate equation, elucidating the distinctions between linear (1.5) and non-linear (1.8) processes. In their exploration, they adopted a well-known scaling solution for the density function, expressed as $c(t,x) \sim s^{-2}\varphi(x/s)$, where s represents the characteristic cluster mass, defined as $s = t^{-1/\lambda}$, for $\lambda > 0$.

Article [74] analyzed the asymptotic behaviour of a simple-minded class of models in which two-particle collision results in either: (1) both particles splitting into two equal pieces, (2) only the larger particle splitting in two, or (3) only the smaller particle splitting. Next, authors in [75] studied the shattering phenomena and also investigated case (2), where particles turn into dust particles due to discontinuous transition. Moreover, case (3) contains the continuous transition with dust gaining mass steadily due to the fragments. The article [76] possessed the information regarding the analytical solutions for two cases, $K(x,y) = 1, b(x,y,z) = 2/y$ and $K(x,y) = xy, b(x,y,z) = 2/y$ with mono-disperse initial condition $\delta(x-1)$. Additionally, self-similar solutions are also explored for sum kernel $K(x,y) = x^{\omega} + y^{\omega}$ and product kernel $K(x,y) = x^{\omega}y^{\omega}$, $\omega > 0$. The existence of mass conserving solution for the CBE (1.8) is established under certain constraints imposed on the breakage function

$$b(x,y,z) \leq \frac{k_1}{y^{\beta}}, \quad \beta > 0$$

and collision kernel

$$K(x,y) \leq k_2(1+x)^{\gamma}(1+y)^{\gamma}, \quad 0 \leq \gamma \leq \alpha, \quad \alpha \in \mathbb{R},$$

see [77]. For the uniqueness, some strong assumption was taken on

$$K(x,y) \leq k_2(1+x)^{\gamma}(1+y)^{\gamma}, \quad 0 \leq \gamma \leq 1.$$

Further, the existence of classical solution with mass conservation for coagulation and CBE is investigated for collision kernels growing indefinitely for large volumes and binary breakage distribution function in [78]. In the continuation, authors in [79] discussed the existence of mass conserving weak solution for collision kernel $K(x,y) = x^{\alpha}y^{\beta} + x^{\beta}y^{\alpha}$, $\alpha \geq 0$, $\alpha \leq \beta \leq 1$, when $\alpha + \beta \in [1,2]$ and non-existence of the mass conserving weak solution rely on the condition $\alpha + \beta \in [0,1), \alpha \geq 0$.
Article [80] focused on the global existence of the solution for the collision kernel featuring a singularity for $\alpha < 0$ or being locally bounded for $\alpha = 0$ for small volumes and proof is relied on a weak L^1 compactness method.

The study of the well-posedness of CBE is exhibited only for very specific kernels. In the sense of the applicability of CBE, numerical methods such as FVM [81–83] and finite element method [84] were investigated recently. FVM was proven to be one of the best algorithms to solve such models, see [49, 85] and further citations for aggregation, breakage and aggregation-breakage equations. The study of weighted FVM has been accomplished with the event-driven constant number Monte Carlo simulation algorithm for several breakage distribution functions in [81]. In [82], two new weighted FVM are introduced to witness the preservation of mass and total number of particles. In addition, convergence analysis and consistency are discovered under some assumptions of collisional kernels and initial condition. In [83], the novel approach (FVM) is achieved through adjusting the birth term within the discretized CBE (1.8). Essential to the efficacy of this proposed method is the strategic allocation of newly generated particles to their adjacent cells. The authors in [84] have introduced a discontinuous Galerkin algorithm that precisely resolves the non-linear CBE on a reduced mass grid in order to account for

the dust particles.

Based on the existing literature and the gap in the research direction, the following objectives are proposed and accomplished during the Ph.D. study.

1.0.3 Objectives of the Thesis

- To prove the weak convergence of discretized weighted finite volume solution towards a solution to coagulation and multiple breakage equation in weighted L^1 space and error estimation.
- To find the weak convergence and error analysis of the discretized finite volume solution to coagulation-multiple fragmentation equation with singular fragmentation kernel using divergence form of the model.
- To conduct weak convergence and error analysis of the finite volume method for non-linear collision-induced breakage equation for locally bounded kernels.
- To implement two semi-analytical schemes, such as are called variational iteration and optimized decomposition methods for non-linear collision-induced breakage equation along with the convergence analysis of the series solutions.
- To show the convergence analysis of the series solution computed using homotopy analysis and accelerated homotopy perturbation methods as well as finite volume implementation for non-linear collision-induced breakage equation.

1.0.4 Organization of the Thesis

The thesis is structured around an exploration of equations CMBE (1.7) and CBE (1.8) utilizing theoretical, numerical, and semi-analytical techniques. The theoretical segment delves into the existence of a weak solution under a stability condition in weighted the L^1 space. Additionally, error estimation for the approximate solution is addressed considering kernels in the $W^{1,\infty}_{loc}$ space. From the numerical aspect, the finite volume method is employed due to its inherent ability to uphold mass conservation. Moreover, multiple

semi-analytical methods are applied to the CBE (1.8) to unveil process dynamics. Simultaneously, the convergence and error analysis are investigated under specific assumptions related to kernels. Let us briefly summarize each chapter of the thesis.

Chapter 2 consists the convergence of weighted FVS for solving CMBE (1.7) having locally bounded coagulation kernel but singularity near the origin due to fragmentation rates. Thanks to the Dunford-Pettis and De La Vall$\acute{e}$e-Poussin theorems, we establish that numerical solution is converging to the weak solution of the continuous model using a weak L^1 compactness argument. A suitable stable condition on time step is taken to achieve the result. Furthermore, when kernels are in $W^{1,\infty}_{loc}$ space, first order error approximation is demonstrated for a uniform mesh. The result is numerically validated by taking four test problems of coupled coagulation-fragmentation models.

Further, Chapter 3 analyzes a FVS for solving coagulation and multiple fragmentation equation (1.7). Here, the conservative form of the problem (1.7) in terms of fluxes is considered for the discretization using FVS. The methodology and kernel assumptions are the same as in Chapter 2. Additionally, convergence analysis and theoretical and experimental error estimation (first-order) in $W^{1,\infty}_{loc}$ space is also delivered for this model.

Chapter 4 presents the pure collisional breakage equation (1.8), which is non-linear in nature and accompanied by a locally bounded breakage kernel and collision kernel. The continuous equation (1.8) is discretized using a FVS, and the weak convergence of the approximated solution towards the exact solution is analyzed for non-uniform mesh using the same idea in Chapter 2. Error analysis is also developed and verified numerically for three test examples of the kernels.

Next, Chapter 5 provides approximate solutions for the non-linear collision-induced breakage equation (1.8) using two different semi-analytical schemes, i.e., variational iteration method (VIM) and optimized decomposition method (ODM). The study also includes the detailed convergence analysis and error estimation for ODM in the case of product collisional ($K(x, y) = xy$) and breakage ($b(x, y, z) = \frac{2}{y}$) kernels with an exponential decay initial condition. By contrasting estimated density function and moments with exact solutions, the novelty of the suggested approaches is presented considering

three numerical examples. Interestingly, in one case, VIM provides a closed-form solution, however, finite term series solutions obtained via both schemes supply a great approximation for density function and moments with the precise solutions.

Finally, Chapter 6 implements two semi-analytical techniques, namely homotopy analysis method (HAM) and accelerated homotopy perturbation method (AHPM) are investigated along with the well-known FVM to comprehend the dynamical behavior of the non-linear system (1.8), i.e., the density function, the total number and the total mass of the particles in the system. The theoretical convergence analyses of the series solutions of HAM and AHPM are discussed. In addition, the error estimations of the truncated solutions of both methods equip the maximum absolute error bound. To justify the applicability and accuracy of these methods, numerical simulations are compared with the findings of FVM and analytical solutions considering three physical problems.

In the end, some conclusions and future works are summarized.

Chapter 2

Convergence and Error Estimation of Weighted Finite Volume Scheme for Coagulation-Fragmentation Equation

---

Recently, in articles [57, 58], a new finite volume scheme is developed directly from the integral equation (1.7). To get the discretized form, quadrature rules are applied to the truncated equation, where the replacement of ∞ with R is implemented. However, such discrete formulation does not follow the mass conservation property. In order to do so, some weight functions are introduced and it was shown that the new scheme gives better predictions for the number density and moments as compared to the previous numerical schemes proposed in [50, 59]. The results are verified numerically by taking several examples. However, the theoretical convergence analysis was still missing.

Hence, it would be interesting to study the convergence analysis of the method using weak L^1 compactness argument, see [50, 56]. Therefore, our aim here is to prove the weak convergence analysis for coagulation-multiple fragmentation equation having unbounded multiple breakage kernel. The idea of the proof is based on Dunford-Pettis

theorem by using weak L^1 compactness method and the De La Vallée Poussin theorem. In addition, we show the error estimation for a uniform mesh by taking the rate of kernels in $W^{1,\infty}_{loc}$. It is observed that the first-order accuracy of the scheme is tested numerically.

Let us recall (1.0.1.3) the following one-dimensional non-linear integro-differential model, known as coagulation and multiple fragmentation equation

$$\begin{aligned}\frac{\partial c(t,x)}{\partial t} =& \frac{1}{2}\int_0^x K(y,x-y)c(t,y)c(t,x-y)dy - \int_0^\infty K(x,y)c(t,x)c(t,y)dy \\ &+ \int_x^\infty B(x,y)S(y)c(t,y)dy - S(x)c(t,x)\end{aligned}$$

with the given initial data

$$c(0,x) \;=\; c^{in}(x) \geq 0, \quad x \in]0,\infty[. \tag{2.1}$$

Besides number density distribution, essential characteristics such as moments are also of relevance. The expression of the moments corresponding to the particle size distribution is

$$\mu_j(t) = \int_0^\infty x^j c(t,x)dx, \tag{2.2}$$

where $\mu_0(t)$ and $\mu_1(t)$ are of special interest, which are proportional to the total number and the total mass of the particles, respectively. One can easily show that the zeroth moment decreases by coagulation and increases by breakage processes although the total mass stays constant. The following integral equality describes the mass conservation property

$$\int_0^\infty xc(t,x)dx = \int_0^\infty xc^{in}(x)dx, \;\; t \geq 0.$$

The contributions in this chapter are structured as follows. In Section 2.1, some relevant definitions and theorems are presented related to Chapters 2, 3, and 4. Section 2.2 starts with the discretization technique based on the finite volume method. Further, representing the mass conservation scheme in Section 2.3, followed by the detailed convergence analysis in Section 2.4. Finally, we discuss the error estimation in Section 2.5 and validation of it is explained in Section 2.6 by taking several examples.

2.1 Preliminaries

Definition 1. Jensen inequality [86]: consider an integrable function c defined on the interval $[a, b]$, and let ϕ be a convex function defined at least over the range $[m, M]$, where m represents the infimum of c and M denotes the supremum of c. Under these conditions, we have the following inequality:

$$\phi\left(\frac{1}{b-a}\int_a^b c\right) \leq \frac{1}{b-a}\int_a^b \phi(c).$$

Definition 2. ([87], Definition 7.19]) A sequence $\{c_n : \mathbb{R} \to \mathbb{R}\}$ of functions is uniformly bounded if there exists a constant $M \geq 0$, such that $\forall n$, we have $\sup_{x\in\mathbb{R}} |c_n(x)| \leq M$.

Definition 3. (Uniform integrability), [33]. A subset I of $L_1(\Omega)$ is uniformly integrable in $L_1(\Omega)$ if I is a bounded subset of $L_1(\Omega)$ such that

$$\lim_{M\to\infty} \sup_{c\in I} \int_{\{|c|\geq M\}} |c| \mathrm{d}\mu = 0.$$

Proposition 2.1.1. ([88]) Let (c_n) be a sequence in space E. Then

- $c_n \to c$ weakly in $\sigma\left(E, E^\star\right) \Leftrightarrow \langle g, c_n\rangle \to \langle g, c\rangle \ \forall g \in E^\star$ (dual of E).
- If $c_n \to c$ weakly in $\sigma\left(E, E^\star\right)$, then $(\|c_n\|)$ is bounded and $\|c\| \leq \liminf \|c_n\|$.

Definition 4. ([33])

- Let $p \in [1, \infty)$. A sequence (c_n) in $L_p(\Omega)$ converges weakly to c in $L_p(\Omega)$ if

  $$\lim_{n\to\infty} \int_\Omega c_n(x)\phi(x)\mathrm{d}\mu(x) = \int_\Omega c(x)\phi(x)\mathrm{d}\mu(x)$$

  for all $\phi \in L_{p'}(\Omega)$ where $p' := \infty$ when $p = 1$ and $p' := p/(p-1)$ when $p \in (1, \infty)$.

- A sequence $(c_n)_{n\geq 1}$ in $L_\infty(\Omega)$ converges $\star$-weakly to c in $L_\infty(\Omega)$ if

  $$\lim_{n\to\infty} \int_\Omega c_n(x)\phi(x)\mathrm{d}\mu(x) = \int_\Omega c(x)\phi(x)\mathrm{d}\mu(x)$$

  for all $\phi \in L_1(\Omega)$.

It is known that for a given p within the interval $(1, \infty)$ and a sequence of functions $(f_n)_{n\geq 1}$ in $L_p(\Omega)$, Kakutani's theorem [[88], Theorem 3.17], coupled with the reflexivity property of $L_p(\Omega)$ [[88], Theorem 4.10], guarantees the existence of a subsequence within any bounded sequence in $L_p(\Omega)$ that converges weakly in $L_p(\Omega)$. Similar in essence, a parallel outcome is attainable for $L_\infty(\Omega)$: due to $L_\infty(\Omega)$ serving as the dual space of the separable domain $L_1(\Omega)$, it can be deduced from the Banach-Alaoglu theorem that a bounded sequence of functions in $L_\infty(\Omega)$ will possess a subsequence that converges $\star$-weakly in $L_\infty(\Omega)$ [[88], Theorem 3.16].

Regrettably, this advantageous property is not extended to the space $L^1(\Omega)$, and a bounded sequence within $L^1(\Omega)$ is not guaranteed to possess a subsequence that converges weakly in $L^1(\Omega)$. Avoiding the emergence of concentration and vanishing scenarios leads to a significant outcome concerning sequential weak compactness within $L^1(\Omega)$. This result is recognized as the Dunford-Pettis theorem.

Theorem 2.1.2. (Dunford-Pettis theorem)[89] Let I be a bounded set of $L_1(\Omega)$. The identical statements are as follows:

- I is relatively sequentially weakly compact in $L_1(\Omega)$.
- I satisfies the following two properties:

$$\eta\{I\} = \lim_{\varepsilon\to 0}\left[\sup\left\{\int_E |c|\mathrm{d}\mu : c \in \mathcal{E}, E \in B, \mu(E) \leq \varepsilon\right\}\right] = 0$$

and, $\forall\, \varepsilon > 0$, $\exists\, \Omega_\varepsilon \in B$ such that $\mu\left(\Omega_\varepsilon\right) < \infty$ and

$$\sup_{c\in I}\int_{\Omega\setminus\Omega_\varepsilon} |f|\mathrm{d}\mu \leq \varepsilon.$$

We now present the link between the Dunford-Pettis theorem and the property of uniform integrability.

Proposition 2.1.3. ([90]) Let $I \subset L^1(\Omega)$. The identical statements are as follows:

- I is uniformly integrable.

- I (bounded) $\subset L^1(\Omega)$ such that $\eta\{I\} = 0$.

Theorem 2.1.4. (The De La Vallée Poussin theorem [91]) Let $I \subset L^1(\Omega)$. The identical statements are as follows:

- I is uniformly integrable.
- I (bounded) $\subset L^1(\Omega)$ and $\exists$ convex function $\Phi \in C^\infty([0,\infty))$ such that $\Phi(0) = \Phi'(0) = 0$, Φ' is a concave function,

$$\Phi'(r) > 0 \quad \text{if} \quad r > 0,$$
$$\lim_{r\to\infty} \frac{\Phi(r)}{r} = \lim_{r\to\infty} \Phi'(r) = \infty,$$

and

$$\sup_{c\in I} \int_\Omega \Phi(|c|) d\mu < \infty.$$

Lemma 2.1.5. [[92], Lemma A.2] Let Π be an open subset of $\mathbb{R}^m$ and let there exists a constant $l > 0$ and two sequences $(z_n^1)_{n\in\mathbb{N}}$ and $(z_n^2)_{n\in\mathbb{N}}$ such that $(z_n^1) \in L^1(\Pi), z^1 \in L^1(\Pi)$ and

$$z_n^1 \rightharpoonup z^1, \quad \text{weakly in } L^1(\Pi) \quad \text{as } n \to \infty,$$

$(z_n^2) \in L^\infty(\Pi), z^2 \in L^\infty(\Pi)$, and for all $n \in \mathbb{N}, |z_n^2| \le l$ with

$$z_n^2 \to z^2, \ \text{ almost everywhere (a.e.) in } \Pi \quad \text{as } n \to \infty.$$

Then

$$\lim_{n\to\infty} \|z_n^1(z_n^2 - z^2)\|_{L^1(\Pi)} = 0$$

and

$$z_n^1 z_n^2 \rightharpoonup z^1 z^2, \quad \text{weakly in } L^1(\Pi) \quad \text{as } n \to \infty.$$

Finally, we provide the Gronwall's lemma which is

Theorem 2.1.6. Version of Gronwall's lemma [93] (The Gollwitzer Inequality) . Assume u, f, g and h are nonnegative continuous functions on $I = [a, b]$, and for all $t \in I$,

$$u(t) \le f(t) + g(t) \int_a^t h(s)u(s)ds.$$

Then for all $t \in I$,

$$u(t) \leq f(t) + g(t) \int_a^t h(s)f(s) \exp\left(\int_s^t h(\sigma)g(\sigma)d\sigma\right) ds.$$

Definition 5. (Contraction mapping [87]) Let (X, d) be a non-empty complete metric space $d : X \to X$ with the property that there is some real number $0 \leq r < 1$ so that $\forall x, y \in X$,

$$d(f(x), f(y)) \leq rd(x, y).$$

Theorem 2.1.7. (Contraction mapping theorem [87]) Let (X, d) be a complete metric space with a contraction mapping $T : X \to X$. Then, T admits a unique fixed point c in X. Furthermore, c can be found as follows: start with an arbitrary element $c_0 \in X$ and define a sequence c_n by $c_n = T(c_{n-1})$ for $n \geq 1$, then $c_n \to c$ as $n \to \infty$. The theorem is also known as the Banach fixed point theorem.

Moreover, to shows how the numerically discretized solution converges to a weak solution for the continuous CMBE, in chapters 2, 3, 4 the following weighted L^1 space X^+ is taken

$$X^+ = \{c \in L^1(\mathbb{R}^+) \cap L^1(\mathbb{R}^+, x\,dx) : c \geq 0, \|c\| < \infty\}, \tag{2.3}$$

where $\|c\| = \int_0^\infty (1 + x)c(x)\,dx$, and $c^{in} \in X^+$.
For the analysis in chapters 2, 3, the following assumptions are taken on coagulation and selection rates, as well as on breakage function

$$H1: \quad K \in L^\infty_{\text{loc}}(\mathbb{R}^+ \times \mathbb{R}^+), \tag{2.4}$$

and

$$H2: \begin{cases} S \in L^\infty_{\text{loc}}(\mathbb{R}^+) \text{ and } S(x) = x^{1+\alpha}, \\ B(x, y) = \frac{\alpha+2}{y}\left(\frac{x}{y}\right)^\alpha, \text{ for } 0 < x < y, \end{cases} \tag{2.5}$$

where $\alpha \in (-1, 0]$, see [94]. It should be mentioned here that such breakage function includes the singularity near the origin.

2.2 Finite Volume Scheme

Consider the CMBE Eq.(1.7) associated with initial datum (2.1). For the numerical scheme, firstly, truncate the computational domain of volume argument $(0, \infty)$ to $(0, R)$. Then, separate the domain into a limited number of grids or subintervals (Λ_i^h). The purpose of discretization is to approximate the total number of particles that exist in these cells. The truncated CMBE equation and all the notations that will be used in the discretization are described below:

The truncated CMBE equation is

$$\begin{aligned}\frac{\partial c(t,x)}{\partial t} =& \frac{1}{2}\int_0^x K(y, x-y)c(t,y)c(t,x-y)dy - \int_0^R K(x,y)c(t,x)c(t,y)dy \\ &+ \int_x^R B(x,y)S(y)c(t,y)dy - S(x)c(t,x) \end{aligned} \tag{2.6}$$

associated initial function, $c(0,x) = c^{in}(x) \geq 0, \quad x \in]0, R]$.

The volume variable x is discretized into cells as

$$\Lambda_i^h =]x_{i-1/2}, x_{i+1/2}] \quad \text{for } i = 1, 2, ..., \mathrm{I}(h),$$

where $x_{1/2} = 0, x_{\mathrm{I}(h)+1/2} = R, \Delta x_i = x_{i+1/2} - x_{i-1/2}$. Let us consider $h = \max\ \Delta x_i \ \forall\ i$. The characterization of each i^{th} cell is portrayed by the center of that cell, i.e., $x_i = (x_{i-1/2} + x_{i+1/2})/2$. This type of cell partitioning is referred to as the central representation of the cell.

For the time argument, the domain is restricted in the range [0, T] and then discretize the domain with time step Δt into N time intervals. We define the interval

$$\tau_n = [t_n, t_{n+1}[,$$

with $t_n = n\Delta t,\ n = 0, 1, ..., N-1$.

We can start the formulation of the scheme on any type of uniform and non-uniform meshes. For non-uniform scheme, merging of j^{th} and k^{th} cells are not exactly overlap with i^{th} cell, i.e., $[x_{j-1/2} + x_{k-1/2},\ \ x_{j+1/2} + x_{k+1/2}] \neq [x_{i-1/2},\ x_{i+1/2}]$. For later use,

consider the two indices [59], $\Pi_{i,j}$ and $\Gamma_{i,j}$ satisfying the condition

$$x_{\Pi_{i,j}+1/2} + x_{j+1/2} < x_{i+1/2},\ x_{\Gamma_{i,j}-1/2} + x_{j-1/2} < x_{i-1/2}.$$

The significant benefit of a non-uniform mesh is that it allows for the inclusion of a larger domain with fewer mesh sizes than a uniform mesh.

Taking into consideration that c_i^n is the mean value of c in cell i and at time t_n, which is an approximation of $c(t_n, x_i)$ and is provided by the following expression

$$c_i^n(t) = \frac{1}{\Delta x_i} \int_{x_{i-1/2}}^{x_{i+1/2}} c(t,x)\, dx. \tag{2.7}$$

Notice that $c_i^n(t)$ and $c(t,x)$ are identical up to the order of two using the mid-point quadrature rule and assuming that point masses are concentrated on the cell representatives, i.e., $c(t,x) \approx \sum_{i=1}^{\mathrm{I(h)}} c_i(t)\Delta x_i \delta(x - x_i)$. Integration of Eq.(2.6) over i^{th} cell provides the following discrete form of the equation

$$\frac{dc_i}{dt} = C(B_i) - C(D_i) + F(B_i) - F(D_i), \tag{2.8}$$

where

$$C(B_i) = \frac{1}{\Delta x_i} \int_{x_{i-1/2}}^{x_{i+1/2}} \frac{1}{2} \int_0^x K(y, x-y)c(t,y)c(t,x-y)dydx$$

$$C(D_i) = \frac{1}{\Delta x_i} \int_{x_{i-1/2}}^{x_{i+1/2}} \int_0^{x_{\mathcal{I}(h)+1/2}} K(x,y)c(t,x)c(t,y)dydx$$

$$F(B_i) = \frac{1}{\Delta x_i} \int_{x_{i-1/2}}^{x_{i+1/2}} \int_x^{x_{\mathcal{I}(h)+1/2}} B(x,y)S(y)c(t,y)dydx$$

$$F(D_i) = \frac{1}{\Delta x_i} \int_{x_{i-1/2}}^{x_{i+1/2}} S(x)c(t,x)dx$$

along with initial datum,

$$c_i(0) = c_i^{in} = \frac{1}{\Delta x_i} \int_{x_{i-1/2}}^{x_{i+1/2}} c_0(x)\, dx. \tag{2.9}$$

Applying the midpoint rule on all the above expressions provides the following semi-discrete equation, see [57, 58] for more detailed explanation

$$\begin{aligned}\frac{dc_i}{dt} =& \frac{1}{2\Delta x_i}\sum_{(j,k)\in\lambda^i} K_{j,k}c_jc_k\Delta x_j\Delta x_k - \frac{1}{\Delta x_i}\sum_{j=1}^{\mathrm{I}(h)} K_{i,j}c_ic_j\Delta x_i\Delta x_j \\ &+ \frac{1}{\Delta x_i}\sum_{k=i}^{\mathrm{I}(h)} S_kc_k\Delta x_k\int_{x_{i-1/2}}^{p_k^i} B(x,x_k)dx - S_ic_i,\end{aligned} \tag{2.10}$$

where λ^i and p_k^i are defined as

$$\lambda^i = \{(j,k)\in\mathbb{N}\times\mathbb{N} : x_{i-1/2} < (x_j + x_k) \le x_{i+1/2}\}, \quad i\in\{1,2,...,\mathrm{I}(h)\}. \tag{2.11}$$

$$p_k^i = \begin{cases} x_i, & \text{if } k = i \\ x_{i+1/2}, & k \neq i. \end{cases} \tag{2.12}$$

Note that such discretization given by Saha and Kumar [57] and Singh et al. [58] is different from the formulations considered in [49] where authors have used equivalent divergence form of CMBE (1.7) which automatically satisfies the mass conservation. The following notation is also essential for further analysis

$$\lambda^* = \{(j,k)\in\mathbb{N}\times\mathbb{N} : (x_j + x_k) \ge R\}. \tag{2.13}$$

Represent the characteristic function $\chi_D(x)$ of a set D as $\chi_D(x) = 1$ if $x \in D$ or 0 elsewhere. Subsequently, define a function c^h on the interval $[0,T]\times]0,R]$ as:

$$c^h(t,x) = \sum_{n=0}^{N-1}\sum_{i=1}^{\mathrm{I}(h)} c_i^n\,\chi_{\Lambda_i^h}(x)\,\chi_{\tau_n}(t), \tag{2.14}$$

which means that the function c^h relies on the volume and time steps. Also noting that

$$c^h(0,\cdot) = \sum_{i=1}^{\mathrm{I}(h)} c_i^{in}\chi_{\Lambda_i^h}(\cdot)$$

converges strongly to c^{in} in $L^1(0,R)$ as $h\to 0$. Further, we take the following forms of aggregation, fragmentation and selection functions in the discrete setting

$$K^h(u,v) = \sum_{i=1}^{\mathrm{I}(h)}\sum_{j=1}^{\mathrm{I}(h)} K_{i,j}\chi_{\Lambda_i^h}(u)\chi_{\Lambda_j^h}(v) \quad \text{where} \quad K_{i,j} = \frac{1}{\Delta x_i\Delta x_j}\int_{\Lambda_j^h}\int_{\Lambda_i^h} K(u,v)dudv, \tag{2.15}$$

$$B^h(u,v) = \sum_{i=1}^{\mathrm{I}(h)} \sum_{j=1}^{\mathrm{I}(h)} B_{i,j} \chi_{\Lambda_i^h}(u) \chi_{\Lambda_j^h}(v) \quad \text{where} \quad B_{i,j} = \frac{1}{\Delta x_i \Delta x_j} \int_{\Lambda_j^h} \int_{\Lambda_i^h} B(u,v) du dv, \tag{2.16}$$

and

$$S^h(v) = \sum_{i=1}^{\mathrm{I}(h)} S_i \chi_{\Lambda_i^h}(v) \quad \text{where} \quad S_i = \frac{1}{\Delta x_i} \int_{\Lambda_i^h} S(v) dv. \tag{2.17}$$

Such discretization ensures that $\|K^h - K\|_{L^1((0,R)\times(0,R))} \to 0$, $\|B^h - B\|_{L^1((0,R)\times(0,R))} \to 0$ and $\|S^h - S\|_{L^1(0,R)} \to 0$ as $h \to 0$, see [50].

2.3 Conservative Formulation

Here, we quickly review the conservative semi-discrete CMBE proposed by authors in [57, 58]. Readers are referred to these references for more detailed explanation. Implementing weight functions, Eq. (2.10) becomes

$$\begin{aligned} \frac{dc_i}{dt} =& \frac{1}{2\Delta x_i} \sum_{(j,k)\in\lambda^i} K_{j,k} c_j c_k \Delta x_j \Delta x_k \omega'_{i,j,k} - \frac{1}{\Delta x_i} \sum_{j=1}^{\mathrm{I}(h)} K_{i,j} c_i c_j \Delta x_i \Delta x_j \\ &+ \frac{1}{\Delta x_i} \sum_{k=i}^{\mathrm{I}(h)} S_k c_k \Delta x_k \int_{x_{i-1/2}}^{p_k^i} B(x, x_k) dx - S_i c_i \omega_{i,j}, \end{aligned} \tag{2.18}$$

where

$$\omega'_{i,j,k} = \begin{cases} \frac{x_j + x_k}{x_i}, & (x_j + x_k) \le R \\ 0, & \text{otherwise}, \end{cases} \tag{2.19}$$

and

$$\omega_{i,j} = \frac{\sum_{j=1}^{i} x_j \int_{x_{j-1/2}}^{p_i^j} B(x, x_i) dx}{x_i}. \tag{2.20}$$

Discretization of the time derivative by the Euler method leads to the fully discrete system

$$\begin{aligned} c_i^{n+1} =& c_i^n + \frac{\Delta t}{2\Delta x_i} \sum_{(j,k)\in\lambda^i} K_{j,k} c_j^n c_k^n \Delta x_j \Delta x_k \omega'_{i,j,k} - \frac{\Delta t}{\Delta x_i} \sum_{j=1}^{\mathrm{I}(h)} K_{i,j} c_i^n c_j^n \Delta x_i \Delta x_j \\ &+ \frac{\Delta t}{\Delta x_i} \sum_{k=i}^{\mathrm{I}(h)} S_k c_k^n \Delta x_k \int_{x_{i-1/2}}^{p_k^i} B(x, x_k) dx - S_i c_i^n \omega_{i,j} \Delta t, \end{aligned} \tag{2.21}$$

which is mass conserving.

2.4 Convergence of Solutions

Theorem 2.4.1. Consider that $c^{in} \in X^+$ and the hypothesis $(H1) - (H2)$ on kernels hold. Also assuming that under the time step Δt and for a constant $\theta > 0$, the following stability condition

$$C(R,T)\Delta t \leq \theta < 1, \tag{2.22}$$

holds for

$$C(R,T) := \max(\|K\|_\infty, \alpha+2)\|c^{in}\|_{L^1} e^{\eta\|S\|_{L^\infty}T} + \|S\|_\infty \eta, \;\; \eta = \frac{\alpha+2}{\alpha+1}. \tag{2.23}$$

Then there exists the extraction of a sub-sequence as

$$c^h \to c \;\text{ in }\; L^\infty((0,T; L^1(0,R)),$$

for c being the weak solution to (1.7) on $[0,T]$ with initial condition c^{in}, implying that $c \geq 0$ satisfies

$$\begin{aligned}
&\int_0^T \int_0^R c(t,x)\frac{\partial \varphi}{\partial t}(t,x)dx\,dt + \int_0^R c^{in}(x)\varphi(0,x)dx + \int_0^T \int_0^R \varphi(t,x)S(x)c(t,x)dx\,dt \\
&- \frac{1}{2}\int_0^T \int_0^R \int_0^x \varphi(t,x)K(y,x-y)c(t,y)c(t,x-y)dy\,dx\,dt \\
&+ \int_0^T \int_0^R \int_0^R \varphi(t,x)K(x,y)c(t,x)c(t,y)dy\,dx\,dt \\
&- \int_0^T \int_0^R \int_x^R \varphi(t,x)B(x,y)S(y)c(t,y)dy\,dx\,dt = 0,
\end{aligned} \tag{2.24}$$

for all smooth functions φ having compactly supported in $[0,T]\times]0,R]$.

By following the above theorem, the main task here certainly is to establish $(c^h) \rightharpoonup c$ in $L^1(0,R)$ as h and Δt go to zero. Thanks to the Dunford-Pettis theorem, we have a reliable criterion that determines compactness in L^1 when weak convergence is present.

Theorem 2.4.2. Let us take follows: $|\Omega| < \infty$ and a sequence $c^h : \Omega \mapsto \mathbb{R}$ in $L^1(\Omega)$. Consider $\{c^h\}$ holds

- $\{c^h\}$ is equibounded in $L^1(\Omega)$, i.e.

$$\sup \|c^h\|_{L^1(\Omega)} < \infty \tag{2.25}$$

- $\{c^h\}$ is equiintegrable, iff

$$\int_\Omega \Phi(|c^h|)dx < \infty \tag{2.26}$$

for Φ being some increasing function taken as $\Phi : [0, \infty[\mapsto [0, \infty[$ such that

$$\lim_{r\to\infty} \frac{\Phi(r)}{r} \to \infty.$$

Then c^h belongs to a weakly compact set in $L^1(\Omega)$ implying that there is a subsequence of c^h that weakly converges in $L^1(\Omega)$.

Hence, to justify Theorem 2.4.1, it is enough to exhibit the equiboundedness and the equiintegrability of the family c^h in L^1 as in (2.25) and (2.26), respectively. The next proposition, deals with the non-negativity and equiboundedness of the function c^h. We have followed the idea of Bourgade and Filbet [50] for the proof.

Proposition 2.4.3. Let us consider that the stability condition (2.22) holds for the time step Δt. Also, assuming that the growth condition on kernels satisfies $(H1) - (H2)$. Then $c^h \geq 0$ holds the estimate

$$\int_0^R c^h(t, x)dx \leq \|c^{in}\|_{L^1} e^{\eta\|S\|_{L^\infty} t}. \tag{2.27}$$

Proof. The non-negativity and the equiboundedness of the function c^h are shown here by using induction. It is known that at $t = 0$, $c^h(0) \geq 0$ and belongs to $L^1(0, R)$. Assuming further that $c^h(t^n) \geq 0$ and

$$\int_0^R c^h(t^n, x)dx \leq \|c^{in}\|_{L^1} e^{\eta\|S\|_{L^\infty} t^n}. \tag{2.28}$$

Then, our first aim is to prove that $c^h(t^{n+1}) \geq 0$. Firstly, consider the cell at the boundary having index $i = 1$. In this case, from the equation (2.21), we get

$$c_1^{n+1} = c_1^n + \frac{\Delta t}{2\Delta x_1} \sum_{(j,k)\in\lambda^1} K_{j,k} c_j^n c_k^n \Delta x_j \Delta x_k \omega'_{1,j,k} - \frac{\Delta t}{\Delta x_1} \sum_{j=1}^{\mathrm{I}(h)} K_{1,j} c_1^n c_j^n \Delta x_1 \Delta x_j$$

$$+\frac{\Delta t}{\Delta x_1}\sum_{k=1}^{\mathrm{I}(h)} S_k c_k^n \Delta x_k \int_{x_{1/2}}^{p_k^1} B(x,x_k)dx - \frac{\sum_{j=1}^{1} x_j \int_{x_{j-1/2}}^{p_1^j} B(x,x_1)dx}{x_1} S_1 c_1^n \Delta t$$

$$\geq c_1^n + \frac{\Delta t}{\Delta x_1}\sum_{k=2}^{\mathrm{I}(h)} S_k c_k^n \Delta x_k \int_{x_{1/2}}^{p_k^1} B(x,x_k)dx - \frac{\Delta t}{\Delta x_1}\sum_{j=1}^{\mathrm{I}(h)} K_{1,j} c_1^n c_j^n \Delta x_1 \Delta x_j$$

$$\geq \big(1 - \Delta t \|K\|_\infty \sum_{j=1}^{\mathrm{I}(h)} c_j^n \Delta x_j\big) c_1^n.$$

Now, using the condition (2.22) and from Eq. (2.28), the non-negativity of c_1^{n+1} follows. For $i \geq 2$, we have

$$c_i^{n+1} \geq\ c_i^n - \frac{\Delta t}{\Delta x_i}\sum_{j=1}^{\mathrm{I}(h)} K_{i,j} c_i^n c_j^n \Delta x_i \Delta x_j - \frac{\sum_{j=1}^{i} x_j \int_{x_{j-1/2}}^{p_i^j} B(x,x_i)dx}{x_i} S_i c_i^n \Delta t.$$

The condition ($x_j \leq x_i$) and Eq. (2.5) lead to the following condition

$$c_i^{n+1} \geq \Big[1 - \Delta t\big(\|K\|_\infty \sum_{j=1}^{\mathrm{I}(h)} c_j^n \Delta x_j + \eta \|S\|_\infty\big)\Big] c_i^n.$$

Hence, following the condition (2.22) and the L^1 bound (2.28) give

$$c^h(t^{n+1}) \geq 0.$$

Next, it is shown that $c^h(t^{n+1})$ follows a similar estimate as (2.28). For this, multiply equation (2.21) by the term Δx_i and using summation with respect to i, provide

$$\sum_{i=1}^{\mathrm{I}(h)} \Delta x_i c_i^{n+1} = \sum_{i=1}^{\mathrm{I}(h)} \Delta x_i c_i^n + \frac{\Delta t}{2}\sum_{i=1}^{\mathrm{I}(h)} \sum_{(j,k)\in\lambda^i} K_{j,k} c_j^n c_k^n \Delta x_j \Delta x_k \omega_{i,j,k}^{'} - \Delta t \sum_{i=1}^{\mathrm{I}(h)}\sum_{j=1}^{\mathrm{I}(h)} K_{i,j} c_i^n c_j^n \Delta x_i \Delta x_j$$

$$+\Delta t \sum_{i=1}^{\mathrm{I}(h)}\sum_{k=i}^{\mathrm{I}(h)} S_k c_k^n \Delta x_k \int_{x_{i-1/2}}^{p_k^i} B(x,x_k)dx - \sum_{i=1}^{\mathrm{I}(h)} S_i c_i^n \omega_{i,j} \Delta t \Delta x_i. \tag{2.29}$$

According to indices λ^*, i.e., $\omega_{i,j,k}^{'} = 0$ for $(j,k) \in \lambda^*$, one has

$$\sum_{(j,k)\in\lambda^*} K_{j,k} c_j^n c_k^n \Delta x_j \Delta x_k \omega_{i,j,k}^{'} = 0. \tag{2.30}$$

Therefore, following equality holds true using symmetricity of K, see [57, 58]

$$\sum_{j=1}^{\mathrm{I}(h)} K_{i,j} c_i^n c_j^n \Delta x_i \Delta x_j = \frac{1}{2}\sum_{(j,k)\in\lambda^i} K_{j,k} c_j^n c_k^n \Delta x_j \Delta x_k \omega_{i,j,k}^{'} + \frac{1}{2}\sum_{(j,k)\in\lambda^*} K_{j,k} c_j^n c_k^n \Delta x_j \Delta x_k \omega_{i,j,k}^{'}. \tag{2.31}$$

Using the Eq.(2.30)-(2.31) in Eq.(2.29) simplified the equation as

$$\sum_{i=1}^{\mathrm{I}(h)} \Delta x_i c_i^{n+1} \leq \sum_{i=1}^{\mathrm{I}(h)} \Delta x_i c_i^n + \Delta t \sum_{i=1}^{\mathrm{I}(h)} \sum_{k=i}^{\mathrm{I}(h)} S_k c_k^n \Delta x_k \int_{x_{i-1/2}}^{p_k^i} B(x, x_k) dx.$$

By altering the summation's order, taking the value of B as in (2.5) and having (2.28) at step n with $1 + x < \exp(x)\ \forall\ x > 0$ imply that

$$\begin{aligned}\sum_{i=1}^{\mathrm{I}(h)} \Delta x_i c_i^{n+1} \leq & \sum_{i=1}^{\mathrm{I}(h)} \Delta x_i c_i^n + \Delta t \|S\|_\infty \eta \sum_{i=1}^{\mathrm{I}(h)} \Delta x_i c_i^n \\ & \leq \Big(1 + \Delta t \|S\|_\infty \eta\Big) \|c^{in}\|_{L^1}\, e^{\eta \|S\|_{L^\infty} t^n} \leq \|c^{in}\|_{L^1}\, e^{\eta \|S\|_{L^\infty} t^{n+1}},\end{aligned}$$

consequently, the outcome (2.27) is obtained. □

In order to prove the uniform integrability of the family of solutions, let us denote a certain category of convex functions as $C_{VP,\infty}$. Further, consider $\Phi \in C^\infty([0,\infty))$, a non-negative and convex function which resides in class $C_{VP,\infty}$ and enjoys the following properties:

(i) $\Phi(0) = 0,\ \Phi'(0) = 1$ and Φ' is concave;

(ii) $\lim_{p\to\infty} \Phi'(p) = \lim_{p\to\infty} \frac{\Phi(p)}{p} = \infty$;

(iii) for $\gamma \in (1, 2)$,

$$T_\gamma(\Phi) := \sup_{p\geq 0} \left\{ \frac{\Phi(p)}{p^\gamma} \right\} < \infty. \tag{2.32}$$

It is given that, $c^{in} \in L^1(0, R)$, therefore, by De La Vallée Poussin theorem, a convex function $\Phi \geq 0$ exists which satisfies

$$\frac{\Phi(p)}{p} \to \infty,\ \text{as}\ p \to \infty \quad \text{and} \quad \mathcal{I} := \int_0^R \Phi(c^{in})(x) dx < +\infty. \tag{2.33}$$

Lemma 2.4.4. [[92], Lemma B.1.] Consider $\Phi \in C_{VP,\infty}$. Then $\forall\ (r, s) \in \mathbb{R}^+ \times \mathbb{R}^+$,

$$r\Phi'(s) \leq \Phi(r) + \Phi(s).$$

Now, in the following proposition, the equiintegrability is discussed.

Proposition 2.4.5. Let $c^{in} \geq 0 \in L^1(0,R)$ and (2.21) constructs the family $(c^h)_{(h,\Delta t)}$ for any h and Δt, where Δt fulfills the relation (2.22). Then (c^h) is weakly relatively sequentially compact in $L^1((0,T)\times(0,R))$.

Proof. Our focus here is to obtain a similar result as (2.33) for the family of function c^h. The integral of $\Phi(c^h)$ by using the sequence c_i^n can be written as

$$\begin{aligned}\int_0^T\int_0^R \Phi(c^h(t,x))dx\,dt &= \sum_{n=0}^{N-1}\sum_{i=1}^{\mathrm{I}(h)}\int_{\tau_n}\int_{\Lambda_i^h}\Phi\Big(\sum_{k=0}^{N-1}\sum_{j=1}^{\mathrm{I}(h)} c_j^k\chi_{\Lambda_j^h}(x)\chi_{\tau_k}(t)\Big)dx\,dt\\ &= \sum_{n=0}^{N-1}\sum_{i=1}^{\mathrm{I}(h)}\Delta t\Delta x_i\Phi(c_i^n).\end{aligned}$$

The convexity of Φ leads to the estimate

$$\left(c_i^{n+1}-c_i^n\right)\Phi^{'}(c_i^{n+1}) \geq \Phi(c_i^{n+1})-\Phi(c_i^n).$$

Next, by multiplying the preceding equation with Δx_i, summing over i on both sides and then substituting the value of $(c_i^{n+1}-c_i^n)$ from Eq. (2.21) leads to

$$\begin{aligned}\sum_{i=1}^{\mathrm{I}(h)}\Delta x_i\left[\Phi(c_i^{n+1})-\Phi(c_i^n)\right] \leq& \sum_{i=1}^{\mathrm{I}(h)}\Delta x_i\left[(c_i^{n+1}-c_i^n)\Phi^{'}(c_i^{n+1})\right]\\ \leq& \frac{\Delta t}{2}\sum_{i=1}^{\mathrm{I}(h)}\sum_{(j,k)\in\lambda^i} K_{j,k}c_j^nc_k^n\Delta x_j\Delta x_k\omega_{i,j,k}^{'}\Phi^{'}(c_i^{n+1})\\ &+\Delta t\sum_{i=1}^{\mathrm{I}(h)}\sum_{k=i+1}^{\mathrm{I}(h)}\Phi^{'}(c_i^{n+1})S_kc_k^n\Delta x_k\int_{x_{i-1/2}}^{p_k^i}B(x,x_k)dx\\ \leq& \Delta t\sum_{i=1}^{\mathrm{I}(h)}\sum_{j=1}^{\mathrm{I}(h)}K_{i,j}c_i^nc_j^n\Delta x_i\Delta x_j\Phi^{'}(c_i^{n+1})\\ &+\Delta t\sum_{i=1}^{\mathrm{I}(h)}\sum_{k=i+1}^{\mathrm{I}(h)}\Phi^{'}(c_i^{n+1})S_kc_k^n\Delta x_k\int_{x_{i-1/2}}^{p_k^i}B(x,x_k)dx.\end{aligned} \tag{2.34}$$

For the coagulation term, i.e., the first part of the right-hand side (RHS) of Eq. (2.34), changing the order of summation and the convexity result given as in Lemma 2.4.4 enable

us to have

$$\Delta t\sum_{i=1}^{\mathrm{I}(h)}\sum_{j=1}^{\mathrm{I}(h)}K_{i,j}c_i^nc_j^n\Delta x_i\Delta x_j\Phi^{'}(c_i^{n+1})\leq\|K\|_{L^\infty}\Delta t\sum_{j=1}^{\mathrm{I}(h)}c_j^n\Delta x_j\sum_{i=1}^{\mathrm{I}(h)}\Delta x_i[\Phi(c_i^n)+\Phi(c_i^{n+1})]. \tag{2.35}$$

While for the fragmentation term, after observing the values of S, B in (2.5), values of p_k^i and Lemma 2.4.4, we obtain

$$\begin{aligned}\Delta t\sum_{i=1}^{\mathrm{I}(h)}\sum_{k=i+1}^{\mathrm{I}(h)}\Phi^{'}(c_i^{n+1})S_kc_k^n\Delta x_k\int_{x_{i-1/2}}^{p_k^i}B(x,x_k)dx\leq&(\alpha+2)\Delta t\sum_{i=1}^{\mathrm{I}(h)}\sum_{k=i+1}^{\mathrm{I}(h)}\Phi^{'}(c_i^{n+1})c_k^n\Delta x_k\int_{x_{i-1/2}}^{x_{i+1/2}}x^\alpha dx\\&\leq\frac{(\alpha+2)}{(\alpha+1)}\Delta t\sum_{i=1}^{\mathrm{I}(h)}\sum_{k=i+1}^{\mathrm{I}(h)}\Phi^{'}(c_i^{n+1})c_k^n\Delta x_k\Big[x_{i+1/2}^{1+\alpha}-x_{i-1/2}^{1+\alpha}\Big].\end{aligned} \tag{2.36}$$

It is noticed that the term $[x_{i+1/2}^{1+\alpha}-x_{i-1/2}^{1+\alpha}]$ as $\Delta x_i\to 0$ leads to

$$x_{i+1/2}^{1+\alpha}-x_{i-1/2}^{1+\alpha}\leq\ \ (1+\alpha)x_{i+1/2}^{\alpha}\Delta x_i. \tag{2.37}$$

Applying Eq. (2.37) into Eq. (2.36), changing the order of summation in the RHS of Eq. (2.36) and additionally enforcing Lemma 2.4.4 yield

$$\begin{aligned}&\Delta t\sum_{i=1}^{\mathrm{I}(h)}\sum_{k=i+1}^{\mathrm{I}(h)}\Phi^{'}(c_i^{n+1})S_kc_k^n\Delta x_k\int_{x_{i-1/2}}^{p_k^i}B(x,x_k)dx\leq(\alpha+2)\Delta t\sum_{k=1}^{\mathrm{I}(h)}c_k^n\Delta x_k\sum_{i=1}^{k-1}\Delta x_i\Phi^{'}(c_i^{n+1})x_{i+1/2}^{\alpha}\\&\leq(\alpha+2)\Delta t\sum_{k=1}^{\mathrm{I}(h)}c_k^n\Delta x_k\sum_{i=1}^{\mathrm{I}(h)}\Phi(c_i^{n+1})\Delta x_i+(\alpha+2)\Delta t\sum_{k=1}^{\mathrm{I}(h)}c_k^n\Delta x_k\sum_{i=1}^{k-1}\Phi(x_{i+1/2}^{\alpha})\Delta x_i.\end{aligned} \tag{2.38}$$

Let us estimate the 2^{nd} part on the RHS of Eq. (2.38) by using (2.32) and using the values of $\gamma\in(1,2)$ & $\alpha\in(-1,0]$

$$\begin{aligned}(\alpha+2)\Delta t\sum_{k=1}^{\mathrm{I}(h)}c_k^n\Delta x_k\sum_{i=1}^{k-1}\Phi(x_{i+1/2}^{\alpha})\Delta x_i=&(\alpha+2)\Delta t\sum_{k=1}^{\mathrm{I}(h)}c_k^n\Delta x_k\sum_{i=1}^{k-1}\frac{\Phi(x_{i+1/2}^{\alpha})}{x_{i+1/2}^{\gamma\alpha}}x_{i+1/2}^{\gamma\alpha}\Delta x_i\\\leq&(\alpha+2)\Delta tT_\gamma(\Phi)\sum_{k=1}^{\mathrm{I}(h)}c_k^n\Delta x_k\sum_{i=1}^{k-1}x_i^{\gamma\alpha}\Delta x_i\\=&\frac{(\alpha+2)}{(1+\gamma\alpha)}\Delta tT_\gamma(\Phi)\sum_{k=1}^{\mathrm{I}(h)}c_k^n\Delta x_kx_k^{1+\gamma\alpha},\end{aligned}$$

which further reduces to

$$(\alpha+2)\Delta t\sum_{k=1}^{\mathrm{I}(h)}c_k^n\Delta x_k\sum_{i=1}^{k-1}\Phi(x_{i+1/2}^{\alpha})\Delta x_i \leq \frac{(\alpha+2)}{(1+\gamma\alpha)}\Delta t T_\gamma(\Phi)\Big[\sum_{k=1}^{\mathrm{I}(h)}c_k^n\Delta x_k+\sum_{k=1}^{\mathrm{I}(h)}x_k c_k^n\Delta x_k\Big]$$
$$\leq \frac{(\alpha+2)}{(1+\gamma\alpha)}\Delta t T_\gamma(\Phi)\Big[\|c^{in}\|_{L^1}\,e^{\eta\|S\|_{L^\infty}t}+\mu_1\Big]. \qquad (2.39)$$

Substituting the results (2.35), (2.38) and (2.39) in (2.34) lead to

$$\sum_{i=1}^{\mathrm{I}(h)}\Delta x_i\left[\Phi(c_i^{n+1})-\Phi(c_i^n)\right]\leq \|K\|_{L^\infty}\Delta t\|c^{in}\|_{L^1}\,e^{\eta\|S\|_{L^\infty}t}\sum_{i=1}^{\mathrm{I}(h)}\Delta x_i[\Phi(c_i^n)+\Phi(c_i^{n+1})]$$
$$+(\alpha+2)\|c^{in}\|_{L^1}\,e^{\eta\|S\|_{L^\infty}t}\Delta t\sum_{i=1}^{\mathrm{I}(h)}\Delta x_i\Phi(c_i^{n+1})+\frac{(\alpha+2)}{(\gamma\alpha+1)}\Delta t T_\gamma(\Phi)\Big[\|c^{in}\|_{L^1}\,e^{\eta\|S\|_{L^\infty}t}+\mu_1\Big],$$

and therefore, one can obtain

$$\Big(1-K_\alpha\|c^{in}\|_{L^1}\,e^{\eta\|S\|_{L^\infty}T}\Delta t\Big)\sum_{i=1}^{\mathrm{I}(h)}\Delta x_i\Phi(c_i^{n+1})\leq$$
$$\Big(1+\|K\|_{L^\infty}\|c^{in}\|_{L^1}\,e^{\eta\|S\|_{L^\infty}T}\Delta t\Big)\sum_{i=1}^{\mathrm{I}(h)}\Delta x_i\Phi(c_i^n)+\frac{(\alpha+2)}{(\gamma\alpha+1)}\Delta t T_\gamma(\Phi)\Big(\|c^{in}\|_{L^1}\,e^{\eta\|S\|_{L^\infty}T}+\mu_1\Big),$$

where $K_\alpha=\max\{\|K\|_{L^\infty},\alpha+2\}$. The above inequality implies that

$$\sum_{i=1}^{\mathrm{I}(h)}\Delta x_i\Phi(c_i^{n+1})\leq A\sum_{i=1}^{\mathrm{I}(h)}\Delta x_i\Phi(c_i^n)+B \qquad (2.40)$$

where

$$A=\frac{\Big(1+\|K\|_{L^\infty}\|c^{in}\|_{L^1}\,e^{\eta\|S\|_{L^\infty}T}\Delta t\Big)}{\Big(1-K_\alpha\|c^{in}\|_{L^1}\,e^{\eta\|S\|_{L^\infty}T}\Delta t\Big)},\quad B=\frac{(\alpha+2)\Delta t T_\gamma(\Phi)\Big(\|c^{in}\|_{L^1}\,e^{\eta\|S\|_{L^\infty}T}+\mu_1\Big)}{(\gamma\alpha+1)\Big(1-K_\alpha\|c^{in}\|_{L^1}\,e^{\eta\|S\|_{L^\infty}T}\Delta t\Big)}.$$

Hence,

$$\sum_{i=1}^{\mathrm{I}(h)}\Delta x_i\Phi(c_i^n)\leq A^n\sum_{i=1}^{\mathrm{I}(h)}\Delta x_i\Phi(c_i^{in})+B\frac{A^n-1}{A-1}. \qquad (2.41)$$

Thanks to Jensen's inequality and having (2.33), we get

$$\int_0^{\mathbb{R}}\Phi(c^h(t,x))\,dx\leq A^n\sum_{i=1}^{\mathrm{I}(h)}\Delta x_i\Phi\Big(\frac{1}{\Delta x_i}\int_{\Lambda_i^h}c^{in}(x)dx\Big)+B\frac{A^n-1}{A-1}$$

$$\leq A^n\mathcal{I} + B\frac{A^n - 1}{A - 1} < \infty, \quad \text{for all} \quad t \in [0, T]. \tag{2.42}$$

Thus, applying Dunford-Pettis theorem, the sequence (c^h) is said to be weakly compact in L^1. Also, it is evenly bounded with respect to h and Δt, condition (2.22) is satisfied which ensures the existence of a subsequence of (c^h) converges weakly to $c \in L^1((0, T)\times (0, R))$ as $h \to 0$. □

Now, the time has come for proving the weak convergence of sequence c_i^n that is made by a sequence of step functions c^h. In order to do so, some point approximations (converge pointwise) are used which are defined as a midpoint, right endpoint and left endpoint approximations as

$$X^h : x \in (0, R) \to X^h(x) = \sum_{i=1}^{\mathrm{I}(h)} x_i \chi_{\Lambda_i^h}(x), \tag{2.43}$$

$$\Xi^h : x \in (0, R) \to \Xi^h(x) = \sum_{i=1}^{\mathrm{I}(h)} x_{i+1/2} \chi_{\Lambda_i^h}(x), \tag{2.44}$$

and

$$\xi^h : x \in (0, R) \to \xi^h(x) = \sum_{i=1}^{\mathrm{I}(h)} x_{i-1/2} \chi_{\Lambda_i^h}(x), \tag{2.45}$$

respectively. Now, we have assembled all the results required to justify Theorem 2.4.1. In order to prove this, we are considering a test function $\varphi \in C^1([0, T]\times]0, R])$ having compact support with respect to t in $[0, t_{N-1}]$ for small Δt. Formalize the finite volume for time variable and left endpoint approximation for space variable of φ on $\tau_n \times \Lambda_i^h$ by

$$\varphi_i^n = \frac{1}{\Delta t}\int_{t_n}^{t_{n+1}} \varphi(t, x_{i-1/2})dt.$$

Multiply Eq.(2.21) by φ_i^n, taking summation over $n \in \{0, \cdots, N-1\}$ and $i \in \{1, \cdots, \mathrm{I(h)}\}$ give

$$\sum_{n=0}^{N-1}\sum_{i=1}^{\mathrm{I}(h)} \Delta x_i (c_i^{n+1} - c_i^n)\varphi_i^n = \frac{\Delta t}{2}\sum_{n=0}^{N-1}\sum_{i=1}^{\mathrm{I}(h)}\sum_{(j,k)\in\lambda^i} K_{j,k} c_j^n c_k^n \Delta x_j \Delta x_k \omega'_{i,j,k}\varphi_i^n$$

$$
\begin{aligned}
&- \Delta t \sum_{n=0}^{N-1} \sum_{i=1}^{\mathrm{I}(h)} \sum_{j=1}^{\mathrm{I}(h)} K_{i,j} c_i^n c_j^n \Delta x_i \Delta x_j \varphi_i^n \\
&+ \Delta t \sum_{n=0}^{N-1} \sum_{i=1}^{\mathrm{I}(h)} \varphi_i^n \sum_{k=i}^{\mathrm{I}(h)} S_k c_k^n \Delta x_k \int_{x_{i-1/2}}^{p_k^i} B(x, x_k) dx \\
&- \sum_{n=0}^{N-1} \sum_{i=1}^{\mathrm{I}(h)} S_i c_i^n \omega_{i,j} \varphi_i^n \Delta t. \qquad (2.46)
\end{aligned}
$$

Splitting the summation for n, the left-hand side (LHS) comes in the following way

$$
\sum_{n=0}^{N-1} \sum_{i=1}^{\mathrm{I}(h)} \Delta x_i (c_i^{n+1} - c_i^n) \varphi_i^n = \sum_{n=0}^{N-1} \sum_{i=1}^{\mathrm{I}(h)} \Delta x_i c_i^{n+1} (\varphi_i^{n+1} - \varphi_i^n) + \sum_{i=1}^{\mathrm{I}(h)} \Delta x_i c_i^{in} \varphi_i^0.
$$

Now, evaluating the LHS of the above equation in relation to the function c^h provides

$$
\begin{aligned}
\sum_{n=0}^{N-1} \sum_{i=1}^{\mathrm{I}(h)} \Delta x_i (c_i^{n+1} - c_i^n) \varphi_i^n &= \sum_{n=0}^{N-1} \sum_{i=1}^{\mathrm{I}(h)} \int_{\tau_{n+1}} \int_{\Lambda_i^h} c^h(t,x) \frac{\varphi(t, \xi^h(x)) - \varphi(t - \Delta t, \xi^h(x))}{\Delta t} dx\, dt \\
&\quad + \sum_{i=1}^{\mathrm{I}(h)} \int_{\Lambda_i^h} c^h(0,x) \frac{1}{\Delta t} \int_0^{\Delta t} \varphi(t, \xi^h(x)) dt\, dx \\
&= \int_{\Delta t}^{T} \int_0^{\mathbb{R}} c^h(t,x) \frac{\varphi(t, \xi^h(x)) - \varphi(t - \Delta t, \xi^h(x))}{\Delta t} dx\, dt \\
&\quad + \int_0^{\mathbb{R}} c^h(0,x) \frac{1}{\Delta t} \int_0^{\Delta t} \varphi(t, \xi^h(x)) dt\, dx.
\end{aligned}
$$

Since, $\varphi \in C^1([0,T] \times]0,R])$ posseses compact support and having bounded derivative

$$
\frac{1}{\Delta t} \int_0^{\Delta t} \varphi(t, \xi^h(x)) dt \to \varphi(0,x)
$$

uniformly with respect to t, x as $\max\{h, \Delta t\} \to 0$ and $c^h(0,x) \to c^{in}$ in $L^1(0,R)$. As a result, we use Lemma 2.1.5 to achieve the following term

$$
\int_0^R c^h(0,x) \frac{1}{\Delta t} \int_0^{\Delta t} \varphi(t, \xi^h(x)) dt dx \to \int_0^R c^{in}(x) \varphi(0,x) dx \qquad (2.47)
$$

as $\max\{h, \Delta t\}$ goes to 0. Further, using the expansion of the smooth function φ through Taylor series implies that

$$
\frac{\varphi(t, \xi^h(x)) - \varphi(t - \Delta t, \xi^h(x))}{\Delta t} \to \frac{\partial \varphi}{\partial t}(t,x)
$$

uniformly as $\max\{h, \Delta t\} \to 0$. Lemma 2.1.5 and Proposition 2.4.5 ensure that for $\max\{h, \Delta t\} \to 0$

$$\int_0^T \int_0^R c^h(t,x) \frac{\varphi(t, \xi^h(x)) - \varphi(t - \Delta t, \xi^h(x))}{\Delta t} dx\, dt \to \int_0^T \int_0^R c(t,x) \frac{\partial \varphi}{\partial t}(t,x) dx\, dt.$$

Hence, for $\max\{h, \Delta t\} \to 0$,

$$\begin{aligned} &\int_{\Delta t}^T \int_0^R \underbrace{c^h(t,x) \frac{\varphi(t, \xi^h(x)) - \varphi(t - \Delta t, \xi^h(x))}{\Delta t}}_{c(\varphi)} dx\, dt \\ &= \int_0^T \int_0^R c(\varphi)\, dx\, dt - \int_0^{\Delta t} \int_0^R c(\varphi)\, dx\, dt \to \int_0^T \int_0^R c(t,x) \frac{\partial \varphi}{\partial t}(t,x) dx\, dt. \quad (2.48) \end{aligned}$$

Now, to deal with the first term on the RHS of Eq. (2.46), applying the condition $\frac{x_j + x_k}{x_i} = 1 \pm \mathcal{O}(h)$ and by following [[59], Proposition 2.1.] yield

$$\begin{aligned} &\frac{\Delta t}{2} \sum_{n=0}^{N-1} \sum_{i=1}^{\mathrm{I}(h)} \sum_{(j,k) \in \lambda^i} \underbrace{K_{j,k} c_j^n c_k^n \Delta x_j \Delta x_k \varphi_i^n (1 \pm \mathcal{O}(h))}_{\Im_{j,k}} \\ &\quad = \frac{\Delta t}{2} \sum_{n=0}^{N-1} \sum_{i=1}^{\mathrm{I}(h)} \sum_{j=1}^{i} \Big(\sum_{k=\Pi_{i-1,j}}^{\Pi_{i,j}} \Im_{j,k} + \sum_{k=\Pi_{i,j}+1}^{\Gamma_{i,j}} \Im_{j,k} - \sum_{k=\Pi_{i-1,j}+1}^{\Gamma_{i-1,j}} \Im_{j,k} \Big) \\ &\quad = \frac{1}{2} \sum_{n=0}^{N-1} \sum_{i=1}^{\mathrm{I}(h)} \int_{\tau_n} \int_{\Lambda_i^h} \int_0^x K^h(y, x-y) c^h(t,y) c^h(t, x-y) \varphi(t, \xi^h(x)) dy\, dx\, dt. \end{aligned}$$

Again, using the Lemma 2.1.5 and Proposition 2.4.5 lead to

$$\begin{aligned} &\frac{1}{2} \sum_{n=0}^{N-1} \sum_{i=1}^{\mathrm{I}(h)} \int_{\tau_n} \int_{\Lambda_i^h} \int_0^x K^h(y, x-y) c^h(t,y) c^h(t, x-y) \varphi(t, \xi^h(x)) dy\, dx\, dt \\ &\qquad \to \frac{1}{2} \int_0^T \int_0^R \int_0^x K(y, x-y) c(t,y) c(t, x-y) \varphi(t,x) dy\, dx\, dt, \quad (2.49) \end{aligned}$$

as $\max\{h, \Delta t\} \to 0$. Dealing with the second term on the RHS of Eq.(2.46), as $\max\{h, \Delta t\} \to 0$,

$$\begin{aligned} &\Delta t \sum_{n=0}^{N-1} \sum_{i=1}^{\mathrm{I}(h)} \sum_{j=1}^{\mathrm{I}(h)} K_{i,j} c_i^n c_j^n \Delta x_i \Delta x_j \varphi_i^n \\ &\qquad = \sum_{n=0}^{N-1} \sum_{i=1}^{\mathrm{I}(h)} \sum_{j=1}^{\mathrm{I}(h)} \int_{\tau_n} \int_{\Lambda_i^h} \int_{\Lambda_j^h} K^h(x,y) c^h(t,x) c^h(t,y) \varphi(t, \xi^h(x)) dy\, dx\, dt \end{aligned}$$

$$\to \int_0^T \int_0^R \int_0^R K(x,y)c(t,x)c(t,y)\varphi(t,x)dy\,dx\,dt. \tag{2.50}$$

Finally, some simplifications in the third and fourth terms on the RHS of Eq.(2.46) by using (2.20) provide

$$\begin{aligned}
&\Delta t \sum_{n=0}^{N-1}\sum_{i=1}^{\mathrm{I}(h)} \varphi_i^n \sum_{k=i}^{\mathrm{I}(h)} S_k c_k^n \Delta x_k \int_{x_{i-1/2}}^{p_k^i} B(x,x_k)dx - \sum_{n=0}^{N-1}\sum_{i=1}^{\mathrm{I}(h)} S_i c_i^n \omega_{i,j}\varphi_i^n \Delta t \\
&= \sum_{n=0}^{N-1}\sum_{i=1}^{\mathrm{I}(h)} \int_{\tau_n}\int_{\Lambda_i^h} \frac{1}{\Delta s}\int_{t_n}^{t_{n+1}} \varphi(s,\xi^h(x))ds\Big[\sum_{k=i+1}^{\mathrm{I}(h)} \int_{\Lambda_k^h} S^h(y)c^h(t,y)\frac{1}{\Delta x_i}\int_{\Lambda_i^h} B(r,X^h(y))dr\,dy\Big]dx\,dt \\
&- \sum_{n=0}^{N-1}\sum_{i=1}^{\mathrm{I}(h)} \int_{\tau_n}\int_{\Lambda_i^h} \frac{\sum_{j=1}^{i-1}\int_{\Lambda_j^h} X^h(r)B(X^h(r),X^h(x))dr}{X^h(x)} S^h(x)c^h(t,x)\frac{1}{\Delta s}\int_{t_n}^{t_{n+1}} \varphi(s,\xi^h(x))ds\,dx\,dt.
\end{aligned}$$

Again using Lemma 2.1.5, Proposition 2.4.5 and the fact that $\frac{\int_0^x rB(r,x)\,dr}{x} = 1$, one can claim that

$$\begin{aligned}
LHS &= \int_0^T\int_0^R \frac{1}{\Delta s}\int_{t_n}^{t_{n+1}} \varphi(s,\xi^h(x))ds \int_{\Xi^h(x)}^R S^h(y)c^h(t,y)B^h(x,X^h(y))dy\,dx\,dt \\
&- \int_0^T\int_0^R \frac{\int_0^{\xi^h(x)} X^h(r)B(X^h(r),X^h(x))dr}{X^h(x)} S^h(x)c^h(t,x)\frac{1}{\Delta s}\int_{t_n}^{t_{n+1}} \varphi(s,\xi^h(x))ds\,dx\,dt. \\
&\to \int_0^T\int_0^R\int_x^R S(y)c(t,y)B(x,y)\varphi(t,x)dy\,dx\,dt - \int_0^T\int_0^R S(x)c(t,x)\varphi(t,x)dx\,dt
\end{aligned} \tag{2.51}$$

as $\max\{h,\Delta t\} \to 0$. Eq.(2.47)-(2.51) yields the result for the weak convergence as given in (2.24).

2.5 Error Simulation

For estimating the error part, taking a uniform mesh is essential, i.e., $\Delta x_i = h\,\forall i = 1,2,\ldots,\mathrm{I(h)}$. Also, some assumptions are taken on the kernels and initial datum as mentioned in the following theorem.

Theorem 2.5.1. Let the kernels hold $K, B \in W_{loc}^{1,\infty}(\mathbb{R}^+\times\mathbb{R}^+)$, selection rate and initial datum $S, c^{in} \in W_{loc}^{1,\infty}(\mathbb{R}^+)$. Moreover, assume a uniform volume mesh and time step Δt

that fulfill the condition (2.22). Then, the error estimates

$$\|c^h - c\|_{L^\infty(0,T;L^1(0,R))} \leq H(T,R)(h + \Delta t) \tag{2.52}$$

holds, for c being the weak solution to (1.7) and $H(T,R)$ is a constant depending on R and T.

The following estimates on the c^h and c are necessary in order to establish the above theorem.

Proposition 2.5.2. Assume that kinetic parameters $K, B \in L^\infty_{loc}(\mathbb{R}^+ \times \mathbb{R}^+)$, $S \in L^\infty_{loc}(\mathbb{R}^+)$ and the condition (2.22) holds for time step Δt. Also, let the initial datum c^{in} is restricted in L^∞_{loc}. Then, solution c^h and c to (1.7) are essentially bounded in $(0,T) \times (0,R)$ as

$$\|c^h\|_{L^\infty((0,T)\times(0,R))} \leq H(T,R), \quad \|c\|_{L^\infty((0,T)\times(0,R))} \leq H(T,R).$$

Furthermore, if $K, B \in W^{1,\infty}_{loc}(\mathbb{R}^+ \times \mathbb{R}^+)$ and $S, c^{in} \in W^{1,\infty}_{loc}(\mathbb{R}^+)$, then a positive constant $H(T,R)$ exists such that

$$\|c\|_{W^{1,\infty}(0,R)} \leq H(T,R). \tag{2.53}$$

Proof. The aim here is to bound the solution c to the continuous equation (1.7). The discrete case can be handled similar to the non-negativity of c^h. Integrating Eq.(2.6) with respect to t and leaving the negative terms out yield

$$\begin{aligned} c(t,x) &\leq c^{in} + \frac{1}{2}\int_0^t \int_0^x K(y, x-y)c(s,y)c(s,x-y)dy\,ds + \int_0^t \int_x^R B(x,y)S(y)c(s,y)dy\,ds \\ &\leq \underbrace{c^{in}(x) + \|BS\|_{L^\infty}\|c\|_{\infty,1}t}_{\alpha(t)} + \underbrace{\|K\|_{L^\infty}\|c\|_{\infty,1}}_{\beta}\int_0^t \sup_{y\in(0,R)} c(s,y)\,ds, \end{aligned}$$

for $\|c\|_{\infty,1}$ being the norm of c in $L^\infty(0,T;L^1(0,R))$. Subsequently, using Gronwall's lemma and integration by parts to accomplish the proof as

$$\begin{aligned} \sup_{x\in(0,R)} c(t,x) &\leq \alpha(t) + \int_0^t \alpha(s)\beta e^{\int_s^t \beta\,dr}\,ds \\ &\leq \alpha(t) + \beta\Big[\frac{\alpha(s)e^{\beta(t-s)}}{-\beta}\Big|_0^t - \int_0^t \|BS\|_{L^\infty}\|c\|_{\infty,1}\frac{e^{\beta(t-s)}}{-\beta}\,ds\Big] \end{aligned}$$

$$\leq \alpha(0)e^{\beta t} + \frac{\|BS\|_{L^\infty}\|c\|_{\infty,1}}{\beta}[(e^{\beta t}-1)].$$

Therefore,

$$\|c\|_{L^\infty((0,T)\times(0,R))} \leq H(T,R).$$

Now, to establish the relation (2.53), integrating Eq.(2.6) again with respect to t, differentiating with respect to x and then considering the maximum value over the domain of x give

$$\begin{aligned}\left\|\frac{\partial c}{\partial x}(x)\right\|_{L^\infty} \leq \left\|\frac{\partial c^{in}}{\partial x}\right\|_{L^\infty} + \Big\{&\frac{1}{2}\|K\|_{L^\infty}\|c\|^2_{L^\infty} + 2\|K\|_{W^{1,\infty}}\|c\|_{L^\infty}\|c\|_{\infty,1}R + \|BS\|_{L^\infty}\|c\|_{L^\infty}\\ &+ 2\|B\|_{W^{1,\infty}}\|S\|_{L^\infty}\|c\|_{\infty,1}R + \|S\|_{W^{1,\infty}}\|c\|_{L^\infty}\Big\}t\\ &+ (2\|K\|_{L^\infty}\|c\|_{\infty,1}R + \|S\|_{L^\infty})\int_0^t \left\|\frac{\partial c}{\partial x}\right\|_{L^\infty} ds.\end{aligned}$$

Applying Gronwall's lemma as used in priori boundedness of c accomplishes the result.

□

The discrete coagulation and fragmentation terms given as in (2.21) expressed like

$$\mathbb{C}(c_i) = \frac{1}{2\Delta x_i}\sum_{j=1}^{i-1} K_{j,i-j}c_j^n c_{i-j}^n \Delta x_j \Delta x_{i-j} - \frac{1}{\Delta x_i}\sum_{j=1}^{\mathrm{I}(h)} K_{i,j}c_i^n c_j^n \Delta x_i \Delta x_j, \tag{2.54}$$

and

$$\mathbb{F}(c_i) = \frac{1}{\Delta x_i}\sum_{k=i}^{\mathrm{I}(h)} S_k c_k^n \Delta x_k \int_{x_{i-1/2}}^{p_k^i} B(x,x_k)dx - \frac{\sum_{j=1}^{i} x_j \int_{x_{j-1/2}}^{p_i^j} B(x,x_i)dx}{x_i} S_i c_i^n, \tag{2.55}$$

respectively, for a uniform mesh. The following lemma yields the continuous version of the above discrete terms.

Lemma 2.5.3. Consider the initial condition $c^{in} \in W^{1,\infty}_{loc}$ and uniform mesh, $\Delta x_i = h$ $\forall i$. Also assuming that K, B and S follow the conditions $K, B, S \in W^{1,\infty}_{loc}$. Let $(s,x) \in \tau_n \times \Lambda_i^h$, where $n \in \{0,1,\cdots,N-1\}, i \in \{1,2,\cdots,\mathrm{I}(h)\}$. Then

$$\mathbb{C}(c_i) = \frac{1}{2}\int_0^{\xi^h(x)} K^h(x', x-x')c^h(s,x')c^h(s,x-x')\,dx' - \int_0^R K^h(x,x')c^h(s,x)c^h(s,x')\,dx', \tag{2.56}$$

$$\mathbb{F}(c_i) = \int_{\Xi^h(x)}^{R} S^h(x^{'})B^h(x,x^{'})c^h(s,x^{'})\,dx^{'} - S^h(x)c^h(s,x) + \varepsilon(\mathbb{F},h), \tag{2.57}$$

where $\varepsilon(\mathbb{F},h)$ expresses the first-order term concerning h within L^1 framework,

$$\|\varepsilon(\mathbb{F},h)\|_{L^1} \leq \frac{R}{2}\|BS\|_{L^\infty}\|c^h\|_{\infty,1}h. \tag{2.58}$$

Proof. First, start with discrete coagulation term (2.54) to change into a continuous form using a uniform mesh and having $x \in \Lambda_i^h$,

$$\begin{aligned}
&\frac{1}{2\Delta x_i}\sum_{j=1}^{i-1} K_{j,i-j}c_j^n c_{i-j}^n \Delta x_j \Delta x_{i-j} - \frac{1}{\Delta x_i}\sum_{j=1}^{\mathrm{I}(h)} K_{i,j}c_i^n c_j^n \Delta x_i \Delta x_j \\
&\quad = \frac{1}{2}\int_0^{\xi^h(x)} K^h(x^{'},x-x^{'})c^h(s,x^{'})c^h(s,x-x^{'})\,dx' - \int_0^R K^h(x,x^{'})c^h(s,x)c^h(s,x^{'})\,dx^{'}.
\end{aligned}$$

Now, moving to equation (2.55), the following continuous expression is obtained by using the fact that $\omega_{i,j} = 1 + \mathcal{O}(h^2)$, see [57], and $(s,x) \in \tau_n \times \Lambda_i^h$

$$\begin{aligned}
&\frac{1}{\Delta x_i}\sum_{k=i}^{\mathrm{I}(h)} S_k c_k^n \Delta x_k \int_{x_{i-1/2}}^{p_k^i} B(x,x_k)dx - \frac{\sum_{j=1}^{i} x_j \int_{x_{j-1/2}}^{p_i^j} B(x,x_i)dx}{x_i} S_i c_i^n \\
&= \sum_{k=i+1}^{\mathrm{I}(h)} S_k c_k^n \Delta x_k \frac{1}{\Delta x_i}\int_{x_{i-1/2}}^{x_{i+1/2}} B(x,x_k)dx + S_i c_i^n \int_{x_{i-1/2}}^{x_i} B(x,x_i)\,dx - (1+\mathcal{O}(\Delta {x_i}^2))S_i c_i^n \\
&\qquad = \int_{\Xi^h(x)}^{R} S^h(x^{'})B^h(x,x^{'})c^h(s,x^{'})\,dx^{'} - S^h(x)c^h(s,x) + \varepsilon(\mathbb{F},h)
\end{aligned}$$

where $\varepsilon(\mathbb{F},h) = S_i c_i^n \int_{x_{i-1/2}}^{x_i} B(x,x_i)\,dx$. Calculating the L^1 norm of $\varepsilon(\mathbb{F},h)$ leads to

$$\begin{aligned}
\|\varepsilon(\mathbb{F},h)\|_{L^1} &\leq \|BS\|_{L^\infty}\sum_{i=1}^{\mathrm{I(h)}}\int_{\Lambda_i^h} c_i^n \int_{x_{i-1/2}}^{x_i} dx\,dy \\
&\leq \|BS\|_{L^\infty}\|c^h\|_{\infty,1}\frac{R}{2}h.
\end{aligned}$$

□

Now, to prove the main result Theorem 2.5.1, using Eq. (2.21), (2.56) and (2.57) lead to

$$\frac{\partial c^h(t,x)}{\partial t} = \frac{1}{2}\int_0^{\xi^h(x)} K^h(x^{'},x-x^{'})c^h(s,x^{'})c^h(s,x-x^{'})\,dx' - \int_0^R K^h(x,x^{'})c^h(s,x)c^h(s,x^{'})\,dx^{'}$$

$$+\int_{\Xi^h(x)}^{R} S^h(x^{'})B^h(x,x^{'})c^h(s,x^{'})\,dx^{'} - S^h(x)c^h(s,x) + \varepsilon(\mathbb{F},h). \tag{2.59}$$

Finally, from Eq.(1.7) and Eq.(2.59), we get the error formulation for $t \in \tau_n$ as

$$\int_0^R |c^h(t,x) - c(t,x)|dx \leq \int_0^R |c^h(0,x) - c(0,x)|dx + \sum_{\beta=1}^{3}[\epsilon_\beta(\mathbb{C},h) + \epsilon_\beta(\mathbb{F},h)]$$
$$+\int_0^R |\epsilon(t,n)|\,dx + \|\varepsilon(\mathbb{F},h)\|_{L^1}t, \tag{2.60}$$

where error terms are expressed by $\epsilon_\beta(\mathbb{C},h)$ for $\beta = 1,2,3$ related to the coagulation part as

$$\epsilon_1(\mathbb{C},h) = \frac{1}{2}\int_0^t\int_0^R\int_0^{\xi^h(x)} |K^h(x^{'},x-x^{'})c^h(s,x^{'})c^h(s,x-x^{'})$$
$$-K(x^{'},x-x^{'})c(s,x^{'})c(s,x-x^{'})|\,dx^{'}\,dx\,ds,$$

$$\epsilon_2(\mathbb{C},h) = \frac{1}{2}\int_0^t\int_0^R\int_{\xi^h(x)}^{x} K(x^{'},x-x^{'})c(s,x^{'})c(s,x-x^{'})\,dx^{'}\,dx\,ds,$$

and

$$\epsilon_3(\mathbb{C},h) = \int_0^t\int_0^R\int_0^R |K^h(x,x^{'})c^h(s,x)c^h(s,x^{'}) - K(x,x^{'})c(s,x)c(s,x^{'})|\,dx^{'}\,dx\,ds.$$

While error terms due to the fragmentation part are expressed by $\epsilon_\beta(\mathbb{F},h)$ for $\beta = 1,2,3$ as

$$\epsilon_1(\mathbb{F},h) = \int_0^t\int_0^R\int_{\Xi^h(x)}^R |S^h(x^{'})B^h(x,x^{'})c^h(s,x^{'}) - S(x^{'})B(x,x^{'})c(s,x^{'})|\,dx^{'}\,dx\,ds,$$

$$\epsilon_2(\mathbb{F},h) = \int_0^t\int_0^R\int_x^{\Xi^h(x)} S(x^{'})B(x,x^{'})c(s,x^{'})\,dx^{'}\,dx\,ds,$$

and

$$\epsilon_3(\mathbb{F},h) = \int_0^t\int_0^R |S^h(x)c^h(s,x) - S(x)c(s,x)|\,dx\,ds.$$

Additionally, due to time discretization, considering $|t-t_n| \leq \Delta t$ yields

$$\int_0^R |\epsilon(t,n)|\,dx \leq \frac{1}{2}\int_{t_n}^t\int_0^R\int_0^{\xi^h(x)} K^h(x^{'},x-x^{'})c^h(s,x^{'})c^h(s,x-x^{'})\,dx^{'}\,dx\,ds$$

$$+\int_{t_n}^{t}\int_0^R\int_0^R K^h(x,x^{'})c^h(s,x)c^h(s,x^{'})\,dx^{'}\,dx\,ds$$
$$+\int_{t_n}^{t}\int_0^R\int_{\Xi^h(x)}^R S^h(x^{'})B^h(x,x^{'})c^h(s,x^{'})\,dx^{'}\,dx\,ds$$
$$+\int_{t_n}^{t}\int_0^R S^h(x)c^h(s,x)\,dx\,ds+\int_{t_n}^{t}\int_0^R \varepsilon(\mathbb{F},h)\,dx\,ds.$$

Given K, B and $S \in W^{1,\infty}_{loc}$, we have for all $x, y \in (0, R)$

$$|K^h(x,y)-K(x,y)| \le \|K\|_{W^{1,\infty}}h.$$

Thus, it provides the estimation of $\epsilon_1(\mathbb{C},h)$ using the L^∞ bound on c^h and c as in [50]. Firstly, the change of variable $z = x - x^{'}$ is executed and then splitting the expression into three parts

$$\epsilon_1(\mathbb{C},h) \le \frac{1}{2}\int_0^t\int_0^R\int_0^R |K^h(x^{'},z)-K(x^{'},z)|c(s,x^{'})c(s,z)\,dx^{'}\,dz\,ds$$
$$+\frac{1}{2}\int_0^t\int_0^R\int_0^R K^h(x^{'},z)|c^h(s,x^{'})-c(s,x^{'})|c(s,z)\,dx^{'}\,dz\,ds$$
$$+\frac{1}{2}\int_0^t\int_0^R\int_0^R K^h(x^{'},z)c^h(s,x^{'})|c^h(s,z)-c(s,z)|\,dx^{'}\,dz\,ds.$$

By simplifying and using Proposition 2.5.2, the above can be reduced to

$$\epsilon_1(\mathbb{C},h) \le \frac{1}{2}tR^2\|c\|_\infty^2\|K\|_{W^{1,\infty}}h+\frac{R}{2}\|K\|_\infty(\|c\|_\infty+\|c^h\|_\infty)\int_0^t \|c^h(s)-c(s)\|_{L^1}\,ds. \tag{2.61}$$

A similar estimates can also be obtained for $\epsilon_3(\mathbb{C},h)$, $\epsilon_1(\mathbb{F},h)$ and $\epsilon_3(\mathbb{F},h)$ utilizing the above explanation as

$$\epsilon_3(\mathbb{C},h) \le tR^2\|K\|_{W^{1,\infty}}\|c\|_\infty^2h+R\|K\|_\infty(\|c\|_\infty+\|c^h\|_\infty)\int_0^t \|c^h(s)-c(s)\|_{L^1}\,ds, \tag{2.62}$$

$$\epsilon_1(\mathbb{F},h) \le tR^2\|c\|_\infty(\|B\|_\infty\|S\|_{W^{1,\infty}}+\|S\|_\infty\|B\|_{W^{1,\infty}})h+R\|BS\|_\infty\int_0^t \|c^h(s)-c(s)\|_{L^1}\,ds, \tag{2.63}$$

and

$$\epsilon_3(\mathbb{F},h) \leq \|c\|_\infty \|S\|_{W^{1,\infty}} tRh + \|S\|_\infty \int_0^t \|c^h(s) - c(s)\|_{L^1}\, ds. \tag{2.64}$$

Now, moving to the remaining terms $\epsilon_2(\mathbb{C},h)$ and $\epsilon_2(\mathbb{F},h)$, it seems easy to notice that

$$\epsilon_2(\mathbb{C},h) \leq \frac{tR^2}{4}\|K\|_\infty \|c\|_\infty^2 h, \tag{2.65}$$

and

$$\epsilon_2(\mathbb{F},h) \leq \frac{tR}{2}\|BS\|_\infty \|c\|_\infty h. \tag{2.66}$$

Finally, the error caused by the time discretization is dealt and bound is obtained as

$$\int_0^R |\epsilon(t,n)|\, dx \leq \Big(\frac{3}{2}\|K\|_\infty \|c^h\|_\infty^2 R^2 + (\|B\|_\infty R + 1)\|S\|_\infty \|c^h\|_\infty R + \|\varepsilon(\mathbb{F},h)\|_{L^1}\Big)\Delta t. \tag{2.67}$$

Substituting all the bound estimations from Eq.(2.61)-(2.67) in Eq.(2.60) and using Gronwall's lemma provide the order of error as in (2.52), i.e.,

$$\|c^h - c\|_{L^\infty(0,T;L^1(0,R))} \leq H(T,R)(h + \Delta t)$$

to complete the proof.

2.6 Numerical Results

The CMBE for two test cases, consisting of a constant and sum coagulation kernel ($K(x,y) = 1, x+y$) with linear and quadratic selection functions ($S(x) = x, x^2$), is used to prove the mathematical results on error analysis numerically. In all the cases, breakage function $B(x,y) = \frac{\alpha+2}{y}\left(\frac{x}{y}\right)^\alpha$, $\alpha = -1/2$ and the initial condition $c(x,0) = e^{-x}$ are considered. Since, analytical solutions are not available for such cases, experimental order of convergence (EOC) on uniform mesh is computed using the numerical simulations. The EOC can be computed numerically using the following expression

$$EOC = \ln\left(\frac{\|N^{num}_{\mathrm{I}(h)} - N^{num}_{\mathrm{2I}(h)}\|}{\|N^{num}_{\mathrm{2I}(h)} - N^{num}_{\mathrm{4I}(h)}\|}\right) / \ln(2), \tag{2.68}$$

where, the total number of particles created by the Finite volume scheme (2.21) with a mesh of $\mathrm{I}(h)$ number of cells is denoted by $N^{num}_{\mathrm{I}(h)}$. For the simulations computational domain [$1e^{-3}$,10] and time $t = 100$ are taken. As expected from mathematical results first order error estimates is noticed in all the examples. It should be also mentioned the EOC is computed for several other values of α, K and S . However, similar observations are marked in all the cases. Therefore, results are omitted here.

Test Case 1: Consider the constant coagulation kernel,i.e., $K(x, y) = 1$ with selection function $S(x) = x, x^2$. The numerical EOC for uniform meshes is shown in Table 2.1. It is clear from the table that the FVS produces first-order convergence.

$S(x) = x$		
Cells	Error	EOC
30	-	-
60	1.0295	-
120	0.1489	0.8714
240	0.0111	0.9850
480	0.0022	0.9988

$S(x) = x^2$		
Cells	Error	EOC
30	-	-
60	0.0358	-
120	0.0094	0.9884
240	0.0012	0.9953
480	0.0001	0.9990

Table 2.1: EOC for Test Case 1

Test Case 2: Now, we assume sum coagulation kernel,i.e., $K(x, y) = x+y$ with selection functions $S(x) = x, x^2$. The error and EOC of the scheme are reported in Table 2.2, and again it is observed that the EOC is 1 for the finite volume scheme for a CMBE.

$S(x) = x$		
Cells	Error	EOC
30	-	-
60	1.2652	-
120	0.2495	0.8721
240	0.0342	0.9713
480	0.0054	0.9952

$S(x) = x^2$		
Cells	Error	EOC
30	-	-
60	0.0677	-
120	0.0194	0.9606
240	0.0026	0.9794
480	0.0006	0.9949

Table 2.2: EOC for Test Case 2

Chapter 3

Finite Volume Scheme for Coagulation-Fragmentation Equation with Singular Rates

---

Bourgade et al. [50] considered the binary coagulation and binary fragmentation equation and showed the convergence analysis for locally bounded kernels using the compactness method. Additionally, they proved the first-order error estimation for the finite volume scheme when kernels belong to $W_{loc}^{1,\infty}$.

The motivation for this chapter is the study of their extension. Hence, here we discuss the weak convergence analysis for the binary coagulation and multiple fragmentation equation (1.7) having the singular breakage kernel. In addition, the error analysis is demonstrated when kernels belong to space $W_{loc}^{1,\infty}$. It is important to mention that the finite volume method is deployed on the non-conservative divergence form of the equation.

The chapter is organized as follows. The non-conservative formulation of the combined coagulation and multiple fragmentation equations is discussed in Section 3.1 together with the numerical approximations. Further in Section 3.2, the main result of

convergence analysis is explained for the approximated solutions using the weak compactness argument. Section 3.3 deals with the first-order error estimation theoretically for a uniform mesh which is verified numerically in Section 3.4.

3.1 Non-conservative Formulation

Thanks to the Leibniz integral rule, CMBE (1.7) for continuous coagulation-multiple fragmentation processes can be written in divergence form in terms of the mass density $xc(t,x)$ as

$$\frac{x\partial c(t,x)}{\partial t} = -\frac{\partial \mathcal{C}(c)(t,x)}{\partial x} + \frac{\partial \mathcal{F}(c)(t,x)}{\partial x}, \quad (t,x) \in \mathbb{R}^2_{>0} :=]0,\infty[^2 \tag{3.1}$$

where the continuous fluxes are being taken as

$$\mathcal{C}(c)(t,x) := \int_0^x \int_{x-u}^{\infty} uK(u,v)c(t,u)c(t,v)dvdu, \tag{3.2}$$

for aggregation and for the breakage, the following form is obtained

$$\mathcal{F}(c)(t,x) := \int_0^x \int_x^{\infty} uB(u,v)S(v)c(t,v)dvdu. \tag{3.3}$$

Similar to the previous chapter, the following assumptions on kinetic parameters are taken

$$K \in L^{\infty}_{\text{loc}}(\mathbb{R}_{>0} \times \mathbb{R}_{>0}), \tag{3.4}$$

$$S \in L^{\infty}_{\text{loc}}(\mathbb{R}_{>0}) \text{ and } S(x) = x^{1+\alpha}, \tag{3.5}$$

and

$$B(x,y) = \frac{\alpha+2}{y}\left(\frac{x}{y}\right)^{\alpha}, \text{ for } 0 < x < y, \tag{3.6}$$

where $\alpha \in (-1, 0]$. Now, in the next subsection, a numerical method to solve the equation (3.1) is described. For this a finite volume approximation [54] is taken for the volume variable x while an explicit Euler method is used to discretize the time variable t.

3.1.1 Numerical approximation

In order to consider the more realistic case, in this section, the coagulation part is truncated non-conservatively as

$$\mathcal{C}^R_{nc}(c)(t,x) := \int_0^x \int_{x-u}^{R} uK(u,v)c(t,u)c(t,v)dvdu \tag{3.7}$$

by replacing ∞ for a positive real constant R in the equation (3.2). While for the breakage, using R, equation (3.3) leads to a conservative approximation as

$$\mathcal{F}_c^R(c)(t,x) := \int_0^x \int_x^R uB(u,v)S(v)c(t,v)dvdu. \tag{3.8}$$

Thus, the coupled non-conservative form of the truncation is governed by

$$\begin{cases} x\frac{\partial c}{\partial t} = -\frac{\partial \mathcal{C}_{nc}^R(c)}{\partial x} + \frac{\partial \mathcal{F}_c^R(c)}{\partial x}, & (t,x) \in \mathbb{R}_{>0}\times]0,R]; \\ \\ c(0,x) = c^{in}(x), & x \in]0,R]. \end{cases} \tag{3.9}$$

Such truncation is chosen so that it enables for the simulation of gelation phenomena. Although, it depends on mainly the higher rate of kernels K and B, it should be mentioned here that flux (3.7) leads to the decrease in total mass in the system while expression (3.8) yields the total mass conservation. One can easily verify these by having

$$\frac{d}{dt}\int_0^R xc(t,x)dx = -\mathcal{C}_{nc}^R(c)(t,R) \leq 0$$

in case of pure coagulation and

$$\frac{d}{dt}\int_0^R xc(t,x)dx = 0$$

for the pure breakage case.

Now, to apply the numerical scheme and to discretize the volume variable of the equation (3.9), consider a partitioning of the truncated computational range $(0,R]$ into tiny cells $\Lambda_i^h =]x_{i-1/2}, x_{i+1/2}]$, $i = 0,1,2,...,\mathrm{I}^h$, where $x_{-1/2} = 0$, $x_{\mathrm{I}^h+1/2} = R$, $\Delta x_i = x_{i+1/2} - x_{i-1/2} \leq h$ for $0 < h < 1$. For integers i and j, let us introduce $x_{i+1/2} - x_j \in \Lambda_{\gamma_{i,j}}^h$, where $\gamma_{i,j} \in \{0,\ldots,\mathrm{I}^h\}$.

For non-uniform mesh, introduce $\delta_h = \min \Delta x_i$ and consider a positive constant L as

$$\frac{h}{\delta_h} \leq L, \tag{3.10}$$

while for the uniform mesh, i.e., $\Delta x_i = h \,\forall\, i$, one obtains that $x_{i-1/2} = ih$ and $\gamma_{i,j} = i-j$. Further, for discretizing the time variable t, assuming Δt being the time step and truncated

time domain $[0, T]$, we have $T = \Delta t N$ for a large $N \in \mathbb{N}$. Consider $\tau_n := [t_n, t_{n+1}[$ as a time interval having $t_n = n\Delta t,\ n \geq 0$.

By having the above discretizations for volume variable x and time t, let us begin with the study of FVS for the Eq.(3.9). Consider c_i^n as an approximation of $c(t, x)$ in i^{th} cell at $t \in \tau_n$. Further, for the kinetic parameters K, B, and S, for the time being, assume the discretized form as $K(u, v) \approx K^h(u, v) = K_{j,i}$, $S(v) \approx S^h(v) = S_i$ and $B(u, v) \approx B^h(u, v) = B_{j,i}$ for $v \in \Lambda_i^h$ and $u \in \Lambda_j^h$.

The following equation is obtained by integrating Eq.(3.9) with respect to x and t

$$\int_{t_n}^{t_{n+1}} \int_{x_{i-1/2}}^{x_{i+1/2}} \frac{\partial(xc(t,x))}{\partial t} dx\, dt = -\int_{t_n}^{t_{n+1}} \int_{x_{i-1/2}}^{x_{i+1/2}} \frac{\partial \mathcal{C}_{nc}^R(c)(t,x)}{\partial x} dx\, dt + \int_{t_n}^{t_{n+1}} \int_{x_{i-1/2}}^{x_{i+1/2}} \frac{\partial \mathcal{F}_c^R(c)(t,x)}{\partial x} dx\, dt.$$

Simplifying the above equation leads to the following discretized formulation

$$\Delta x_i x_i (c_i^{n+1} - c_i^n) = -\Delta t \left(\mathcal{C}_{i+1/2}^n - \mathcal{C}_{i-1/2}^n\right) + \Delta t \left(\mathcal{F}_{i+1/2}^n - \mathcal{F}_{i-1/2}^n\right) \tag{3.11}$$

where $\mathcal{C}_{i+1/2}^n$ and $\mathcal{F}_{i+1/2}^n$ are the approximations of continuous fluxes $\mathcal{C}_{nc}^R(c)(x)$ and $\mathcal{F}_c^R(c)(x)$. Therefore, these are computed as

$$\begin{aligned}
\mathcal{C}_{nc}^R(c)(x_{i+1/2}) &= \int_0^{x_{i+1/2}} \int_{x_{i+1/2}-u}^{R} uK(u,v)c(u)c(v)dv\, du \\
&= \sum_{j=0}^{i} \int_{\Lambda_j^h} uc(u) \sum_{K=\gamma_{i,j}}^{\mathrm{I}^h} \int_{\Lambda_k^h} K(u,v)c(v)dv\, du \\
&\approx \sum_{j=0}^{i} \sum_{k=\gamma_{i,j}}^{\mathrm{I}^h} x_j K_{j,k} c_j^n c_k^n \Delta x_j \Delta x_k := \mathcal{C}_{i+1/2}^n.
\end{aligned} \tag{3.12}$$

Similarly, for the breakage,

$$\begin{aligned}
\mathcal{F}_c^R(c)(x_{i+1/2}) &= \int_0^{x_{i+1/2}} \int_{x_{i+1/2}}^{R} uB(u,v)S(v)c(v)dv\, du \\
&= \sum_{j=0}^{i} \int_{\Lambda_j^h} \sum_{k=i+1}^{\mathrm{I}^h} \int_{\Lambda_k^h} uS(v)c(v)B(u,v)dv\, du \\
&\approx \sum_{j=0}^{i} \sum_{k=i+1}^{\mathrm{I}^h} x_j S_k B_{j,k} c_k^n \Delta x_k \Delta x_j := \mathcal{F}_{i+1/2}^n.
\end{aligned} \tag{3.13}$$

Also, the initial condition is approximated as

$$c_i^{in} = \frac{1}{\triangle x_i} \int_{\Lambda_i^h} c^{in}(x)dx, \quad i \in \{0, \ldots, \mathrm{I}^h\}.$$

Then a function c^h on $[0,T]\times]0,R]$ is defined as in 2.14 and also noting that

$$c^h(0,\cdot) = \sum_{i=0}^{\mathrm{I}^h} c_i^{in} \chi_{\Lambda_i^h}(\cdot) \to c^{in} \in L^1]0,R] \text{ as } h \to 0.$$

Further, the discrete forms of aggregation, fragmentation and selection functions are taken as defined in Eqs.(2.15-2.17).

3.2 Convergence of Solutions

Below, the main findings of this work, i.e., the sequence of approximated functions converges to a weak solution of the continuous problem (3.9) is discussed.

Theorem 3.2.1. Assume that $c^{in} \in X^+$. Let the kernels K, S and B satisfy, (3.4), (3.5), and (3.6), respectively. Also assuming that under the time step Δt and for a constant $\theta > 0$, the following stability condition

$$C(R,T)\Delta t \leq \theta < 1, \tag{3.14}$$

holds where

$$C(R,T) := \max(M, \alpha+2)\ \max(\|K\|_\infty, 1)\|c^{in}\|_{L^1}\, e^{\eta\|S\|_{L^\infty}T} + R^{1+\alpha}\eta. \tag{3.15}$$

Then through the extraction of a subsequence,

$$c^h \to c \ \text{ in } \ L^\infty(0,T;L^1\,]0,R]),$$

for c being the weak solution to (3.9) on $[0,T]$ with initial condition c^{in}. This implies that, the function $c \geq 0$ satisfies

$$\begin{aligned} &\int_0^T \int_0^R xc(t,x)\frac{\partial\varphi}{\partial t}(t,x)dx\,dt + \int_0^R xc^{in}(x)\varphi(0,x)dx \\ &+ \int_0^T \int_0^R [\mathcal{C}_{nc}^R(t,x) - \mathcal{F}_c^R(t,x)]\frac{\partial\varphi}{\partial x}(t,x)dx\,dt = \int_0^T \mathcal{C}_{nc}^R(t,R)\varphi(t,R)dt \end{aligned} \tag{3.16}$$

for φ being the smooth functions having compact support in $[0,T[\times[0,R]$.

By following the above theorem, the main task here certainly is to establish $(c^h) \rightharpoonup c$ in $L^1(0,R)$ as h and Δt go to zero. The idea is picked from the Dunford-Pettis theorem that provides the guarantee for weak sequential compactness in L^1.

For proving Theorem 3.2.1, it is enough to establish the equiboundedness and the equiintegrability of the family c^h in L^1 as given in (2.25) and (2.26), respectively. Let us begin with the proof of non-negativity and the equiboundedness of the function c^h in the following proposition. In order to proceed this, let us denote $X^h(x) = x_i$ for $x \in \Lambda_i^h$.

Proposition 3.2.2. Let us consider that the stability condition (3.14) holds for the time step Δt. Also, assuming that the growth conditions on kernels satisfy (3.4)-(3.6). Then function $c^h \geq 0$ follows

$$\int_0^R X^h(x)c^h(t,x)dx \leq \int_0^R X^h(x)c^h(s,x)dx \leq \int_0^R X^h(x)c^h(0,x)dx =: \mu_1^{in}, \quad (3.17)$$

where $0 \leq s \leq t \leq T$. Also, the following estimates obtained

$$\int_0^R c^h(t,x)dx \leq \|c^{in}\|_{L^1}\, e^{\eta\|S\|_{L^\infty} t}. \quad (3.18)$$

Proof. The non-negativity and the equiboundedness of the function c^h are shown here by using induction. It is known that $c^h(0) \in L^1]0,R]$ and is non-negative at $t = 0$. Assuming further that $c^h(t^n) \geq 0$ and

$$\int_0^R c^h(t^n,x)dx \leq \|c^{in}\|_{L^1}\, e^{\eta\|S\|_{L^\infty} t^n}. \quad (3.19)$$

Then, our first aim is to prove that $c^h(t^{n+1}) \geq 0$. Firstly, consider the boundary cell with index $i = 0$. By (3.12) and (3.13), we have $\mathcal{C}^n_{i\pm1/2} \geq 0$, $\mathcal{F}^n_{i\pm1/2} \geq 0$. Therefore, in this case, from the equation (3.11) and by using the fluxes at boundaries, we obtain

$$\begin{aligned} x_0 c_0^{n+1} =& x_0 c_0^n - \frac{\Delta t}{\Delta x_0}\mathcal{C}^n_{1/2} + \frac{\Delta t}{\Delta x_0}\mathcal{F}^n_{1/2} \\ \geq& x_0 c_0^n - \frac{\Delta t}{\Delta x_0}\mathcal{C}^n_{1/2} \\ \geq& \left(1 - \Delta t \sum_{k=0}^{\mathrm{I}^h} \Delta x_k K_{0,k} c_k^n\right) x_0 c_0^n. \end{aligned}$$

Now, having the condition on Δt (3.14) and from equation (3.19), the non-negativity of c_0^{n+1} follows. For $i \geq 1$, one has

$$x_i c_i^{n+1} = x_i c_i^n - \frac{\Delta t}{\Delta x_i}\left(\mathcal{C}_{i+1/2}^n - \mathcal{C}_{i-1/2}^n\right) + \frac{\Delta t}{\Delta x_i}\left(\mathcal{F}_{i+1/2}^n - \mathcal{F}_{i-1/2}^n\right).$$

Following the equations (3.12), (3.13) and the non-negativity of $c^h(t^n)$ imply that

$$\begin{aligned}
-\frac{\mathcal{C}_{i+1/2}^n - \mathcal{C}_{i-1/2}^n}{\Delta x_i} =& \frac{1}{\Delta x_i}\Bigg[-\sum_{j=0}^{i}\sum_{k=\gamma_{i,j}}^{\mathrm{I}^h} x_j K_{j,k} c_j^n c_k^n \Delta x_j \Delta x_k + \sum_{j=0}^{i-1}\sum_{k=\gamma_{i-1,j}}^{\mathrm{I}^h} x_j K_{j,k} c_j^n c_k^n \Delta x_j \Delta x_k \Bigg] \\
=& \frac{1}{\Delta x_i}\Bigg[-\sum_{k=\gamma_{i,i}}^{\mathrm{I}^h} x_i K_{i,k} c_i^n c_k^n \Delta x_i \Delta x_k + \sum_{j=0}^{i-1}\sum_{k=\gamma_{i-1,j}}^{\gamma_{i,j}-1} x_j K_{j,k} c_j^n c_k^n \Delta x_j \Delta x_k \Bigg] \\
\geq& -\sum_{k=0}^{\mathrm{I}^h} \Delta x_k K_{i,k} x_i c_k^n c_i^n, \qquad (3.20)
\end{aligned}$$

and

$$\begin{aligned}
\frac{\mathcal{F}_{i+1/2}^n - \mathcal{F}_{i-1/2}^n}{\Delta x_i} =& \frac{1}{\Delta x_i}\Bigg[\sum_{j=0}^{i}\sum_{k=i+1}^{\mathrm{I}^h} x_j S_k B_{j,k} c_k^n \Delta x_j \Delta x_k - \sum_{j=0}^{i-1}\sum_{k=i}^{\mathrm{I}^h} x_j S_k B_{j,k} c_k^n \Delta x_j \Delta x_k \Bigg] \\
=& \frac{1}{\Delta x_i}\Bigg[-\sum_{j=0}^{i-1} x_j S_i B_{j,i} c_i^n \Delta x_i \Delta x_j + \sum_{k=i+1}^{\mathrm{I}^h} x_i S_k B_{i,k} c_k^n \Delta x_k \Delta x_i \Bigg] \\
\geq& -\sum_{j=0}^{i-1} S_i B_{j,i} \Delta x_j x_i c_i^n, \quad \text{as } x_j < x_i \text{ for } j < i. \qquad (3.21)
\end{aligned}$$

By using the above bounds and then the assumptions taken in expressions (3.4), (3.6) and (3.5) lead to

$$\begin{aligned}
x_i c_i^{n+1} \geq& \left(1 - \Delta t\left(\sum_{k=0}^{\mathrm{I}^h} \Delta x_k K_{i,k} c_k^n + \sum_{k=0}^{\mathrm{I}^h} S_i B_{k,i} \Delta x_k\right)\right) x_i c_i^n \\
\geq& \left(1 - \Delta t\left(\|K\|_\infty \sum_{k=0}^{\mathrm{I}^h} \Delta x_k c_k^n + \eta R^{1+\alpha}\right)\right) x_i c_i^n, \quad \text{for} \quad \eta = \frac{\alpha+2}{\alpha+1}.
\end{aligned}$$

Hence, following the stability condition (3.14) on Δt and the L^1 bound (3.19) give $c^h(t^{n+1}) \geq 0$. Further, by summing (3.11) over i and using the fluxes at boundaries, the following time monotonicity result is obtained for the total mass from the non-negativity

of c^h as

$$\sum_{i=0}^{\mathrm{I}^h} \Delta x_i x_i c_i^{n+1} = \sum_{i=0}^{\mathrm{I}^h} \Delta x_i x_i c_i^n - \Delta t\, \mathcal{C}^n_{\mathrm{I}^h+1/2} \leq \sum_{i=0}^{\mathrm{I}^h} \Delta x_i x_i c_i^n.$$

Next, it is shown that $c^h(t^{n+1})$ follows a similar estimate as (3.19). For this, multiply Eq. (3.11) with the term $\Delta x_i/x_i$ and using summation over i, provide

$$\sum_{i=0}^{\mathrm{I}^h} \Delta x_i c_i^{n+1} = \sum_{i=0}^{\mathrm{I}^h} \Delta x_i c_i^n - \Delta t \sum_{i=0}^{\mathrm{I}^h} \frac{\left(\mathcal{C}^n_{i+1/2} - \mathcal{C}^n_{i-1/2}\right)}{x_i} + \Delta t \sum_{i=0}^{\mathrm{I}^h} \frac{\left(\mathcal{F}^n_{i+1/2} - \mathcal{F}^n_{i-1/2}\right)}{x_i}. \tag{3.22}$$

The second component of the RHS of the above expression can be simplified as

$$-\sum_{i=0}^{\mathrm{I}^h} \frac{\left(\mathcal{C}^n_{i+1/2} - \mathcal{C}^n_{i-1/2}\right)}{x_i} \leq -\sum_{i=0}^{\mathrm{I}^h} \mathcal{C}^n_{i+1/2}\left(\frac{1}{x_i} - \frac{1}{x_{i+1}}\right) \leq 0, \quad \text{due to } \mathcal{C}^n_{i+1/2} \geq 0\ \forall\, i. \tag{3.23}$$

Now, dealing with third component, it leads to

$$\sum_{i=0}^{\mathrm{I}^h} \frac{\mathcal{F}^n_{i+1/2} - \mathcal{F}^n_{i-1/2}}{x_i} \leq \sum_{i=0}^{\mathrm{I}^h} \sum_{k=i+1}^{\mathrm{I}^h} \Delta x_i \Delta x_k S_k B_{i,k} c_k^n.$$

Let us alter the order of summation and then using the conditions (3.5) and (3.6) on the selection rate and fragmentation function, it is easy to see that

$$\begin{aligned}\sum_{i=0}^{\mathrm{I}^h} \frac{\mathcal{F}^n_{i+1/2} - \mathcal{F}^n_{i-1/2}}{x_i} &\leq \sum_{k=0}^{\mathrm{I}^h} \Delta x_k c_k^n \sum_{i=0}^{k-1} \Delta x_i S_k B_{i,k} \\ &\leq \|S\|_{L^\infty} \sum_{k=0}^{\mathrm{I}^h} \Delta x_k c_k^n \int_0^{x_k} B(x, x_k)dx \leq \|S\|_{L^\infty} \frac{\alpha+2}{\alpha+1} \sum_{k=0}^{\mathrm{I}^h} \Delta x_k c_k^n. \end{aligned} \tag{3.24}$$

By using (3.23) and (3.24) into (3.22), we find that for $\eta = \frac{\alpha+2}{\alpha+1}$

$$\sum_{i=0}^{\mathrm{I}^h} \Delta x_i c_i^{n+1} \leq (1 + \eta \|S\|_{L^\infty} \Delta t) \sum_{i=0}^{\mathrm{I}^h} \Delta x_i c_i^n.$$

Finally, having (3.19) at time t^n and the relation $1 + z < \exp(z)$ for all $z > 0$ provide

$$\sum_{i=0}^{\mathrm{I}^h} \Delta x_i c_i^{n+1} \leq (1 + \eta \|S\|_{L^\infty} \Delta t)\, \|c^{in}\|_{L^1}\, e^{\eta \|S\|_{L^\infty} t^n} \leq \|c^{in}\|_{L^1}\, e^{\eta \|S\|_{L^\infty} t^{n+1}},$$

consequently, the outcome (3.18) is obtained. □

In order to prove uniform integrability of the family of solutions, let us denote a particular class of convex functions as $C_{VP,\infty}$. Further, consider $\Phi \in C^{\infty}([0,\infty))$, a non-negative and convex function which belongs to the class $C_{VP,\infty}$ and enjoys the following properties:

(i) $\Phi(0) = 0,\ \Phi'(0) = 1$ and Φ' is concave;

(ii) $\lim_{p\to\infty} \Phi'(p) = \lim_{p\to\infty} \frac{\Phi(p)}{p} = \infty$;

(iii) for some $\lambda \in (1,2)$,

$$T_{\lambda}(\Phi) := \sup_{p\geq 0} \left\{ \frac{\Phi(p)}{p^{\lambda}} \right\} < \infty. \tag{3.25}$$

Example of such a $C_{VP,\infty}$ function is $\Phi(p) = 2(1+p)\ln(1+p) - p$. It is given that, $c^{in} \in L^1(0,R)$, therefore, by De La Vallée Poussin theorem, a convex function $\Phi \geq 0$ exists which satisfies

$$\frac{\Phi(p)}{p} \to \infty, \ \text{ as } \ p \to \infty$$

and

$$\mathcal{I} := \int_0^R \Phi(c^{in})(x)dx < \infty. \tag{3.26}$$

Now, in the following proposition, the equi-integrability is discussed.

Proposition 3.2.3. Let $c^{in} \geq 0 \in L^1]0,R]$ and the family $(c^h)_{(h,\Delta t)}$ is expressed by (2.14), where the relation (3.14) holds by Δt. Then (c^h) is weakly sequentially compact in $L^1(]0,T[\times]0,R])$.

Proof. Our focus here is to obtain a similar result as (3.26) for the family of function c^h. The integral of $\Phi(c^h)$ by using the sequence c_i^n can be written as

$$\begin{aligned}\int_0^T \int_0^R \Phi(c^h(t,x))dx\,dt &= \sum_{n=0}^{N-1}\sum_{i=0}^{\mathrm{I}^h} \int_{\tau_n}\int_{\Lambda_i^h} \Phi\bigg(\sum_{k=0}^{N-1}\sum_{j=0}^{\mathrm{I}^h} c_j^k \chi_{\Lambda_j^h}(x)\chi_{\tau_k}(t)\bigg)dx\,dt \\ &= \sum_{n=0}^{N-1}\sum_{i=0}^{\mathrm{I}^h} \Delta t \Delta x_i \Phi(c_i^n).\end{aligned}$$

The convexity of the function Φ leads to the estimate

$$\left(c_i^{n+1} - c_i^n\right) \Phi^{'}(c_i^{n+1}) \geq \Phi(c_i^{n+1}) - \Phi(c_i^n).$$

Now, multiply with Δx_i and having summation over i display the following equation

$$\sum_{i=0}^{\mathrm{I}^h} \Delta x_i \left[\Phi(c_i^{n+1}) - \Phi(c_i^n)\right] \leq \sum_{i=0}^{\mathrm{I}^h} \Delta x_i \left[(c_i^{n+1} - c_i^n)\Phi^{'}(c_i^{n+1})\right].$$

By using discrete coagulation and fragmentation terms, it can further be rewritten as

$$\begin{aligned}\sum_{i=0}^{\mathrm{I}^h} \Delta x_i \left[\Phi(c_i^{n+1}) - \Phi(c_i^n)\right] \leq & \|K\|_{L^\infty} \Delta t \sum_{i=0}^{\mathrm{I}^h} \sum_{j=0}^{i-1} \Delta x_j c_j^n \sum_{k=\gamma_{i-1,j}}^{\gamma_{i,j}-1} \Delta x_k c_k^n \Phi^{'}(c_i^{n+1}) \\ & + \Delta t \sum_{i=0}^{\mathrm{I}^h} \sum_{k=i+1}^{\mathrm{I}^h} S_k B_{i,k} c_k^n \Delta x_k \Delta x_i \Phi^{'}(c_i^{n+1}). \end{aligned} \tag{3.27}$$

For the coagulation component, i.e., the first part on the RHS of Eq.(3.27), altering the order of summation and the convexity result given as in Lemma 2.4.4 enable us to have

$$\begin{aligned}& \|K\|_{L^\infty} \Delta t \sum_{i=0}^{\mathrm{I}^h} \sum_{j=0}^{i-1} \Delta x_j c_j^n \sum_{k=\gamma_{i-1,j}}^{\gamma_{i,j}-1} \Delta x_k c_k^n \Phi^{'}(c_i^{n+1}) \\ & \qquad \leq \|K\|_{L^\infty} \Delta t \sum_{j=0}^{\mathrm{I}^h} \Delta x_j c_j^n \sum_{i=j+1}^{\mathrm{I}^h} \sum_{k=\gamma_{i-1,j}}^{\gamma_{i,j}-1} \Delta x_k [\Phi(c_k^n) + \Phi(c_i^{n+1})],\end{aligned}$$

and

$$\sum_{i=j+1}^{\mathrm{I}^h} \sum_{k=\gamma_{i-1,j}}^{\gamma_{i,j}-1} \Delta x_k \Phi(c_k^n) = \sum_{k=\gamma_{j,j}}^{\gamma_{\mathrm{I}^h,j}-1} \Delta x_k \Phi(c_k^n) \leq \sum_{k=0}^{\mathrm{I}^h} \Delta x_k \Phi(c_k^n). \tag{3.28}$$

Further, to simplify the term

$$\sum_{i=j+1}^{\mathrm{I}^h} \sum_{k=\gamma_{i-1,j}}^{\gamma_{i,j}-1} \Delta x_k \Phi(c_i^{n+1}),$$

we proceed as follows. Notice that

$$\sum_{k=\gamma_{i-1,j}}^{\gamma_{i,j}-1} \Delta x_k = x_{\gamma_{i,j}-1/2} - x_{\gamma_{i-1,j}-1/2},$$

where $x_{i+1/2} - x_j$ and $x_{i-1/2} - x_j$ represent $x_{\gamma_{i,j}-1/2}$ and $x_{\gamma_{i-1,j}-1/2}$ as left point approximations. Hence, by following [50], the inequality

$$x_{\gamma_{i,j}-1/2} - x_{\gamma_{i-1,j}-1/2} \leq Q\Delta x_i$$

holds for $Q = 1 + L$ or $Q = 2$. Therefore,

$$\sum_{i=j+1}^{\mathrm{I}^h} \sum_{k=\gamma_{i-1,j}}^{\gamma_{i,j}-1} \Delta x_k \Phi(c_i^{n+1}) \leq Q \sum_{i=0}^{\mathrm{I}^h} \Delta x_i \Phi(c_i^{n+1}). \tag{3.29}$$

Again, using the convexity results on fragmentation term in the equation (3.27), growth conditions (3.5)-(3.6) on selection and breakage functions and changing the order of summation yield

$$\begin{aligned}
\Delta t \sum_{i=0}^{\mathrm{I}^h} \sum_{k=i+1}^{\mathrm{I}^h} S_k B_{i,k} c_k^n \Delta x_k \Delta x_i \Phi^{'}(c_i^{n+1}) =& (\alpha+2)\Delta t \sum_{i=0}^{\mathrm{I}^h} \sum_{k=i+1}^{\mathrm{I}^h} x_i^{\alpha} c_k^n \Delta x_k \Delta x_i \Phi^{'}(c_i^{n+1}) \\
&\leq (\alpha+2)\Delta t \sum_{k=0}^{\mathrm{I}^h} c_k^n \Delta x_k \sum_{i=0}^{k-1} \Delta x_i [\Phi(c_i^{n+1}) + \Phi(x_i^{\alpha})] \\
&\leq (\alpha+2)\Delta t \sum_{k=0}^{\mathrm{I}^h} c_k^n \Delta x_k \left(\sum_{i=0}^{\mathrm{I}^h} \Phi(c_i^{n+1}) \Delta x_i + \sum_{i=0}^{k-1} \Phi(x_i^{\alpha}) \Delta x_i \right).
\end{aligned} \tag{3.30}$$

Let us assess the two expressions on the RHS of equation (3.30) separately. The first summation is evaluated as

$$(\alpha+2)\Delta t \sum_{k=0}^{\mathrm{I}^h} c_k^n \Delta x_k \sum_{i=0}^{\mathrm{I}^h} \Phi(c_i^{n+1}) \Delta x_i \leq (\alpha+2) \|c^{in}\|_{L^1} e^{\eta \|S\|_{L^\infty} t} \Delta t \sum_{i=0}^{\mathrm{I}^h} \Phi(c_i^{n+1}) \Delta x_i. \tag{3.31}$$

Using the Proposition 3.3, for the second term, we proceed as follows

$$\begin{aligned}
(\alpha+2)\Delta t \sum_{k=0}^{\mathrm{I}^h} \Delta x_k c_k^n \sum_{i=0}^{k-1} \Phi(x_i^{\alpha}) \Delta x_i =& (\alpha+2)\Delta t \sum_{k=0}^{\mathrm{I}^h} \Delta x_k c_k^n \sum_{i=0}^{k-1} \frac{\Phi(x_i^{\alpha})}{x_i^{\lambda\alpha}} x_i^{\lambda\alpha} \Delta x_i \\
&\leq (\alpha+2)\Delta t T_\lambda(\Phi) \sum_{k=0}^{\mathrm{I}^h} \Delta x_k c_k^n \sum_{i=0}^{k-1} x_i^{\lambda\alpha} \Delta x_i \ \text{ (by having } (4.26))
\end{aligned}$$

$$
\begin{aligned}
&\leq (\alpha+2)\Delta t T_\lambda(\Phi)\sum_{k=0}^{\mathrm{I}^h}\Delta x_k c_k^n\int_0^{x_k} x^{\lambda\alpha}dx\\
&=\frac{(\alpha+2)}{(\lambda\alpha+1)}\Delta t T_\lambda(\Phi)\sum_{k=0}^{\mathrm{I}^h} c_k^n x_k^{\lambda\alpha+1}\Delta x_k\\
&\leq\frac{(\alpha+2)}{(\lambda\alpha+1)}\Delta t T_\lambda(\Phi)\bigg(\sum_{k=0}^{\mathrm{I}^h} c_k^n\Delta x_k+\sum_{k=0}^{\mathrm{I}^h} x_k c_k^n\Delta x_k\bigg)\\
&\leq\frac{(\alpha+2)}{(\lambda\alpha+1)}\Delta t T_\lambda(\Phi)\bigg(\|c^{in}\|_{L^1}\,e^{\eta\|S\|_{L^\infty}t}+\mu_1^{in}\bigg).
\end{aligned}
\tag{3.32}
$$

Consequently, all the results (3.28)-(3.32) used in (3.27) lead to

$$
\begin{aligned}
\sum_{i=0}^{\mathrm{I}^h}\Delta x_i\left[\Phi(c_i^{n+1})-\Phi(c_i^n)\right]\leq\|K\|_{L^\infty}\Delta t\sum_{j=0}^{\mathrm{I}^h}\Delta x_j c_j^n\bigg(\sum_{i=0}^{\mathrm{I}^h}\Delta x_i\Phi(c_i^n)+Q\sum_{i=0}^{\mathrm{I}^h}\Delta x_i\Phi(c_i^{n+1})\bigg)\\
+(\alpha+2)\|c^{in}\|_{L^1}\,e^{\eta\|S\|_{L^\infty}t}\Delta t\sum_{i=0}^{\mathrm{I}^h}\Delta x_i\Phi(c_i^{n+1})\\
+\frac{(\alpha+2)}{(\lambda\alpha+1)}\Delta t T_\lambda(\Phi)\bigg(\|c^{in}\|_{L^1}\,e^{\eta\|S\|_{L^\infty}t}+\mu_1^{in}\bigg).
\end{aligned}
\tag{3.33}
$$

It can further be simplified as

$$
\begin{aligned}
&\bigg(1-Q^*N^*\|c^{in}\|_{L^1}\,e^{\eta\|S\|_{L^\infty}T}\Delta t\bigg)\sum_{i=0}^{\mathrm{I}^h}\Delta x_i\Phi(c_i^{n+1})\\
&\leq\bigg(1+\|K\|_{L^\infty}\|c^{in}\|_{L^1}\,e^{\eta\|S\|_{L^\infty}T}\Delta t\bigg)\sum_{i=0}^{\mathrm{I}^h}\Delta x_i\Phi(c_i^n)\\
&\quad+\frac{(\alpha+2)}{(\lambda\alpha+1)}\Delta t T_\lambda(\Phi)\bigg(\|c^{in}\|_{L^1}\,e^{\eta\|S\|_{L^\infty}t}+\mu_1^{in}\bigg),
\end{aligned}
\tag{3.34}
$$

where Q^* and N^* denote $\max(Q,\alpha+2)$ and $\max(\|K\|_{L^\infty},1)$, respectively. The former inequality implies that

$$
\sum_{i=0}^{\mathrm{I}^h}\Delta x_i\Phi(c_i^{n+1})\leq A\sum_{i=0}^{\mathrm{I}^h}\Delta x_i\Phi(c_i^n)+B \tag{3.35}
$$

where

$$
A=\frac{\bigg(1+\|K\|_{L^\infty}\|c^{in}\|_{L^1}\,e^{\eta\|S\|_{L^\infty}T}\Delta t\bigg)}{\bigg(1-Q^*N^*\|c^{in}\|_{L^1}\,e^{\eta\|S\|_{L^\infty}T}\Delta t\bigg)}\ \text{and}\ B=\frac{(\alpha+2)\Delta t T_\lambda(\Phi)\bigg(\|c^{in}\|_{L^1}\,e^{\eta\|S\|_{L^\infty}t}+\mu_1^{in}\bigg)}{(\lambda\alpha+1)\bigg(1-Q^*N^*\|c^{in}\|_{L^1}\,e^{\eta\|S\|_{L^\infty}T}\Delta t\bigg)}.
$$

Hence, the following is obtained

$$\sum_{i=0}^{\mathrm{I}^h} \Delta x_i \Phi(c_i^n) \leq A^n \sum_{i=0}^{\mathrm{I}^h} \Delta x_i \Phi(c_i^{in}) + B\frac{A^{n-1}-1}{A-1}.$$

By using Jensen's inequality and (3.26), finally we get

$$\begin{aligned}\int_0^R \Phi(c^h(t,x))\,dx \leq & A^n \sum_{i=0}^{\mathrm{I}^h} \Delta x_i \Phi\left(\frac{1}{\Delta x_i}\int_{\Lambda_i^h} c^{in}(x)dx\right) + B\frac{A^{n-1}-1}{A-1} \\ \leq & A^n \sum_{i=0}^{\mathrm{I}^h} \int_{\Lambda_i^h} \Phi(c^{in}(x))dx + B\frac{A^{n-1}-1}{A-1} \\ = & A^n\mathcal{I} + B\frac{A^{n-1}-1}{A-1} < \infty, \quad \text{for all} \quad t \in [0,T].\end{aligned}$$

□

Thus, applying the Dunford-Pettis theorem, one can say that the sequence $(c^h)_{h\in(0,1)}$ is weakly compact in L^1. This guarantees that a subsequence of $(c^h)_{h\in(0,1)}$ exists and $c \in L^1(]0,T[\times]0,R])$ is such that $c^h \rightharpoonup c$ for $h \to 0$.

Remark 3.2.4. By a diagonal procedure, subsequences of $(c^h)_h$,$(K^h)_h$ and $(B^h)_h$ can be extracted such that

$$K^h(z_1,z_2) \to K(z_1,z_2) \quad \text{and} \quad B^h(z_1,z_2) \to B(z_1,z_2),$$

for almost every $(z_1,z_2) \in (0,R)\times(0,R)$ as $h \to 0$.

Now, we show that the discrete aggregation and fragmentation fluxes converge weakly to the continuous fluxes written in terms of the function c^h. In order to do so, some point approximations are used which are given below. The notations of the midpoint, right and left approximations are in (2.43-2.45). Also, define

$$\Theta^h : (x,z) \in]0,R[^2 \to \Theta^h(x,z) = \sum_{i=0}^{\mathrm{I}^h}\sum_{j=0}^{i} x_{\gamma_{i,j}} \chi_{\Lambda_i^h}(x)\chi_{\Lambda_j^h}(z).$$

Note that the above approximations converge pointwise to x, $\forall\ x\ \in]0,R[$ as $h \to 0$. Further, $\forall\ (z_1,z_2) \in]0,R[^2$, one has

$$\begin{cases} \Theta^h : (z_1, z_2) \to z_1 - z_2, \quad z_1 \geq z_2, \\ \Theta^h : (z_1, z_2) \to 0, \quad z_1 \leq z_2. \end{cases}$$

Thanks to the Dunford-Pettis and Egorov theorems, the Lemma 2.1.5 is also needed to exhibit the convergence of the truncated flux towards the continuous flux. Finally, the following result explains the convergence of the numerical fluxes. For this, definitions of c^h, K^h, B^h and S^h given by (2.14), (2.15), (2.16) and (2.17), respectively, are considered.

Lemma 3.2.5. Consider the approximations of the coagulation term as

$$\mathcal{C}^h(t,x) = \int_0^R \int_0^R \chi_{[0,\Xi^h(x)]}(u)\chi_{[\Theta^h(x,u),R]}(v)X^h(u)K^h(u,v)c^h(t,u)c^h(t,v)dvdu,$$

and for the fragmentation

$$\mathcal{F}^h(t,x) = \int_0^R \int_0^R \chi_{[0,\Xi^h(x)]}(u)\chi_{[\Xi^h(x),R]}(v)X^h(u)B^h(u,v)S^h(v)c^h(t,v)dvdu.$$

Subsequently, a subsequence of $(c^h)_{h\in(0,1)}$ exists, which

$$\mathcal{C}^h \rightharpoonup \mathcal{C}^R_{nc} \quad \text{and} \quad \mathcal{F}^h \rightharpoonup \mathcal{F}^R_c$$

in $L^1(]0,T[\times]0,R])$ as $h \to 0$.

Proof. Before we begin the proof, it is worth noting that the terms $\mathcal{C}^h(t,x)$ and $\mathcal{F}^h(t,x)$ coincide with the terms $\mathcal{C}^n_i$ and $\mathcal{F}^n_i$, respectively, whenever $t \in \tau_n$ and $x \in \Lambda^h_i$. It is straightforward to notice that

$$\mathcal{C}^h(t,x) = \int_0^{x_{i+1/2}} \int_{\Theta^h(x,u)}^R X^h(u)K^h(u,v)c^h(t,v)c^h(t,u)dvdu,$$

$$= \sum_{j=0}^{i} \int_{\Lambda^h_j} \sum_{k=\gamma_{i,j}}^{\mathrm{I^h}} \int_{\Lambda^h_k} \left[X^h(u) \left(\sum_{a=0}^{\mathrm{I}^h} \sum_{b=0}^{\mathrm{I}^h} K_{a,b}\chi_{\Lambda^h_a}(u)\chi_{\Lambda^h_b}(v) \right) \left(\sum_{b=0}^{\mathrm{I}^h} c_b \chi_{\Lambda^h_b}(v) \right) \left(\sum_{a=0}^{\mathrm{I}^h} c^n_a \chi_{\Lambda^h_a}(u) \right) \right] dvdu$$

$$= \sum_{j=0}^{i} \sum_{k=\gamma_{i,j}}^{\mathrm{I^h}} \int_{\Lambda^h_j} \int_{\Lambda^h_k} x_j K_{j,k} c^n_j c^n_k dvdu = \mathcal{C}^n_{i+1/2},$$

while

$$\mathcal{F}^h(t,x) = \int_0^{x_{i+1/2}} \int_{x_{i+1/2}}^R X^h(u)B^h(u,v)S^h(v)c^h(t,v)dvdu$$

$$= \sum_{j=0}^{i} \int_{\Lambda_j^h} \sum_{k=i+1}^{\mathrm{I^h}} \int_{\Lambda_k^h} \Big[X^h(u) \Big(\sum_{a=0}^{\mathrm{I}^h} \sum_{b=0}^{\mathrm{I}^h} B_{a,b} \chi_{\Lambda_a^h}(u) \chi_{\Lambda_b^h}(v) \Big) \Big(\sum_{b=0}^{\mathrm{I}^h} S_b \chi_{\Lambda_b^h}(v) \Big) \Big(\sum_{b=0}^{\mathrm{I}^h} c_b^n \chi_{\Lambda_b^h}(v) \Big) \Big] dvdu$$

$$= \sum_{j=0}^{i} \sum_{k=i+1}^{\mathrm{I^h}} \int_{\Lambda_j^h} \int_{\Lambda_k^h} x_j B_{j,k} S_k c_k^n dvdu = \mathcal{F}_{i+1/2}^n.$$

Moving further, by following Remark 3.6, we know that for $(t,x) \in]0,T[\times]0,R]$ and $(u,v) \in]0,R]\times]0,R]$ almost everywhere, the sequence $X^h(\cdot)K^h(\cdot,v)$ is bounded in L^∞. Also,

$$\chi_{[0,\Xi^h(x)]}(u)\chi_{[\Theta^h(x,u),R]}(v)X^h(u)K^h(u,v) \to \chi_{[0,x]}(u)\chi_{[x-u,R]}(v)uK(u,v)$$

as $h \to 0$. Hence, having Lemma 2.1.5 leads to

$$\int_0^R \chi_{[0,\Xi^h(x)]}(u)\chi_{[\Theta^h(x,u),R]}(v)X^h(u)K^h(u,v)c^h(t,u)du \\ \to \int_0^R \chi_{[0,x]}(u)\chi_{[x-u,R]}(v)uK(u,v)c(t,u)du. \tag{3.36}$$

The above expression entails that (3.36) holds for every $(t,x) \in (]0,T[\times]0,R])$ as well as almost every v and c^h converges weakly. Again using Lemma 2.1.5, it yields

$$\mathcal{C}^h(t,x) \to \mathcal{C}_{nc}^R(t,x)$$

for every $(t,x) \in (]0,T[\times]0,R])$. Note that the weak convergence for $\mathcal{C}^h$ follows by this pointwise convergence. A similar approach shows the convergence of $\mathcal{F}^h$ as below,

$X^h(\cdot)B^h(\cdot,v)S^h(v) = (\alpha+2)x\dfrac{x^\alpha}{v^{\alpha+1}}v^{\alpha+1} = (\alpha+2)x^{1+\alpha} \in L^\infty]0,R]$ for almost all $v \in]0,R]$.

Since, the above is uniformly bounded and

$$\chi_{[0,\Xi^h(x)]}(u)\chi_{[\Xi^h(x),R]}(v)X^h(u)B^h(u,v)S^h(v) \to \chi_{[0,x]}(u)\chi_{[x,R]}(v)uB(u,v)S(v)$$

pointwise almost everywhere as $h \to 0$. Hence, one has

$$\int_0^R \chi_{[0,\Xi^h(x)]}(u)\chi_{[\Xi^h(x),R]}(v)X^h(u)B^h(u,v)S^h(v)du \\ \to \int_0^R \chi_{[0,x]}(u)\chi_{[x,R]}(v)uB(u,v)S(v)du \tag{3.37}$$

which holds for every $(t,x) \in (]0,T[\times]0,R])$ and almost every v. We also know that c^h weakly converges to c in $L^1]0,R]$. So, applying Lemma 2.1.5 entails that

$$\int_0^R \chi_{[0,\Xi^h(x)]}(u)\chi_{[\Xi^h(x),R]}(v)X^h(u)B^h(u,v)S^h(v)c^h(t,v)dvdu \\ \to \int_0^R \chi_{[0,x]}(u)\chi_{[x,R]}(v)uB(u,v)S(v)c(t,v)dvdu, \tag{3.38}$$

and therefore,

$$\mathcal{F}^h(t,x) \to \mathcal{F}_c^R(t,x)$$

for every $(t,x) \in (]0,T[\times]0,R])$. Thanks to boundedness of $\mathcal{F}^h$, the pointwise convergence gives weak convergence. Finally, we may demonstrate the main Theorem 3.2.1 below. For the proof, a compactly supported test function $\varphi \in C^1([0,T[\times[0,R])$ is taken. The function φ is having the compact support over $t \in [0,t_{N-1}]$ for small enough time step Δt. Let us consider finite volume and left endpoint approximations for time and space variables of φ on $\tau_n \times \Lambda_i^h$ by

$$\varphi_i^n := \frac{1}{\Delta t}\int_{t_n}^{t_{n+1}} \varphi(t,x_{i-1/2})dt.$$

Now, a multiplication of Eq.(3.11) by φ_i^n & taking summations over n & i provide

$$\sum_{n=0}^{N-1}\sum_{i=0}^{\mathrm{I}^h}\left[\Delta x_i x_i(c_i^{n+1}-c_i^n)\varphi_i^n + \Delta t\left(\mathcal{C}_{i+1/2}^n - \mathcal{C}_{i-1/2}^n\right)\varphi_i^n - \Delta t\left(\mathcal{F}_{i+1/2}^n - \mathcal{F}_{i-1/2}^n\right)\varphi_i^n\right] = 0.$$

Moreover, upon expanding the summations for each i and n, a discrete integration by parts yields

$$\sum_{n=0}^{N-1}\sum_{i=0}^{\mathrm{I}^h}\Delta x_i x_i c_i^{n+1}(\varphi_i^{n+1}-\varphi_i^n) + \sum_{n=0}^{N-1}\sum_{i=0}^{\mathrm{I}^h-1}\Delta t[\mathcal{C}_{i+1/2}^n - \mathcal{F}_{i+1/2}^n](\varphi_{i+1}^{n+1}-\varphi_i^n) \\ + \sum_{i=0}^{\mathrm{I}^h}\Delta x_i x_i c_i^{in}\varphi_i^0 - \sum_{n=0}^{N-1}\Delta t\,\mathcal{C}_{\mathrm{I}^h+1/2}^n\varphi_{\mathrm{I}^h}^n = 0. \tag{3.39}$$

The first and third expressions of the above equation are simplified using only the function c^h while remaining terms are expressed in terms of the functions c^h and $\mathcal{F}^h$. For the first

part, consider

$$\sum_{n=0}^{N-1}\sum_{i=0}^{\mathrm{I}^h}\Delta x_i x_i c_i^{n+1}(\varphi_i^{n+1}-\varphi_i^n)+\sum_{i=0}^{\mathrm{I}^h}\Delta x_i x_i c_i^{in}\varphi_i^0 =$$
$$\sum_{n=0}^{N-1}\sum_{i=0}^{\mathrm{I}^h}\int_{\tau_{n+1}}\int_{\Lambda_i^h} X^h(x)c^h(t,x)\frac{\varphi(t,\xi^h(x))-\varphi(t-\Delta t,\xi^h(x))}{\Delta t}dxdt$$
$$+\sum_{i=0}^{\mathrm{I}^h}\int_{\Lambda_i^h} X^h(x)c^h(0,x)\frac{1}{\Delta t}\int_0^{\Delta t}\varphi(t,\xi^h(x))dtdx,$$

which can be further rewritten as

$$\sum_{n=0}^{N-1}\sum_{i=0}^{\mathrm{I}^h}\Delta x_i x_i c_i^{n+1}(\varphi_i^{n+1}-\varphi_i^n)+\sum_{i=0}^{\mathrm{I}^h}\Delta x_i x_i c_i^{in}\varphi_i^0 =$$
$$\int_{\Delta t}^{T}\int_0^{R} X^h(x)c^h(t,x)\frac{\varphi(t,\xi^h(x))-\varphi(t-\Delta t,\xi^h(x))}{\Delta t}dxdt$$
$$+\int_0^{R} X^h(x)c^h(0,x)\frac{1}{\Delta t}\int_0^{\Delta t}\varphi(t,\xi^h(x))dtdx. \tag{3.40}$$

Since, the derivative of φ is bounded and $\varphi\in C^1([0,T[\times[0,R])$ is having compact support, thus

$$\frac{1}{\Delta t}\int_0^{\Delta t}\varphi(t,\xi^h(x))dt\to\varphi(0,x)\quad\text{as}\quad\max\{h,\Delta t\}\to 0$$

uniformly with respect to t and x. Since, $c^h(0,x)\to c^{in}$ in $L^1]0,R]$, Lemma 2.1.5 yields

$$\int_0^{R} X^h(x)c^h(0,x)\frac{1}{\Delta t}\int_0^{\Delta t}\varphi(t,\xi^h(x))dtdx\to\int_0^{R} xc^{in}(x)\varphi(0,x)dx$$

as $X^h(x)$ converges pointwise in $[0,R]$. To treat the first part on the RHS of (3.40), used the expansion of the function φ through a Taylor series provides

$$\frac{\varphi(t,\xi^h(x))-\varphi(t-\Delta t,\xi^h(x))}{\Delta t}$$
$$=\frac{\varphi(t,x)+(x-\xi^h(x))\frac{\partial\varphi}{\partial x}-\varphi(t,x)+\Delta t\frac{\partial\varphi}{\partial t}-(x-\xi^h(x))\frac{\partial\varphi}{\partial x}+O(h\,\Delta t)}{\Delta t},$$

which means that, as max $\{h,\Delta t\}\to 0$,

$$\frac{\varphi(t,\xi^h(x))-\varphi(t-\Delta t,\xi^h(x))}{\Delta t}\to\frac{\partial\varphi}{\partial t}(t,x)$$

uniformly. Again an application of Lemma 2.1.5 and from Proposition 3.2.3, one has

$$\int_0^T \int_0^R X^h(x)c^h(t,x)\frac{\varphi(t,\xi^h(x))-\varphi(t-\Delta t,\xi^h(x))}{\Delta t}dx\,dt \to \int_0^T \int_0^R xc(t,x)\frac{\partial\varphi}{\partial t}(t,x)dx\,dt.$$

Therefore,

$$\int_{\Delta t}^T \int_0^R \underbrace{X^h(x)c^h(t,x)\frac{\varphi(t,\xi^h(x))-\varphi(t-\Delta t,\xi^h(x))}{\Delta t}}_{A} dx\,dt =$$

$$\int_0^T \int_0^R A\,dx\,dt - \int_0^{\Delta t} \int_0^R A\,dx\,dt \to \int_0^T \int_0^R xc(t,x)\frac{\partial\varphi}{\partial t}(t,x)dx\,dt$$

is established. At the end, taking the remaining terms of the equation (3.39) and writing them in terms of $\mathcal{C}^h$ and $\mathcal{F}^h$ lead to

$$\begin{aligned}
&\sum_{n=0}^{N-1}\sum_{i=0}^{\mathrm{I}^h-1}\Delta t[\mathcal{C}^n_{i+1/2}-\mathcal{F}^n_{i+1/2}](\varphi^n_{i+1}-\varphi^n_i)-\sum_{n=0}^{N-1}\Delta t\mathcal{C}^n_{\mathrm{I}^h+1/2}\varphi^n_{\mathrm{I}^h}\\
&=\sum_{n=0}^{N-1}\sum_{i=0}^{\mathrm{I}^h-1}\int_{\tau_n}\int_{\Lambda^h_i}[\mathcal{C}^n_{i+1/2}-\mathcal{F}^n_{i+1/2}]\frac{1}{\Delta x_i}\left[\varphi(t,x_{i+1/2})-\varphi(t,x_{i-1/2})\right]dxdt\\
&\quad-\sum_{n=0}^{N-1}\int_{\tau_n}\mathcal{C}^n_{\mathrm{I}^h+1/2}\varphi(t,R-\Delta x_{\mathrm{I}^h})dt\\
&=\int_0^T\int_0^{R-\Delta x_{\mathrm{I}^h}}[\mathcal{C}^h(t,x)-\mathcal{F}^h(t,x)]\frac{\partial\varphi}{\partial x}(t,x)dxdt-\int_0^T\mathcal{C}^h(t,R)\varphi(t,R-\Delta x_{\mathrm{I}^h})dt.
\end{aligned}$$

Finally, thanks to Lemma 3.2.5, the weak convergence for the fluxes $\mathcal{C}^h \rightharpoonup \mathcal{C}^R_{nc}$ and $\mathcal{F}^h \rightharpoonup \mathcal{F}^R_c$ exist in $L^1(]0,T[\times]0,R])$ which determine

$$\begin{aligned}
&\int_0^T\int_0^{R-\Delta x_{\mathrm{I}^h}}[\mathcal{C}^h(t,x)-\mathcal{F}^h(t,x)]\frac{\partial\varphi}{\partial x}(t,x)dxdt-\int_0^T\mathcal{C}^h(t,R)\varphi(t,R-\Delta x_{\mathrm{I}^h})dt\\
&=\left(\int_0^T\int_0^R-\int_0^T\int_{\Delta x_{\mathrm{I}^h}}\right)[\mathcal{C}^h(t,x)-\mathcal{F}^h(t,x)]\frac{\partial\varphi}{\partial x}(t,x)dxdt-\int_0^T\mathcal{C}^h(t,R)\varphi(t,R-\Delta x_{\mathrm{I}^h})dt\\
&\to\int_0^T\int_0^R[\mathcal{C}^R_{nc}-\mathcal{F}^R_c]\frac{\partial\varphi}{\partial x}(t,x)dxdt-\int_0^T\mathcal{C}^R_{nc}(t,R)\varphi(t,R)dt\quad\text{as } h\to 0.
\end{aligned}$$

It thus completes the validation of Theorem 3.2.1 as all the terms in the equation (3.16) are obtained. □

3.3 Error Analysis

Here, we have discussed the error estimates for the coagulation and multiple fragmentation equations. It is important to mention here that, for the coagulation, results are taken from [50]. So, our focus is to develop the study for multiple breakage model and combine the findings with the outcomes of [50] for coagulation. Taking the uniform mesh is essential for estimating the error component, i.e., $\Delta x_i = h \; \forall i \in \{0, 1, 2, \ldots, \mathrm{I}^h\}$. The following theorem provides the first order error estimates by taking some assumptions about the kernels and initial datum.

Theorem 3.3.1. Let the coagulation and fragmentation kernels hold $K, B \in W^{1,\infty}_{loc}(\mathbb{R}^+ \times \mathbb{R}^+)$ and selection rate, initial datum $S, c^{in} \in W^{1,\infty}_{loc}(\mathbb{R}^+)$. Moreover, stability condition (3.14) on Δt and uniform mesh are considered. Then, the following error estimates

$$\|c^h - c\|_{L^\infty(0,T;L^1(0,R))} \leq D(T,R)(h + \Delta t) \tag{3.41}$$

holds, where c is the weak solution to (1.7) and $D(T,R)$ is a constant depending on R and T.

Before proving the theorem, consider the following proposition, which estimates the approximate solution c^h and the exact solution c with certain additional assumptions. These computations are significant in predicting the error.

Proposition 3.3.2. Assume that kinetic parameters $K, B \in L^\infty_{loc}(\mathbb{R}^+ \times \mathbb{R}^+)$ and $S \in L^\infty_{loc}(\mathbb{R}^+)$ and the condition (3.14) holds for time step Δt. Also, let the function c^{in} is restricted in L^∞_{loc}. Then, solutions c^h and c to (1.7) are bounded in $(0,T) \times (0,R)$ as

$$\|c^h\|_{L^\infty((0,T)\times(0,R))} \leq D(T,R), \quad \|c\|_{L^\infty((0,T)\times(0,R))} \leq D(T,R).$$

Furthermore, if the kernels $K, B \in W^{1,\infty}_{loc}(\mathbb{R}^+ \times \mathbb{R}^+)$ and $S, c^{in} \in W^{1,\infty}_{loc}(\mathbb{R}^+)$. Then the following inequality holds:

$$\|c\|_{W^{1,\infty}(0,R)} \leq D(T,R). \tag{3.42}$$

Proof. The aim is to bound the solution c of the continuous equation (1.7). For this, integrating Eq. (3.9) concerning the time variable and leaving the negative terms out yield

$$c(t,x) \leq c^{in}(x) + \frac{1}{2}\int_0^t \int_0^x K(y,x-y)c(s,y)c(s,x-y)dy\,ds + \int_0^t \int_x^R B(x,y)S(y)c(s,y)dy\,ds.$$

Thus, it follows

$$\sup_{x\in(\,0,\,R)} c(t,x) \leq \underbrace{c^{in}(x) + \|BS\|_{L^\infty}\|c\|_{\infty,1}t}_{\alpha(t)} + \underbrace{\|K\|_{L^\infty}\|c\|_{\infty,1}}_{\beta}\int_0^t \sup_{y\in(\,0,R)} c(s,y)\,ds,$$

where $\|c\|_{\infty,1}$ symbolizes the norm of c in $L^\infty(0,T;L^1(\,0,R)\,)$. Subsequently, using Gronwall's lemma and integration by parts lead to accomplish the proof as

$$\begin{aligned}
\sup_{x\in(\,0,R)} c(t,x) &\leq \alpha(t) + \int_0^t \alpha(s)\beta e^{\int_s^t \beta\,dr}\,ds \\
&\leq \alpha(t) + \beta\Big[\frac{\alpha(s)e^{\beta(t-s)}}{-\beta}\Big|_0^t - \int_0^t \|SB\|_{L^\infty}\|c\|_{\infty,1}\frac{e^{\beta(t-s)}}{-\beta}\,ds\Big] \\
&\leq \alpha(0)e^{\beta t} + \frac{\|BS\|_{L^\infty}\|c\|_{\infty,1}}{\beta}[(e^{\beta t}-1)].
\end{aligned}$$

Therefore,

$$\|c\|_{L^\infty((0,T)\times(\,0,R)\,)} \leq D(T,R).$$

Now, moving to the conclusion of an estimate of (3.42). To obtain this, firstly we integrate Eq. (3.9) with respect to time variable t and then differentiate it with respect to the volume variable x. Hence, the maximum value over the domain of x is achieved as

$$\begin{aligned}
\left\|\frac{\partial c}{\partial x}(x)\right\|_{L^\infty} \leq \left\|\frac{\partial c^{in}}{\partial x}\right\|_{L^\infty} &+ \Big\{\frac{1}{2}\|K\|_{L^\infty}\|c\|_{L^\infty}^2 + 2\|K\|_{W^{1,\infty}}\|c\|_{L^\infty}\|c\|_{\infty,1}R + \|BS\|_{L^\infty}\|c\|_{L^\infty} \\
&+ 2\|B\|_{W^{1,\infty}}\|S\|_{L^\infty}\|c\|_{\infty,1}R + \|S\|_{W^{1,\infty}}\|c\|_{L^\infty}\Big\}t \\
&+ (2\|K\|_{L^\infty}\|c\|_{\infty,1}R + \|S\|_{L^\infty})\int_0^t \left\|\frac{\partial c}{\partial x}\right\|_{L^\infty} ds.
\end{aligned}$$

An application of Gronwall's lemma as used in the priori boundedness of c is enough to establish (3.42). □

Next, we proceed to write the continuous expressions for the following discrete coagulation and fragmentation terms given in (3.11), for a uniform mesh

$$-\frac{\mathcal{C}^n_{i+1/2}-\mathcal{C}^n_{i-1/2}}{h}=h\sum_{j=0}^{i-1}x_jK_{j,i-j-1}c^n_ic^n_{i-j-1}-h\sum_{j=0}^{\mathrm{I}^h}x_iK_{i,j}c^n_ic^n_j, \tag{3.43}$$

and

$$\frac{\mathcal{F}^n_{i+1/2}-\mathcal{F}^n_{i-1/2}}{h}=-\sum_{j=0}^{i-1}x_jS_iB_{j,i}c^n_i\Delta x_j+\sum_{j=i+1}^{\mathrm{I}^h}x_iS_jB_{i,j}c^n_j\Delta x_j. \tag{3.44}$$

The following lemma solves our purpose.

Lemma 3.3.3. Consider the initial condition $c^{in}\in W^{1,\infty}_{loc}$ and uniform mesh, $\Delta x_i=h$ $\forall i$. Also assuming that K, B, and S follow the conditions $K,B,S\in W^{1,\infty}_{loc}$. Let $(s,x)\in \tau_n\times\Lambda^h_i$, where $n\in\{0,1,\ldots,N-1\}$, $i\in\{0,1,2,\ldots,\mathrm{I}^h\}$. Then

$$\begin{aligned}-\frac{\mathcal{C}^n_{i+1/2}-\mathcal{C}^n_{i-1/2}}{x_ih}=&\frac{1}{2}\int_0^{\xi^h(x)}K^h(x',x-\Xi^h(x'))c^h(s,x')c^h(s,x-\Xi^h(x'))\,dx'\\&-\int_0^R K^h(x,x')c^h(s,x)c^h(s,x')\,dx'+\varepsilon(\mathbb{C},h),\end{aligned} \tag{3.45}$$

$$\frac{\mathcal{F}^n_{i+1/2}-\mathcal{F}^n_{i-1/2}}{x_ih}=\int_{\Xi^h(x)}^R S^h(x')B^h(x,x')c^h(s,x')\,dx'-S^h(x)c^h(s,x)+\varepsilon(\mathbb{F},h), \tag{3.46}$$

where $\varepsilon(\mathbb{C},h)$ and $\varepsilon(\mathbb{F},h)$ express signify the first-order terms concerning h within the L^1 framework:

$$\|\varepsilon(\mathbb{C},h)\|_{L^1}\le\frac{R}{2}\|c^h\|^2_{L^\infty}\|K\|_{L^\infty}h, \tag{3.47}$$

$$\|\varepsilon(\mathbb{F},h)\|_{L^1}\le R\|BS\|_{L^\infty}\|c^h\|_{\infty,1}h. \tag{3.48}$$

Proof. The simplified version of the coagulation part (3.45) from (3.43) has been investigated in [50]. Here, we discuss only the multiple fragmentation variation rate (3.44) to convert into Eq. (3.46) using a uniform mesh and having $x\in\Lambda^h_i$. Consider

$$\frac{\mathcal{F}^n_{i+1/2}-\mathcal{F}^n_{i-1/2}}{x_ih}=\sum_{j=i+1}^{\mathrm{I}^h}x_iS_jB_{i,j}c^n_j\Delta x_j-\frac{S_ic^n_i}{x_i}\sum_{j=0}^{i-1}x_jB_{j,i}\Delta x_j$$

$$= \sum_{j=i+1}^{\mathrm{I}^h} x_i S_j B_{i,j} c_j^n \Delta x_j - \frac{S_i c_i^n}{x_i} \sum_{j=0}^{i} x_j B_{j,i} \Delta x_j + S_i c_i^n B_{i,i} \Delta x_i$$
$$= \int_{\Xi^h(x)}^{R} S^h(x^{'}) B^h(x, x^{'}) c^h(s, x^{'})\, dx^{'} - S^h(x) c^h(s, x) + \varepsilon(\mathbb{F}, h),$$

for $\varepsilon(\mathbb{F}, h) := S_i c_i^n B_{i,i} h$. When the L_1 norm of $\varepsilon(\mathbb{F}, h)$ is calculated, the following term emerges

$$\begin{aligned} \|\varepsilon(\mathbb{F}, h)\|_{L^1} &\leq \|BS\|_{L^\infty} h \sum_{i=1}^{\mathrm{I(h)}} \int_{\Lambda_i^h} c_i^n\, dx \\ &\leq \|BS\|_{L^\infty} \|c^h\|_{\infty,1} h \sum_{i=1}^{\mathrm{I(h)}} \int_{\Lambda_i^h} dx \\ &\leq R \|BS\|_{L^\infty} \|c^h\|_{\infty,1} h. \end{aligned}$$

Now, to demonstrate the essential fact, i.e., Theorem 3.3.1, combination of Eqs. (3.11), (3.45) and (3.46) yields

$$\begin{aligned} \frac{\partial c^h(t,x)}{\partial t} =& \frac{1}{2} \int_0^{\xi^h(x)} K^h(x^{'}, x - \Xi^h(x^{'})) c^h(s, x^{'}) c^h(s, x - \Xi^h(x^{'}))\, dx' \\ &- \int_0^R K^h(x, x^{'}) c^h(s, x) c^h(s, x^{'})\, dx^{'} + \int_{\Xi^h(x)}^R S^h(x^{'}) B^h(x, x^{'}) c^h(s, x^{'})\, dx^{'} \\ &- S^h(x) c^h(s, x) + \varepsilon(\mathbb{C}, h) + \varepsilon(\mathbb{F}, h). \end{aligned} \tag{3.49}$$

Finally, we may derive the error formulation for $t \in \tau_n$ from Eqs. (3.9) and (3.49) as

$$\begin{aligned} \int_0^R |c^h(t,x) - c(t,x)| dx \leq& \int_0^R |c^h(0,x) - c(0,x)| dx + \sum_{\beta=1}^{4} \epsilon_\beta(\mathbb{C}, h) + \sum_{\beta=1}^{3} \epsilon_\beta(\mathbb{F}, h) \\ &+ \int_0^R |\epsilon(t,n)|\, dx + \|\varepsilon(\mathbb{C}, h)\|_{L^1} t + \|\varepsilon(\mathbb{F}, h)\|_{L^1} t, \end{aligned} \tag{3.50}$$

where error terms due to coagulation operator are denoted by $\epsilon_\beta(\mathbb{C}, h)$ with β= 1,2,3,4 and estimation of these terms are calculated in [50]. In this article, only $\epsilon_\beta(\mathbb{F}, h)$ with β= 1,2,3 for the fragmentation operator and $\int_0^R |\epsilon(t,n)|\, dx$ would be estimated. Here,

$$\epsilon_1(\mathbb{F}, h) = \int_0^t \int_0^R \int_{\Xi^h(x)}^R |S^h(x^{'}) B^h(x, x^{'}) c^h(s, x^{'}) - S(x^{'}) B(x, x^{'}) c(s, x^{'})|\, dx^{'}\, dx\, ds,$$

$$\epsilon_2(\mathbb{F},h)=\int_0^t\int_0^R\int_x^{\Xi^h(x)} S(x^{'})B(x,x^{'})c(s,x^{'})\,dx^{'}\,dx\,ds,$$

and

$$\epsilon_3(\mathbb{F},h)=\int_0^t\int_0^R |S^h(x)c^h(s,x)-S(x)c(s,x)|\,dx\,ds.$$

Furthermore, due to time discretization, assuming $|t-t_n|\leq\Delta t$ produces

$$\begin{aligned}\int_0^R|\epsilon(t,n)|\,dx\leq&\frac{1}{2}\int_{t_n}^t\int_0^R\int_0^{\xi^h(x)}K^h(x^{'},x-x^{'})c^h(s,x^{'})c^h(s,x-x^{'})\,dx^{'}\,dx\,ds\\&+\int_{t_n}^t\int_0^R\int_0^R K^h(x,x^{'})c^h(s,x)c^h(s,x^{'})\,dx^{'}\,dx\,ds\\&+\int_{t_n}^t\int_0^R\int_{\Xi^h(x)}^R S^h(x^{'})B^h(x,x^{'})c^h(s,x^{'})\,dx^{'}\,dx\,ds\\&+\int_{t_n}^t\int_0^R S^h(x)c^h(s,x)\,dx\,ds+\int_{t_n}^t\int_0^R\varepsilon(\mathbb{C},h)\,dx\,ds+\int_{t_n}^t\int_0^R\varepsilon(\mathbb{F},h)\,dx\,ds.\end{aligned}$$

Utilizing the smoothness property of kernels, i.e., K,B and $S\in W^{1,\infty}_{loc}$, we have for all $x,y\in(0,R)$

$$|B^h(x,y)-B(x,y)|\leq\|B\|_{W^{1,\infty}}h.$$

Thus, it provides the estimation of $\epsilon_1(\mathbb{F},h)$ using the L^∞ bound on c^h and c. To see this, we split the expression into three parts as

$$\begin{aligned}\epsilon_1(\mathbb{F},h)\leq&\int_0^t\int_0^R\int_0^R|S^h(x^{'})-S(x^{'})|B(x,x^{'})c(s,x^{'})\,dx^{'}\,dx\,ds\\&+\int_0^t\int_0^R\int_0^R S^h(x^{'})|B^h(x,x^{'})-B(x,x^{'})|c(s,x^{'})\,dx^{'}\,dx\,ds\\&+\int_0^t\int_0^R\int_0^R S^h(x^{'})B^h(x,x^{'})|c^h(s,x^{'})-c(s,x^{'})\,dx^{'}\,dx\,ds.\end{aligned}$$

The above may be transformed to, by simplifying and using Proposition 3.3.2

$$\epsilon_1(\mathbb{F},h)\leq tR^2\|c\|_\infty(\|B\|_\infty\|S\|_{W^{1,\infty}}+\|S\|_\infty\|B\|_{W^{1,\infty}})h+R\|BS\|_\infty\int_0^t\|c^h(s)-c(s)\|_{L^1}\,ds. \tag{3.51}$$

Similarly, one can compute

$$\epsilon_3(\mathbb{F},h)\leq\|c\|_\infty\|S\|_{W^{1,\infty}}tRh+\|S\|_\infty\int_0^t\|c^h(s)-c(s)\|_{L^1}\,ds, \tag{3.52}$$

and

$$\epsilon_2(\mathbb{F}, h) \leq \frac{tR}{2}\|BS\|_\infty\|c\|_\infty h. \tag{3.53}$$

Now, let us move on to the remaining term $\int_0^R |\epsilon(t,n)|\, dx$, the error introduced by the time discretization is resolved, and a bound is found as

$$\int_0^R |\epsilon(t,n)|\, dx \leq \Big(\frac{3}{2}\|K\|_\infty\|c^h\|_\infty^2 R^2 + (\|B\|_\infty R + 1)\|S\|_\infty\|c^h\|_\infty R + \|\varepsilon(\mathbb{C}, h)\|_{L^1} + \|\varepsilon(\mathbb{F}, h)\|_{L^1}\Big)\Delta t. \tag{3.54}$$

In conclusion, assemble all the bound estimations on $\epsilon_\beta(\mathbb{C}, h)$ for β=1,2,3,4 from [50], $\epsilon_\beta(\mathbb{F}, h)$ for β=1,2,3 from Eq. (3.51)-(3.53) and the relation (3.54). Substituting all these estimations in (3.50) and applying the Gronwall's lemma conclude

$$\|c^h - c\|_{L^\infty(0,T;L^1(0,R))} \leq D(T, R)(h + \Delta t),$$

which completes the required result. □

3.4 Numerical Validation

In this section, we numerically validate the conclusions obtained in Section 3.3 for two test cases of CMBE with physically relevant kernels. In each case, two different problems are taken into account for which experimental error and experimental order of convergence (EOC) are evaluated on a uniform mesh. The analytical solutions for such cases are not available due to singularity in breakage kernel; the EOC computation formula is as follows:

$$\text{EOC} = \ln\left(\frac{\|N^{num}_{\mathrm{I}^h} - N^{num}_{2\mathrm{I}^h}\|}{\|N^{num}_{2\mathrm{I}^h} - N^{num}_{4\mathrm{I}^h}\|}\right) / \ln(2). \tag{3.55}$$

Here, the total number of particles created by the FVS (3.11) with a mesh of I^h number of cells is denoted by $N^{num}_{\mathrm{I}^h}$. The computational domain for the volume and time arguments, for the numerical simulations, are taken as $x = [1e-3, 100]$ and $t = 100$ along with e^{-x} as the initial condition.

Test Case 1: Consider the CMBE with sum coagulation kernel, i.e., $K(x, y) = x + y$, selection function $S(x) = x^{1/2}, x^{1/4}$ and breakage function $B(x, y) = \frac{\alpha+2}{y}\left(\frac{x}{y}\right)^{\alpha}$, $\alpha = -1/2$. The EOC for taking two different selection rates are computed for a uniform mesh and the results are shown in Table 3.1. As expected from theoretical outcomes, it is clear from the table that the FVS produces first-order convergence for both the problems. The numerical errors are evaluated using 30, 60, 120, 240 and 480 degrees of freedom.

$S(x) = x^{1/2}$		
Cells	Error	EOC
30	-	-
60	0.1499	-
120	0.0272	0.9743
240	0.0039	0.9953
480	0.0005	0.9992

$S(x) = x^{1/4}$		
Cells	Error	EOC
30	-	-
60	0.0014	-
120	0.0005	0.9997
240	0.0002	1.0001
480	0.0001	1.0000

Table 3.1: EOC for Test Case 1

Test Case 2: Let us take the CMBE again with the same coagulation kernel and the selection functions taken in the previous test case but $B(x, y)$ is used with $\alpha = -3/4$. Again by computing the errors using 30, 60, 120, 240 and 480 number of grid points, the error and the EOC of the scheme are reported in Table 3.2. It is observed here as well that the FVS is first order accurate in each case. We would like to mention that the EOC has been evaluated for several other cases of α, K, and S but there was no marked difference in the output, so discussion is omitted here.

$S(x) = x^{1/2}$		
Cells	Error	EOC
30	-	-
60	0.1179	-
120	0.0195	0.9784
240	0.0026	0.9965
480	0.0003	0.9995

$S(x) = x^{1/4}$		
Cells	Error	EOC
30	-	-
60	0.0830	-
120	0.0371	0.9801
240	0.0062	0.9930
480	0.0008	0.9988

Table 3.2: EOC for Test Case 2

Chapter 4

Finite Volume Convergence Analysis and Error Estimation for Non-linear Collision-Induced Breakage Equation

---

According to the existing literature, none of the prior studies account for the weak convergence of the numerical scheme (FVM) for solving the collisional breakage equation (1.8). Therefore, this chapter is an attempt to study the weak convergence analysis of the FVM for solving the model with non-singular unbounded kernels and then error estimation for kernels being in $W^{1,\infty}_{loc}$ space over a uniform mesh. Thanks to the idea taken from Bourgade and Filbet [50] and the proof employs the weak L^1 compactness approach. The solution space weighted L^1 is same as in Chapters 2, 3.

Now, the specifications of the collisional kernel K and breakage distribution function b are expressed in the following expression: both functions are symmetric and measurable over the domain. There exist ζ, η with $0 < \zeta \leq \eta \leq 1$, $\zeta + \eta \leq 1$ and $\alpha \geq 0$, $\lambda > 0$ such that

$$H1: \quad b \in L^{\infty}_{\text{loc}}(\mathbb{R}^+ \times \mathbb{R}^+ \times \mathbb{R}^+), \tag{4.1}$$

$H2$:

$$K(x,y) = \begin{cases} \lambda xy & (x,y) \in]0,1[\times]0,1[\\ \lambda xy^{-\alpha} & (x,y) \in]0,1[\times]1,\infty[\\ \lambda x^{-\alpha}y & (x,y) \in]1,\infty[\times]0,1[\\ \lambda(x^{\zeta}y^{\eta} + x^{\eta}y^{\zeta}) & (x,y) \in]1,\infty[\times]1,\infty[. \end{cases} \tag{4.2}$$

This chapter's contents are organized as follows. The discretization methodology based on the FVM and non-conservative form of fully discretized CBE are introduced in Section 4.1, followed by the detailed convergence analysis in Section 4.2. In Section 4.3, we examine the first order error estimates of FVM on uniform meshes. Additionally, we have justified the theoretical error estimation via numerical results in Section 4.4.

4.1 Numerical Scheme

In this section, we commence exploring the FVM for the solution of Eq.(1.8). Particle volumes ranging from 0 to ∞ are taken into account in Eq.(1.8). Nevertheless, we define the particle volumes to be in a finite domain for practical purposes. The scheme considers $]0,R]$ as truncated domain with $0 < R < \infty$. Thus the collisional breakage equation is truncated as

$$\frac{\partial c(t,x)}{\partial t} = \int_0^R \int_x^R K(y,z)b(x,y,z)c(t,y)c(t,z)\,dy\,dz - \int_0^R K(x,y)c(t,x)c(t,y)\,dy, \tag{4.3}$$

and

$$c(0,x) \;=\; c^{in}(x) \geq 0, \quad x \in]0,R]. \tag{4.4}$$

Consider a partitioning of the operating domain $]0,R]$ into small cells as

$$\Lambda_i^h :=]x_{i-1/2}, x_{i+1/2}],\ i = 1,2,\ldots,\mathrm{I},$$

where $x_{1/2} = 0,\ \ x_{\mathrm{I}+1/2} = R,\ \ \Delta x_i = x_{i+1/2} - x_{i-1/2}$ and consider $h = \max \Delta x_i\ \forall\ i$. The grid points are the midpoints of each subinterval and are designated as $x_i\ \forall\, i$. Now,

the expression of the mean value of the concentration function $c_i(t)$ in the cell Λ_i^h is determined by

$$c_i(t) = \frac{1}{\Delta x_i} \int_{x_{i-1/2}}^{x_{i+1/2}} c(t,x)\, dx. \tag{4.5}$$

The domain is confined in the range [0, T] for the time parameter, and it is discretized into N time intervals with time step Δt. The interval is defined as

$$\tau_n = [t_n, t_{n+1}[,\ n = 0, 1, \ldots, N-1.$$

We now begin developing the scheme on non-uniform meshes. It has the significant advantage of allowing the inclusion of a more extensive domain with fewer mesh points than a uniform mesh. Here, in this work, we have used a non-conservative scheme [81] which is based on using finite volume implementation from the continuous equation (1.8). To derive the discretized version of the CBE (4.3), we proceed as follows: integrating the Eq.(4.3) with respect to x over i^{th} cell yields the following discrete form

$$\frac{dc_i}{dt} = B_C(i) - D_C(i), \tag{4.6}$$

where

$$B_C(i) = \frac{1}{\Delta x_i} \int_{x_{i-1/2}}^{x_{i+1/2}} \int_0^{x_{\mathrm{I}+1/2}} \int_x^{x_{\mathrm{I}+1/2}} K(y,z) b(x,y,z) c(t,y) c(t,z) dy\, dz\, dx$$

$$D_C(i) = \frac{1}{\Delta x_i} \int_{x_{i-1/2}}^{x_{i+1/2}} \int_0^{x_{\mathrm{I}+1/2}} K(x,y) c(t,x) c(t,y) dy\, dx$$

along with initial distribution,

$$c_i(0) = c_i^{in} = \frac{1}{\Delta x_i} \int_{x_{i-1/2}}^{x_{i+1/2}} c_0(x)\, dx. \tag{4.7}$$

Implementing the midpoint rule to all of the above representations provide the semi-discrete equation after some simplifications as, see [81],

$$\frac{dc_i}{dt} = \frac{1}{\Delta x_i} \sum_{l=1}^{\mathrm{I}} \sum_{j=i}^{\mathrm{I}} K_{j,l} c_j(t) c_l(t) \Delta x_j \Delta x_l \int_{x_{i-1/2}}^{p_j^i} b(x, x_j, x_l)\, dx - \sum_{j=1}^{\mathrm{I}} K_{i,j} c_i(t) c_j(t) \Delta x_j, \tag{4.8}$$

where the term p_j^i is expressed by

$$p_j^i = \begin{cases} x_i, & \text{if } j = i \\ x_{i+1/2}, & j \neq i. \end{cases} \tag{4.9}$$

Now, to obtain a fully discrete system, applying explicit Euler discretization to time variable t leads to

$$c_i^{n+1} - c_i^n = \frac{\Delta t}{\Delta x_i} \sum_{l=1}^{\mathrm{I}} \sum_{j=i}^{\mathrm{I}} K_{j,l} c_j^n c_l^n \Delta x_j \Delta x_l \int_{x_{i-1/2}}^{p_j^i} b(x, x_j, x_l)\, dx - \Delta t \sum_{j=1}^{\mathrm{I}} K_{i,j} c_i^n c_j^n \Delta x_j. \tag{4.10}$$

For the convergence analysis, consider a function c^h on $[0,T]\times]0,R]$ which is representated in 2.14 and also mentioning that

$$c^h(0,\cdot) = \sum_{i=1}^{\mathrm{I}} c_i^{in} \chi_{\Lambda_i^h}(\cdot) \to c^{in} \in L^1]0,R[\text{ as } h \to 0.$$

The discrete form of the kernels $K^h(x,y)$ and $b^h(x,y,z)$ are formed using FVS that are similar to (2.15, 2.16).

4.2 Weak Convergence

The objective of this section is to study the convergence of solution c^h to a function c as h and $\Delta t \to 0$.

Theorem 4.2.1. Consider that $c^{in} \in X^+$ and the hypothesis $(H1) - (H2)$ on kernels hold. Also assuming that under the time step Δt and for a constant $\theta > 0$, the following stability condition

$$C(R,T)\Delta t \leq \theta < 1, \tag{4.11}$$

holds for

$$C(R,T) := \lambda(2R\|c^{in}\|_{L^1} e^{2\lambda R\|b\|_{L^\infty} M_1^{in} T} + M_1^{in}). \tag{4.12}$$

Then there exists the extraction of a sub-sequence as

$$c^h \to c \ \text{ in } \ L^\infty([0,T];L^1]0,R[),$$

for c being the weak solution to (1.8-1.9) on $[0,T]$. This implies that, the function $c \geq 0$ satisfies

$$\int_0^T \int_0^R c(t,x)\frac{\partial \varphi}{\partial t}(t,x)dx\,dt - \int_0^T \int_0^R \int_0^R \int_x^R \varphi(t,x)K(y,z)b(x,y,z)c(t,y)c(t,z)dy\,dz\,dx\,dt$$
$$+ \int_0^R c^{in}(x)\varphi(0,x)dx + \int_0^T \int_0^R \int_0^R \varphi(t,x)K(x,y)c(t,x)c(t,y)dy\,dx\,dt = 0, \tag{4.13}$$

where φ is compactly supported smooth functions on $[0,T]\times]0,R]$.

By following the above theorem, the main task here certainly is to establish $(c^h) \rightharpoonup c$ in $L^1(0,R)$ as h and Δt go to zero. The idea is picked from the Dunford-Pettis theorem that provides the guarantee for weak sequential compactness in L^1.

As a result, demonstrating the properties of the family c^h in L^1 as given in (2.25) and (2.26), respectively, are sufficient to establish Theorem 4.2.1. The following proposition addresses the same.

Proposition 4.2.2. Assume that the stability criterion (4.11) holds for time step Δt. Furthermore, assuming that the kernel growth condition satisfies $(H1)-(H2)$. Then c^h is a non-negative function that fulfills the estimation given below

$$\int_0^R X^h(x)c^h(t,x)dx \leq \int_0^R X^h(x)c^h(s,x)dx \leq \int_0^R X^h(x)c^h(0,x)dx =: M_1^{in}, \tag{4.14}$$

where $0 \leq s \leq t \leq T$, and

$$\int_0^R c^h(t,x)dx \leq \|c^{in}\|_{L^1}\, e^{2\lambda R\|b\|_{L^\infty} M_1^{in} t}. \tag{4.15}$$

Proof. Mathematical induction is used to demonstrate the non-negativity and equiboundedness of the function c^h. At $t=0$, it is known that $c^h(0) \geq 0$ and included in $L^1]0,R[$. Assuming that the functions $c^h(t^n) \geq 0$ and

$$\int_0^R c^h(t^n,x)dx \leq \|c^{in}\|_{L^1}\, e^{2\lambda R\|b\|_{L^\infty} M_1^{in} t^n}. \tag{4.16}$$

Then, our first goal is to demonstrate that $c^h(t^{n+1}) \geq 0$. Consider the cell at the boundary with index $i = 1$. As a result, in this situation, we obtain from Eq.(4.10),

$$\begin{aligned} c_1^{n+1} =& c_1^n + \frac{\Delta t}{\Delta x_1} \sum_{l=1}^{\mathrm{I}} \sum_{j=1}^{\mathrm{I}} K_{j,l} c_j^n c_l^n \Delta x_j \Delta x_l \int_{x_{1/2}}^{p_j^1} b(x, x_j, x_l)\, dx - \Delta t \sum_{j=1}^{\mathrm{I}} K_{1,j} c_1^n c_j^n \Delta x_j \\ \geq& c_1^n - \Delta t \sum_{j=1}^{\mathrm{I}} K_{1,j} c_1^n c_j^n \Delta x_j. \end{aligned} \tag{4.17}$$

Moving further, we choose the first case for collisional kernel, case-(1): $K(x, y) = \lambda(x^\zeta y^\eta + x^\eta y^\zeta)$, when $(x, y) \in]1, R[\times]1, R[$. Thus,

$$c_1^{n+1} \geq c_1^n - \Delta t \sum_{j=1}^{\mathrm{I}} \lambda(x_1^\zeta x_j^\eta + x_1^\eta x_j^\zeta) c_1^n c_j^n \Delta x_j,$$

using the fact that $\lambda(x_i^\zeta x_j^\eta + x_i^\eta x_j^\zeta) \leq \lambda(x_i + x_j)$, thanks to Young's inequality, we convert the above inequality into the following one

$$\begin{aligned} c_1^{n+1} \geq\ & c_1^n - \lambda \Delta t \sum_{j=1}^{\mathrm{I}} (x_1 + x_j) c_1^n c_j^n \Delta x_j \\ & \geq [1 - \lambda \Delta t (R \sum_{j=1}^{\mathrm{I}} c_j^n \Delta x_j + M_1^{in})] c_1^n. \end{aligned} \tag{4.18}$$

Now, consider case-(2): $K(x, y) = \lambda x^{-\alpha} y$, when $(x, y) \in]1, R[\times]0, 1[$. Putting this value in Eq.(4.17) and then imposing the condition $x^{-\alpha} \leq 1$ yield

$$\begin{aligned} c_1^{n+1} \geq\ & c_1^n - \lambda \Delta t \sum_{j=1}^{\mathrm{I}} x_j c_1^n c_j^n \Delta x_j \\ & \geq (1 - \lambda \Delta t M_1^{in}) c_1^n. \end{aligned} \tag{4.19}$$

For case-(3): $K(x, y) = \lambda x y^{-\alpha}$, when $(x, y) \in]0, 1[\times]1, R[$ with $y^{-\alpha} \leq 1$ and for case-(4): $K(x, y) = \lambda(xy)$, when $(x, y) \in]0, 1[\times]0, 1[$ provide

$$c_1^{n+1} \geq (1 - \lambda \Delta t \sum_{j=1}^{\mathrm{I}} c_j^n \Delta x_j) c_1^n. \tag{4.20}$$

All the results from case(1)-case(4) are collected, and the following inequality is achieved

$$c_1^{n+1} \geq [1 - \lambda \Delta t (R \sum_{j=1}^{\mathrm{I}} c_j^n \Delta x_j + M_1^{in})] c_1^n. \tag{4.21}$$

Using conditions (4.11), (4.12) and Eq.(4.16), the non-negativity of c_1^{n+1} is obtained. Thus, we assume that the computations for $i \geq 2$ go similar to $i = 1$ for all four cases and the results are obtained like the previous ones. Then, applying the stability condition (4.11) and the L^1 bound on c^h yield $c^h(t^{n+1}) \geq 0$.

Further, by summing (4.10) over i, the following time monotonicity result is obtained for the total mass as

$$\sum_{i=0}^{\mathrm{I}} \Delta x_i x_i c_i^{n+1} = \sum_{i=0}^{\mathrm{I}} \Delta x_i x_i c_i^n + \Delta t \sum_{i=1}^{\mathrm{I}} \sum_{l=1}^{\mathrm{I}} \sum_{j=i}^{\mathrm{I}} x_i K_{j,l} c_j^n c_l^n \Delta x_j \Delta x_l \int_{x_{i-1/2}}^{p_j^i} b(x, x_j, x_l)\, dx$$
$$- \Delta t \sum_{i=1}^{\mathrm{I}} \sum_{j=1}^{\mathrm{I}} x_i K_{i,j} c_i^n c_j^n \Delta x_j \Delta x_i. \tag{4.22}$$

Change the order of summation, taking the upper limit of p_j^i and Eq.(1.10) in the second term on the right-hand side (RHS) of equation (4.22) leads to

$$\Delta t \sum_{i=1}^{\mathrm{I}} \sum_{l=1}^{\mathrm{I}} \sum_{j=i}^{\mathrm{I}} x_i K_{j,l} c_j^n c_l^n \Delta x_j \Delta x_l \int_{x_{i-1/2}}^{p_j^i} b(x, x_j, x_l)\, dx$$
$$\leq \Delta t \sum_{l=1}^{\mathrm{I}} \sum_{j=1}^{\mathrm{I}} K_{j,l} c_j^n c_l^n \Delta x_j \Delta x_l \sum_{i=1}^{j} x_i \int_{x_{i-1/2}}^{x_{i+1/2}} b(x, x_j, x_l)\, dx$$
$$= \Delta t \sum_{l=1}^{\mathrm{I}} \sum_{j=1}^{\mathrm{I}} K_{j,l} c_j^n c_l^n \Delta x_j \Delta x_l \sum_{i=1}^{j} x_i b(x_i, x_j, x_l) \Delta x_i = \Delta t \sum_{l=1}^{\mathrm{I}} \sum_{j=1}^{\mathrm{I}} x_j K_{j,l} c_j^n c_l^n \Delta x_j \Delta x_l. \tag{4.23}$$

Eqs.(4.22) and (4.23) indicate about the approximate mass loss property

$$\sum_{i=0}^{\mathrm{I}} \Delta x_i x_i c_i^{n+1} \leq \sum_{i=0}^{\mathrm{I}} \Delta x_i x_i c_i^n \leq M_1^{in}. \tag{4.24}$$

Following that, it is demonstrated that $c^h(t^{n+1})$ follows a similar estimation as (4.16). To see this, multiply equation (4.10) by the term Δx_i, leaving the negative term out, and determine the result using summation with respect to i, as

$$\sum_{i=1}^{\mathrm{I}} c_i^{n+1} \Delta x_i \leq \sum_{i=1}^{\mathrm{I}} c_i^n \Delta x_i + \Delta t \sum_{i=1}^{\mathrm{I}} \sum_{l=1}^{\mathrm{I}} \sum_{j=i}^{\mathrm{I}} K_{j,l} c_j^n c_l^n \Delta x_j \Delta x_l \int_{x_{i-1/2}}^{p_j^i} b(x, x_j, x_l)\, dx$$
$$\leq \sum_{i=1}^{\mathrm{I}} c_i^n \Delta x_i + \Delta t \|b\|_\infty \sum_{i=1}^{\mathrm{I}} \sum_{l=1}^{\mathrm{I}} \sum_{j=1}^{\mathrm{I}} K_{j,l} c_j^n c_l^n \Delta x_j \Delta x_l \int_{x_{i-1/2}}^{x_{i+1/2}} dx$$

$$\leq \sum_{i=1}^{\mathrm{I}} c_i^n \Delta x_i + \Delta t R \|b\|_\infty \sum_{l=1}^{\mathrm{I}} \sum_{j=1}^{\mathrm{I}} K_{j,l} c_j^n c_l^n \Delta x_j \Delta x_l. \tag{4.25}$$

Again, the above will be simplified for four cases of kernels:

Case-(1): $K(x,y) = \lambda(x^\zeta y^\eta + x^\eta y^\zeta)$, when $(x,y) \in]1,R[\times]1,R[$. Substitute the value of $K(x,y)$ in Eq.(4.25) and use the Young's inequality to get

$$\begin{aligned}\sum_{i=1}^{\mathrm{I}} c_i^{n+1} \Delta x_i &\leq \sum_{i=1}^{\mathrm{I}} c_i^n \Delta x_i + \lambda \Delta t R \|b\|_\infty \sum_{l=1}^{\mathrm{I}} \sum_{j=1}^{\mathrm{I}} (x_j + x_l) c_j^n c_l^n \Delta x_j \Delta x_l \\ &\leq (1 + 2\lambda \Delta t R \|b\|_\infty M_1^{in}) \sum_{i=1}^{\mathrm{I}} c_i^n \Delta x_i.\end{aligned}$$

Finally, having (4.16) the L^1 bound of c^h at time step n and $1 + x < \exp(x)\ \forall\ x > 0$ imply that

$$\sum_{i=1}^{\mathrm{I}} c_i^{n+1} \Delta x_i \leq \|c^{in}\|_{L^1}\, e^{2\lambda R \|b\|_{L^\infty} M_1^{in} t^{n+1}}.$$

As a consequence, the result (4.15) is accomplished.

Case-(2): $K(x,y) = \lambda x^{-\alpha} y$, when $(x,y) \in]1,R[\times]0,1[$, and case-(3): $K(x,y) = \lambda x y^{-\alpha}$, when $(x,y) \in]0,1[\times]1,R[$ have similar computations. The value of $K(x,y)$ after substituting in Eq.(4.25) yields

$$\begin{aligned}\sum_{i=1}^{\mathrm{I}} c_i^{n+1} \Delta x_i &\leq \sum_{i=1}^{\mathrm{I}} c_i^n \Delta x_i + \lambda \Delta t R \|b\|_\infty \sum_{l=1}^{\mathrm{I}} \sum_{j=1}^{\mathrm{I}} (x_j^{-\alpha} x_l) c_j^n c_l^n \Delta x_j \Delta x_l \\ &\leq \sum_{i=1}^{\mathrm{I}} c_i^n \Delta x_i + \lambda \Delta t R \|b\|_\infty \sum_{l=1}^{\mathrm{I}} \sum_{j=1}^{\mathrm{I}} x_l c_j^n c_l^n \Delta x_j \Delta x_l \\ &\leq (1 + \lambda \Delta t R \|b\|_\infty M_1^{in}) \sum_{i=1}^{\mathrm{I}} c_i^n \Delta x_i.\end{aligned}$$

Again, using (4.16) and $1 + x < \exp(x)\ \forall\ x > 0$ provide the L^1 bound for c^h at time step $n+1$.

Case-(4): For $K(x,y) = \lambda(xy)$, when $(x,y) \in]0,1[\times]0,1[$, inserting the value of K in Eq.(4.25) employs

$$\sum_{i=1}^{\mathrm{I}} c_i^{n+1} \Delta x_i \leq \sum_{i=1}^{\mathrm{I}} c_i^n \Delta x_i + \lambda \Delta t R \|b\|_\infty \sum_{l=1}^{\mathrm{I}} \sum_{j=1}^{\mathrm{I}} x_j x_l c_j^n c_l^n \Delta x_j \Delta x_l$$

$$\leq \sum_{i=1}^{\mathrm{I}} c_i^n \Delta x_i + \lambda \Delta t R \|b\|_\infty \sum_{l=1}^{\mathrm{I}} \sum_{j=1}^{\mathrm{I}} x_l c_j^n c_l^n \Delta x_j \Delta x_l.$$

To get the result (4.15) for $c^h(t^{n+1})$, the computations are similar to the previous case. □

To demonstrate the family of solutions's uniform integrability, let us designate a specific category of convex functions as $C_{VP,\infty}$. Consider $\Phi \in C^\infty([0,\infty[)$, a non-negative and convex function that belongs to the $C_{VP,\infty}$ class and has the following properties [92]:

(i) $\Phi(0) = 0,\ \Phi'(0) = 1$ and Φ' is concave;

(ii) $\lim_{p\to\infty} \Phi'(p) = \lim_{p\to\infty} \frac{\Phi(p)}{p} = \infty$;

(iii) for $\theta \in]1,2[$,

$$\Pi_\theta(\Phi) := \sup_{p\geq 0} \left\{ \frac{\Phi(p)}{p^\theta} \right\} < \infty. \tag{4.26}$$

It is given that, $c^{in} \in L^1(0,R)$, therefore, by De La Vallée Poussin theorem, a convex function $\Phi \geq 0$ exists which satisfies

$$\frac{\Phi(p)}{p} \to \infty, \ \text{ as } \ p \to \infty$$

and

$$\mathcal{I} := \int_0^R \Phi(c^{in})(x)dx < \infty. \tag{4.27}$$

The equiintegrability is now examined in the following statement.

Proposition 4.2.3. Let $c^{in} \geq 0 \in L^1]0,R[$ and (4.10) constructs the family (c^h) for any h and Δt, where Δt fulfills the relation (4.11). Then (c^h) is weakly sequentially compact in $L^1(]0,T[\times]0,R[)$.

Proof. The objective here is to acquire a result comparable to (4.27) for the function family c^h. Using the sequence c_i^n, the integral of (c^h) may be expressed as

$$\int_0^T \int_0^R \Phi(c^h(t,x))dx\,dt = \sum_{n=0}^{N-1} \sum_{i=1}^{\mathrm{I}} \int_{\tau_n} \int_{\Lambda_i^h} \Phi\Big(\sum_{k=0}^{N-1} \sum_{j=1}^{\mathrm{I}} c_j^k \chi_{\Lambda_j^h}(x) \chi_{\tau_k}(t) \Big) dx\,dt$$

$$= \sum_{n=0}^{N-1} \sum_{i=1}^{\mathrm{I}} \Delta t \Delta x_i \Phi(c_i^n).$$

It follows from the discrete Eq.(4.10), as well as the convex property of Φ and $\Phi^{'} \geq 0$, that

$$\begin{aligned}
\sum_{i=1}^{\mathrm{I}} [\Phi(c_i^{n+1}) - \Phi(c_i^n)] \Delta x_i &\leq \sum_{i=1}^{\mathrm{I}} \left(c_i^{n+1} - c_i^n\right) \Phi^{'}(c_i^{n+1}) \Delta x_i \\
&\leq \Delta t \sum_{i=1}^{\mathrm{I}} \sum_{l=1}^{\mathrm{I}} \sum_{j=i}^{\mathrm{I}} K_{j,l} c_j^n c_l^n \Phi^{'}(c_i^{n+1}) \Delta x_j \Delta x_l \int_{x_{i-1/2}}^{x_{i+1/2}} b(x, x_j, x_l)\, dx \\
&\leq \Delta t \sum_{i=1}^{\mathrm{I}} \sum_{l=1}^{\mathrm{I}} \sum_{j=1}^{\mathrm{I}} K_{j,l} c_j^n c_l^n \Phi^{'}(c_i^{n+1}) \Delta x_j \Delta x_l b(x_i, x_j, x_l) \Delta x_i.
\end{aligned} \tag{4.28}$$

Case-(1): $K(x,y) = \lambda(x^{\zeta} y^{\eta} + x^{\eta} y^{\zeta})$, when $(x,y) \in]1, R[\times]1, R[$. Substitute the value of $K(x,y)$ in Eq.(4.28) yields

$$\sum_{i=1}^{\mathrm{I}} [\Phi(c_i^{n+1}) - \Phi(c_i^n)] \Delta x_i \leq \lambda \Delta t \sum_{i=1}^{\mathrm{I}} \sum_{l=1}^{\mathrm{I}} \sum_{j=1}^{\mathrm{I}} (x_j + x_l) c_j^n \Delta x_j c_l^n \Delta x_l \Delta x_i b(x_i, x_j, x_l) \Phi^{'}(c_i^{n+1}).$$

The convexity result in Lemma 2.4.4 allows us to obtain

$$\begin{aligned}
\sum_{i=1}^{\mathrm{I}} [\Phi(c_i^{n+1}) - \Phi(c_i^n)] \Delta x_i &\leq 2\lambda \Delta t \sum_{i=1}^{\mathrm{I}} \sum_{l=1}^{\mathrm{I}} \sum_{j=1}^{\mathrm{I}} x_j c_j^n \Delta x_j c_l^n \Delta x_l \Delta x_i [\Phi(c_i^{n+1}) + \Phi(b(x_i, x_j, x_l))] \\
&\leq 2\lambda \Delta t \sum_{i=1}^{\mathrm{I}} \sum_{l=1}^{\mathrm{I}} \sum_{j=1}^{\mathrm{I}} x_j c_j^n \Delta x_j c_l^n \Delta x_l \Delta x_i \Phi(c_i^{n+1}) \\
&+ 2\lambda \Delta t \sum_{i=1}^{\mathrm{I}} \sum_{l=1}^{\mathrm{I}} \sum_{j=1}^{\mathrm{I}} x_j c_j^n \Delta x_j c_l^n \Delta x_l \Delta x_i \Phi(b(x_i, x_j, x_l)).
\end{aligned} \tag{4.29}$$

After employing Eq.(4.26) and Eq.(4.15) into the second term on the RHS of the Eq.(4.29) lead to

$$\begin{aligned}
&2\lambda \Delta t \sum_{i=1}^{\mathrm{I}} \sum_{l=1}^{\mathrm{I}} \sum_{j=1}^{\mathrm{I}} x_j c_j^n \Delta x_j c_l^n \Delta x_l \Delta x_i \Phi(b(x_i, x_j, x_l)) \\
&\qquad = 2\lambda \Delta t \sum_{i=1}^{\mathrm{I}} \sum_{l=1}^{\mathrm{I}} \sum_{j=1}^{\mathrm{I}} x_j c_j^n \Delta x_j c_l^n \Delta x_l \Delta x_i \frac{\Phi(b(x_i, x_j, x_l))}{\{b(x_i, x_j, x_l)\}^{\theta}} b(x_i, x_j, x_l)^{\theta}
\end{aligned}$$

$$\leq 2\lambda\Delta t R\Pi_\theta(\Phi)M_1^{in}\|b\|_\infty^\theta \sum_{l=1}^{\mathrm{I}} c_l^n \Delta x_l$$
$$\leq 2\lambda\Delta t R\Pi_\theta(\Phi)M_1^{in}\|b\|_\infty^\theta \|c^{in}\|_{L^1}\, e^{2\lambda R\|b\|_{L^\infty} M_1^{in}T}. \tag{4.30}$$

Now, Eq.(4.29) and Eq.(4.30) imply that

$$\sum_{i=1}^{\mathrm{I}}[\Phi(c_i^{n+1})-\Phi(c_i^n)]\Delta x_i \leq 2\lambda\Delta t M_1^{in}\|c^{in}\|_{L^1}\, e^{2\lambda R\|b\|_{L^\infty} M_1^{in}T}\sum_{i=1}^{\mathrm{I}}\Delta x_i\Phi(c_i^{n+1})$$
$$+ 2\lambda\Delta t R\Pi_\theta(\Phi)M_1^{in}\|b\|_\infty^\theta \|c^{in}\|_{L^1}\, e^{2\lambda R\|b\|_{L^\infty} M_1^{in}T}.$$

It is reasonable to simplify as

$$(1-2\lambda\Delta t M_1^{in}\|c^{in}\|_{L^1}\, e^{2\lambda R\|b\|_{L^\infty} M_1^{in}T})\sum_{i=1}^{\mathrm{I}}\Delta x_i\Phi(c_i^{n+1}) \leq \sum_{i=1}^{\mathrm{I}}\Delta x_i\Phi(c_i^n)$$
$$+2\lambda\Delta t R\Pi_\theta(\Phi)M_1^{in}\|b\|_\infty^\theta \|c^{in}\|_{L^1}\, e^{2\lambda R\|b\|_{L^\infty} M_1^{in}T}.$$

The above inequality implies that

$$\sum_{i=1}^{\mathrm{I}}\Delta x_i\Phi(c_i^{n+1}) \leq A\sum_{i=1}^{\mathrm{I}}\Delta x_i\Phi(c_i^n) + B,$$

where

$$A=\frac{1}{(1-2\lambda\Delta t M_1^{in}\|c^{in}\|_{L^1}\, e^{2\lambda R\|b\|_{L^\infty} M_1^{in}T})},\ B=\frac{2\lambda\Delta t R\Pi_\theta(\Phi)M_1^{in}\|b\|_\infty^\theta \|c^{in}\|_{L^1}\, e^{2\lambda R\|b\|_{L^\infty} M_1^{in}T}}{(1-2\lambda\Delta t M_1^{in}\|c^{in}\|_{L^1}\, e^{2\lambda R\|b\|_{L^\infty} M_1^{in}T})}.$$

Therefore,

$$\sum_{i=1}^{\mathrm{I}}\Delta x_i\Phi(c_i^n) \leq A^n\sum_{i=1}^{\mathrm{I}}\Delta x_i\Phi(c_i^{in}) + B\frac{A^n-1}{A-1}. \tag{4.31}$$

Thanks to Jensen's inequality and having (4.27), we obtain

$$\int_0^{\mathbb{R}}\Phi(c^h(t,x))\,dx \leq A^n\sum_{i=1}^{\mathrm{I}(h)}\Delta x_i\Phi\left(\frac{1}{\Delta x_i}\int_{\Lambda_i^h} c^{in}(x)dx\right) + B\frac{A^n-1}{A-1}$$
$$\leq A^n\mathcal{I} + B\frac{A^n-1}{A-1} < \infty, \quad \text{for all} \quad t\in[0,T]. \tag{4.32}$$

The computations for Case-(2), Case-(3) and Case-(4) are equivalent to the Case-(1). Only just, we got the different values of A and B, which are the following

$$A=\frac{1}{(1-\lambda\Delta t M_1^{in}\|c^{in}\|_{L^1}\, e^{2\lambda R\|b\|_{L^\infty} M_1^{in}T})},\ B=\frac{\lambda\Delta t R\Pi_\theta(\Phi)M_1^{in}\|b\|_\infty^\theta \|c^{in}\|_{L^1}\, e^{2\lambda R\|b\|_{L^\infty} M_1^{in}T}}{(1-\lambda\Delta t M_1^{in}\|c^{in}\|_{L^1}\, e^{2\lambda R\|b\|_{L^\infty} M_1^{in}T})}.$$

Thus, the sequence (c^h) is said to be weakly compact in L^1 by applying the Dunford-Pettis theorem and ensures the existence of a subsequence of (c^h) that converges weakly to $c \in L^1(]0,T[\times]0,R[)$ as $h \to 0$. □

The time has arrived to demonstrate the weak convergence of the sequence c_i^n, which is formed by a succession of step functions c^h. To do this, various point approximations are utilized, which are as seen in (2.43-2.45).

We have now accumulated all the evidences required to support Theorem 4.2.1. To demonstrate this, take a test function $\varphi \in C^1([0,T]\times]0,R])$ with compact support with respect to t in $[0,t_{N-1}]$ for small t. Establish the finite volume for time variable and left endpoint approximation for space variable of φ on $\tau_n \times \Lambda_i^h$ by

$$\varphi_i^n = \frac{1}{\Delta t}\int_{t_n}^{t_{n+1}} \varphi(t, x_{i-1/2})dt.$$

Multiplication of φ_i^n with (4.10) yields the following equation after employing the summation over n & i

$$\begin{aligned}\sum_{n=0}^{N-1}\sum_{i=1}^{\mathrm{I}} \Delta x_i(c_i^{n+1}-c_i^n)\varphi_i^n =& \Delta t\sum_{n=0}^{N-1}\sum_{i=1}^{\mathrm{I}}\sum_{l=1}^{\mathrm{I}}\sum_{j=i}^{\mathrm{I}} K_{j,l}c_j^n c_l^n \Delta x_j \Delta x_l \varphi_i^n \int_{x_{i-1/2}}^{p_j^i} b(x,x_j,x_l)dx \\ &- \Delta t\sum_{n=0}^{N-1}\sum_{i=1}^{\mathrm{I}}\sum_{j=1}^{\mathrm{I}} K_{i,j}c_i^n c_j^n \Delta x_i \Delta x_j \varphi_i^n. \end{aligned} \tag{4.33}$$

When the summation for n is separated, the LHS resembles like this

$$\sum_{n=0}^{N-1}\sum_{i=1}^{\mathrm{I}} \Delta x_i(c_i^{n+1}-c_i^n)\varphi_i^n = \sum_{n=0}^{N-1}\sum_{i=1}^{\mathrm{I}} \Delta x_i c_i^{n+1}(\varphi_i^{n+1}-\varphi_i^n) + \sum_{i=1}^{\mathrm{I}} \Delta x_i c_i^{in}\varphi_i^0.$$

Moreover, evaluating the latter equation using the function c^h yields

$$\begin{aligned}\sum_{n=0}^{N-1}\sum_{i=1}^{\mathrm{I}} \Delta x_i(c_i^{n+1}-c_i^n)\varphi_i^n =& \sum_{n=0}^{N-1}\sum_{i=1}^{\mathrm{I}}\int_{\tau_{n+1}}\int_{\Lambda_i^h} c^h(t,x)\frac{\varphi(t,\xi^h(x))-\varphi(t-\Delta t,\xi^h(x))}{\Delta t}dx\,dt \\ &+ \sum_{i=1}^{\mathrm{I}}\int_{\Lambda_i^h} c^h(0,x)\frac{1}{\Delta t}\int_0^{\Delta t}\varphi(t,\xi^h(x))dt\,dx \\ =& \int_{\Delta t}^{T}\int_0^{R} c^h(t,x)\frac{\varphi(t,\xi^h(x))-\varphi(t-\Delta t,\xi^h(x))}{\Delta t}dx\,dt\end{aligned}$$

$$+\int_0^R c^h(0,x)\frac{1}{\Delta t}\int_0^{\Delta t}\varphi(t,\xi^h(x))dt\,dx.$$

Since, $\varphi \in C^1([0,T]\times]0,R])$ posseses compact support and having bounded derivative, $c^h(0,x) \to c^{in}$ in $L^1]0,R[$ will provide the following result with the help of Lemma 2.1.5

$$\int_0^R c^h(0,x)\frac{1}{\Delta t}\int_0^{\Delta t}\varphi(t,\xi^h(x))dtdx \to \int_0^R c^{in}(x)\varphi(0,x)dx \tag{4.34}$$

as $\max\{h,\Delta t\}$ goes to 0. Now, applying Taylor series expansion of φ, Lemma 2.1.5 and Proposition 4.2.3 ensure that for $\max\{h,\Delta t\} \to 0$

$$\int_0^T\int_0^R c^h(t,x)\frac{\varphi(t,\xi^h(x))-\varphi(t-\Delta t,\xi^h(x))}{\Delta t}dx\,dt \to \int_0^T\int_0^R c(t,x)\frac{\partial\varphi}{\partial t}(t,x)dx\,dt,$$

and hence, we obtain

$$\begin{aligned}&\int_{\Delta t}^T\int_0^R \underbrace{c^h(t,x)\frac{\varphi(t,\xi^h(x))-\varphi(t-\Delta t,\xi^h(x))}{\Delta t}}_{c(\varphi)}dx\,dt\\ &=\int_0^T\int_0^R c(\varphi)\,dx\,dt-\int_0^{\Delta t}\int_0^R c(\varphi)\,dx\,dt \to \int_0^T\int_0^R c(t,x)\frac{\partial\varphi}{\partial t}(t,x)dx\,dt.\end{aligned} \tag{4.35}$$

Now, the first term in the RHS of Eq.(4.33) is taken for observing the computation

$$\begin{aligned}&\Delta t\sum_{n=0}^{N-1}\sum_{i=1}^{\mathrm{I}}\sum_{l=1}^{\mathrm{I}}\sum_{j=i}^{\mathrm{I}}K_{j,l}c_j^nc_l^n\Delta x_j\Delta x_l\varphi_i^n\int_{x_{i-1/2}}^{p_j^i}b(x,x_j,x_l)dx\\ &\qquad=\Delta t\sum_{n=0}^{N-1}\sum_{i=1}^{\mathrm{I}}\sum_{l=1}^{\mathrm{I}}K_{i,l}c_i^nc_l^n\Delta x_i\Delta x_l\varphi_i^n\int_{x_{i-1/2}}^{x_i}b(x,x_i,x_l)dx\\ &\qquad+\Delta t\sum_{n=0}^{N-1}\sum_{i=1}^{\mathrm{I}}\sum_{l=1}^{\mathrm{I}}\sum_{j=i+1}^{\mathrm{I}}K_{j,l}c_j^nc_l^n\Delta x_j\Delta x_l\varphi_i^n\int_{x_{i-1/2}}^{x_{i+1/2}}b(x,x_j,x_l)dx.\end{aligned} \tag{4.36}$$

The first term on the RHS of Eq.(4.36) simplifies to

$$\begin{aligned}&\Delta t\sum_{n=0}^{N-1}\sum_{i=1}^{\mathrm{I}}\sum_{l=1}^{\mathrm{I}}K_{i,l}c_i^nc_l^n\Delta x_i\Delta x_l\varphi_i^n\int_{x_{i-1/2}}^{x_i}b(x,x_i,x_l)dx\\ &=\sum_{n=0}^{N-1}\sum_{i=1}^{\mathrm{I}}\sum_{l=1}^{\mathrm{I}}\int_{\tau_n}\int_{\Lambda_i^h}\int_{\Lambda_l^h}K^h(x,z)c^h(t,x)c^h(t,z)\varphi(t,\xi^h(x))\int_{\xi^h(x)}^{X^h(x)}b(r,X^h(x),X^h(z))dr\,dz\,dx\,dt\\ &=\int_0^T\int_0^R\int_0^R K^h(x,z)c^h(t,x)c^h(t,z)\varphi(t,\xi^h(x))\int_{\xi^h(x)}^{X^h(x)}b(r,X^h(x),X^h(z))dr\,dz\,dx\,dt.\end{aligned} \tag{4.37}$$

Next, the second term of Eq.(4.36) leads to

$$\Delta t \sum_{n=0}^{N-1} \sum_{i=1}^{\mathrm{I}} \sum_{l=1}^{\mathrm{I}} \sum_{j=i+1}^{\mathrm{I}} K_{j,l} c_j^n c_l^n \Delta x_j \Delta x_l \varphi_i^n \int_{x_{i-1/2}}^{x_{i+1/2}} b(x, x_j, x_l) dx =$$

$$= \sum_{n=0}^{N-1} \sum_{i=1}^{\mathrm{I}} \sum_{l=1}^{\mathrm{I}} \sum_{j=i+1}^{\mathrm{I}} \int_{\tau_n} \int_{\Lambda_i^h} \int_{\Lambda_l^h} \int_{\Lambda_j^h} \Big\{ K^h(y,z) c^h(t,y) c^h(t,z) \varphi(t, \xi^h(x)) \frac{1}{\Delta x_i} \int_{\Lambda_i^h} b(r, X^h(y), X^h(z)) dr \Big\} dy\, dz\, dx\, dt$$

$$= \int_0^T \int_0^R \int_0^R \int_{\Xi^h(x)}^R K^h(y,z) c^h(t,y) c^h(t,z) \varphi(t, \xi^h(x)) b(X^h(x), X^h(y), X^h(z)) dy\, dz\, dx\, dt. \tag{4.38}$$

Eqs.(4.36)-(4.38), Lemma 2.1.5 and Proposition 4.2.3 imply that as $\max\{h, \Delta t\} \to 0$

$$\Delta t \sum_{n=0}^{N-1} \sum_{i=1}^{\mathrm{I}} \sum_{l=1}^{\mathrm{I}} \sum_{j=i}^{\mathrm{I}} K_{j,l} c_j^n c_l^n \Delta x_j \Delta x_l \varphi_i^n \int_{x_{i-1/2}}^{p_j^i} b(x, x_j, x_l) dx$$
$$\to \int_0^T \int_0^R \int_0^R \int_x^R K(y,z) c(t,y) c(t,z) \varphi(t,x) b(x,y,z) dy\, dz\, dx\, dt. \tag{4.39}$$

Taking the second term on the RHS of Eq.(4.33) employs

$$\Delta t \sum_{n=0}^{N-1} \sum_{i=1}^{\mathrm{I}} \sum_{j=1}^{\mathrm{I}} K_{i,j} c_i^n c_j^n \Delta x_i \Delta x_j \varphi_i^n$$
$$= \sum_{n=0}^{N-1} \sum_{i=1}^{\mathrm{I}} \sum_{j=1}^{\mathrm{I}} \int_{\tau_n} \int_{\Lambda_i^h} \int_{\Lambda_j^h} K^h(x,y) c^h(t,x) c^h(t,y) \varphi(t, \xi^h(x)) dy\, dx\, dt$$
$$\to \int_0^T \int_0^R \int_0^R K(x,y) c(t,x) c(t,y) \varphi(t,x) dy\, dx\, dt \tag{4.40}$$

as $\max\{h, \Delta t\} \to 0$. Eqs.(4.33)-(4.40) deliver the desired results for the weak convergence as presented in Eq.(4.13).

4.3 Error Simulation

In this section, the error estimation is explored for CBE, which is based on the idea of [50]. Taking the uniform mesh is crucial for estimating the error component, i.e.,

$\Delta x_i = h \ \forall i \in \{1, 2, \ldots, \mathrm{I}\}$. The error estimate is achieved by providing an estimation on the difference $c^h - c$, where c^h is constructed using the numerical technique and c represents the exact solution to the problem (1.8). By using the following theorem, we can determine the error estimate by making some assumptions about the kernels and the initial datum.

Theorem 4.3.1. Let the collisional and breakage kernels satisfy $K \in W^{1,\infty}_{loc}(\mathbb{R}^+ \times \mathbb{R}^+)$, $b \in W^{1,\infty}_{loc}(\mathbb{R}^+ \times \mathbb{R}^+ \times \mathbb{R}^+)$ and initial datum $c^{in} \in W^{1,\infty}_{loc}(\mathbb{R}^+)$. Moreover, assuming a uniform mesh and Δt that fulfill the condition (4.11). Then the error estimate obtained with a constant $H_{T,R} > 0$ such that

$$\|c^h - c\|_{L^\infty(0,T;L^1]0,R[)} \leq H_{T,R}(h + \Delta t) \tag{4.41}$$

holds, where c is the weak solution to (1.8-1.9).

Before proving the theorem, consider the following proposition, which provides estimates on the approximate and precise solutions c^h and c, respectively, given certain additional assumptions. These estimates are important in the analysis of the error.

Proposition 4.3.2. Assume that kinetic parameters $K \in L^\infty_{loc}(\mathbb{R}^+ \times \mathbb{R}^+)$, $b \in L^\infty_{loc}(\mathbb{R}^+ \times \mathbb{R}^+ \times \mathbb{R}^+)$ and the condition (4.11) holds for time step Δt. Also, let the initial datum c^{in} is restricted in L^∞_{loc}. Then, solutions c^h and c to (1.8-1.9) are bounded on $]0, T[\times]0, R[$ as

$$\|c^h\|_{L^\infty(]0,T[\times]0,R[)} \leq H_{T,R}, \quad \|c\|_{L^\infty(]0,T[\times]0,R[)} \leq H_{T,R}.$$

Furthermore, if the kernels $K \in W^{1,\infty}_{loc}(\mathbb{R}^+ \times \mathbb{R}^+)$, $b \in W^{1,\infty}_{loc}(\mathbb{R}^+ \times \mathbb{R}^+ \times \mathbb{R}^+)$ and $c^{in} \in W^{1,\infty}_{loc}(\mathbb{R}^+)$, then

$$\|c\|_{W^{1,\infty}]0,R[} \leq H_{T,R}. \tag{4.42}$$

Proof. The principal purpose of this proposition is to obtain a bound on the solution c to Eq.(1.8). In consequence, integrating Eq.(4.3) concerning the time variable provides the following result

$$c(t,x) \leq c^{in}(x) + \int_0^t \int_0^R \int_x^R K(y,z)b(x,y,z)c(s,y)c(s,z)dy\,dz\,ds$$

$$\leq c^{in}(x) + \|K\|_\infty \|b\|_\infty \|c\|^2_{\infty,1} t,$$

where $\|c\|_{\infty,1}$ represents the norm of c in $L^\infty(0,T;L^1]0,R[\,)$. Hence,

$$\|c\|_{L^\infty(]0,T[\times]0,R[)} \leq H_{T,R}.$$

Now, let us go to the conclusion of an analysis of (4.42). First, integrate Eq.(4.3) over the time variable t, and then differentiate it with variable x which lead to

$$\frac{\partial c(t,x)}{\partial x} = \frac{\partial c^{in}(x)}{\partial x} + \frac{\partial}{\partial x}\left(\int_0^t \int_0^R \int_x^R K(y,z)b(x,y,z)c(s,y)c(s,z)dy\,dz\,ds\right) - \frac{\partial}{\partial x}\left(\int_0^t \int_0^R K(x,y)c(t,x)c(t,y)\,dy\right).$$

Use of the maximum value across the domain of x and simplification of compuatations yield the following condition

$$\left\|\frac{\partial c(t)}{\partial x}\right\|_\infty \leq \left\|\frac{\partial c^{in}(x)}{\partial x}\right\|_\infty + [\|Kb\|_\infty \|c\|_{\infty,1}\|c\|_\infty + \|K\|_\infty \|b\|_{W^{1,\infty}}\|c\|^2_{\infty,1} + \|K\|_{W^{1,\infty}}\|c\|_{\infty,1}\|c\|_\infty]t + \|K\|_\infty \|c\|_{\infty,1}\int_0^t \left\|\frac{\partial c}{\partial x}\right\|_\infty ds,$$

which can be written in a more coherent way

$$\left\|\frac{\partial c(t)}{\partial x}\right\|_\infty \leq \Upsilon(t) + \upsilon \int_0^t \left\|\frac{\partial c}{\partial x}\right\|_\infty ds,$$

where

$$\Upsilon(t) = \left\|\frac{\partial c^{in}(x)}{\partial x}\right\|_\infty + [\|Kb\|_\infty \|c\|_{\infty,1}\|c\|_\infty + \|K\|_\infty \|b\|_{W^{1,\infty}}\|c\|^2_{\infty,1} + \|K\|_{W^{1,\infty}}\|c\|_{\infty,1}\|c\|_\infty]t,$$

and

$$\upsilon = \|K\|_\infty \|c\|_{\infty,1}.$$

Beyond that, the use of Gronwall's lemma and integration by parts establish the proof as follows

$$\left\|\frac{\partial c(t)}{\partial x}\right\|_\infty \leq \Upsilon(t) + \int_0^t \Upsilon(s)\upsilon e^{\int_s^t \upsilon\,dr}\,ds \leq \Upsilon(0)e^{\upsilon t} + (\|Kb\|_\infty \|c\|_{\infty,1}\|c\|_\infty + \|K\|_\infty \|b\|_{W^{1,\infty}}\|c\|^2_{\infty,1}$$

$$+ \|K\|_{W^{1,\infty}} \|c\|_{\infty,1} \|c\|_{\infty})[(e^{vt} - 1)].$$

Therefore,

$$\left\| \frac{\partial c}{\partial x} \right\|_{L^\infty(]0,T[\times]0,R[)} \leq H_{T,R},$$

which concludes the result (4.42). □

Next, the RHS of equation (4.10) is converted into the continuous form, and we obtain the first-order terms in that process which is explained in the following lemma. The discrete collisional birth-death terms given as in (4.10) expressed like

$$B_C(i) - D_C(i) = \frac{1}{\Delta x_i} \sum_{l=1}^{\mathrm{I}} \sum_{j=i}^{\mathrm{I}} K_{j,l} c_j^n c_l^n \Delta x_j \Delta x_l \int_{x_{i-1/2}}^{p_j^i} b(x, x_j, x_l)\, dx - \sum_{j=1}^{\mathrm{I}} K_{i,j} c_i^n c_j^n \Delta x_j. \tag{4.43}$$

The subsequent lemma offers a simplified version of the preceding discrete terms.

Lemma 4.3.3. Consider the initial condition $c^{in} \in W^{1,\infty}_{loc}$ and uniform mesh, $\Delta x_i = h\ \forall i$. Also assuming that K and b follow the conditions $K, b \in W^{1,\infty}_{loc}$. Let $(s, x) \in \tau_n \times \Lambda_i^h$, where $n \in \{0, 1, \ldots, N-1\}$ and $i \in \{1, 2, \ldots, \mathrm{I}\}$. Then

$$\begin{aligned} B_C(i) - D_C(i) = &\int_0^R \int_{\Xi^h(x)}^R K^h(y, z) b^h(x, y, z) c^h(s, y) c^h(s, z)\, dydz \\ &- \int_0^R K^h(x, y) c^h(s, x) c^h(s, y)\, dy + \varepsilon(h). \end{aligned} \tag{4.44}$$

In the L^1, $\varepsilon(h)$ defines the first order term with regard to h:

$$\|\varepsilon(h)\|_{L^1} \leq \frac{\|Kb\|_{L^\infty}}{2} \|c^{in}\|_{L^1}^2\, e^{4\lambda R \|b\|_{L^\infty} M_1^{in} T} h. \tag{4.45}$$

Proof. Initiate with the discrete birth term of Eq.(4.43) and convert it to the continuous form with a uniform mesh and for $x \in \Lambda_i^h$,

$$\begin{aligned} &\frac{1}{\Delta x_i} \sum_{l=1}^{\mathrm{I}} \sum_{j=i}^{\mathrm{I}} K_{j,l} c_j^n c_l^n \Delta x_j \Delta x_l \int_{x_{i-1/2}}^{p_j^i} b(x, x_j, x_l)\, dx \\ &= \sum_{l=1}^{\mathrm{I}} \sum_{j=i+1}^{\mathrm{I}} K_{j,l} c_j^n c_l^n \Delta x_j \Delta x_l \frac{1}{\Delta x_i} \int_{x_{i-1/2}}^{x_{i+1/2}} b(x, x_j, x_l)\, dx + \sum_{l=1}^{\mathrm{I}} K_{i,l} c_i^n c_l^n \Delta x_l \int_{x_{i-1/2}}^{x_i} b(x, x_i, x_l)\, dx \end{aligned}$$

$$= \int_0^R \int_{\Xi^h(x)}^R K^h(y,z) b^h(x,y,z) c^h(s,y) c^h(s,z)\, dydz + \varepsilon(h), \tag{4.46}$$

where $\varepsilon(h) = \sum_{l=1}^{\mathrm{I}} K_{i,l} c_i^n c_l^n \Delta x_l \int_{x_{i-1/2}}^{x_i} b(x, x_i, x_l)\, dx$ is defined. Calculating the L^1 norm of $\varepsilon(h)$ leads to the following term

$$\begin{aligned}
\|\varepsilon(\mathbb{F}, h)\|_{L^1} &\leq \|Kb\|_{L^\infty} \sum_{i=1}^{\mathrm{I}} c_i^n \Delta x_i \sum_{l=1}^{\mathrm{I}} c_l^n \Delta x_l \int_{x_{i-1/2}}^{x_i} dx \\
&\leq \frac{\|Kb\|_{L^\infty}}{2} \big(\sum_{i=1}^{\mathrm{I}} c_i^n \Delta x_i \big)^2 h \\
&\leq \frac{\|Kb\|_{L^\infty}}{2} \|c^{in}\|_{L^1}^2 \, e^{4\lambda R \|b\|_{L^\infty} M_1^{in} T} h.
\end{aligned}$$

Now, taking the discrete death term of (4.43) yields

$$\sum_{j=1}^{\mathrm{I}} K_{i,j} c_i^n c_j^n \Delta x_j = \int_0^R K^h(x,y) c^h(s,x) c^h(s,y)\, dy. \tag{4.47}$$

Using the formula (4.44), Eq.(4.3) and Eq.(4.10) lead to the error formulation for $t \in \tau_n$ as

$$\begin{aligned}
\int_0^R |c^h(t,x) - c(t,x)| dx \leq \int_0^R |c^h(0,x) - c(0,x)| dx + \sum_{\beta=1}^{3} (CB)_\beta(h) \\
+ \int_0^R |\epsilon(t,n)|\, dx + \|\varepsilon(h)\|_{L^1} t,
\end{aligned} \tag{4.48}$$

where error terms are expressed by $(CB)_\beta(h)$ for $\beta = 1, 2, 3$ as

$$\begin{aligned}
(CB)_1(h) = \int_0^t \int_0^R \int_0^R \int_{\Xi^h(x)}^R |K^h(y,z) b^h(x,y,z) c^h(s,y) c^h(s,z) \\
- K(y,z) b(x,y,z) c(s,y) c(s,z)|\, dy\, dz\, dx\, ds,
\end{aligned}$$

$$(CB)_2(h) = \int_0^t \int_0^R \int_0^R \int_x^{\Xi^h(x)} K(y,z) b(x,y,z) c(s,y) c(s,z)\, dy\, dz\, dx\, ds,$$

and

$$(CB)_3(h) = \int_0^t \int_0^R \int_0^R |K^h(x,y) c^h(s,x) c^h(s,y) - K(x,y) c(s,x) c(s,y)|\, dy\, dx\, ds.$$

Considering $|t - t_n| \leq \Delta t$, the time discretization provides the following expression

$$\int_0^R |\epsilon(t,n)|\,dx \leq \int_{t_n}^t \int_0^R \int_0^R \int_{\Xi^h(x)}^R K^h(y,z) b^h(x,y,z) c^h(s,y) c^h(s,z)\,dy\,dz\,dx\,ds + \int_{t_n}^t \int_0^R \int_0^R K^h(x,y) c^h(s,x) c^h(s,y)\,dy\,dx\,ds + \int_{t_n}^t \int_0^R \varepsilon(h)\,dx\,ds.$$

Given $K, b \in W^{1,\infty}_{loc}$ and for $x, y \in]0, R]$, we have

$$|K^h(x,y) - K(x,y)| \leq \|K\|_{W^{1,\infty}} h.$$

As a result, it produces an estimate of $(CB)_1(h)$ using the L^1 bounds on c^h and c. To begin, divide the expression into four segments

$$\begin{aligned}(CB)_1(h) \leq & \int_0^t \int_0^R \int_0^R \int_0^R |K^h(y,z) - K(y,z)| b(x,y,z) c(s,y) c(s,z)\,dy\,dz\,dx\,ds \\ & + \int_0^t \int_0^R \int_0^R \int_0^R K^h(y,z) |b^h(x,y,z) - b(x,y,z)| c(s,y) c(s,z)\,dy\,dz\,dx\,ds \\ & + \int_0^t \int_0^R \int_0^R \int_0^R K^h(y,z) b^h(x,y,z) |c^h(s,y) - c(s,y)| c(s,z)\,dy\,dz\,dx\,ds \\ & + \int_0^t \int_0^R \int_0^R \int_0^R K^h(y,z) b^h(x,y,z) c^h(s,y) |c^h(s,z) - c(s,z)|\,dy\,dz\,dx\,ds.\end{aligned}$$

By simplifying and employing Proposition 4.3.2, the above may be transformed to

$$\begin{aligned}(CB)_1(h) \leq & (\|K\|_{W^{1,\infty}} \|b\|_\infty + \|K\|_\infty \|b\|_{W^{1,\infty}}) t R^3 \|c\|_\infty^2 h \\ & + R^2 \|K\|_\infty \|b\|_\infty (\|c\|_\infty + \|c^h\|_\infty) \int_0^t \|c^h(s) - c(s)\|_{L^1}\,ds, \end{aligned} \tag{4.49}$$

and similar estimation for $(CB)_3(h)$ gives

$$(CB)_3(h) \leq \|K\|_{W^{1,\infty}} t R^2 \|c\|_\infty^2 h + R \|K\|_\infty (\|c\|_\infty + \|c^h\|_\infty) \int_0^t \|c^h(s) - c(s)\|_{L^1}\,ds. \tag{4.50}$$

Moving on to the remaining terms, $(CB)_2(h)$ and $\int_0^R |\epsilon(t,n)|\,dx$, it is clear that

$$(CB)_2(h) \leq \frac{tR^2}{2} \|Kb\|_\infty \|c\|_\infty^2 h, \tag{4.51}$$

and

$$\int_0^R |\epsilon(t,n)|\,dx \leq (\|Kb\|_\infty \|c^h\|_\infty^2 R^3 + \|K\|_\infty \|c^h\|_\infty^2 R^2 + \|\epsilon(h)\|_{L^1})\Delta t. \tag{4.52}$$

Furthermore, substituting all the estimations (4.49)-(4.52) in (4.48) and applying the Gronwall's lemma conclude the result in (4.41). □

4.4 Numerical Testing

To test the problem's theoretical error estimation, in this part of the article, the discussion over experimental error and experimental order of convergence (EOC) are concluded for three combinations of collision kernel and breakage distribution function. In the first test case, an analytical solution of the model is available while such an expression does not exist for the other two test problems.

The experimental domain for the volume variable is taken as $[1e{-}3, 10]$ and computations are run from time 0 to 1. In the availability of analytical solution for CBE, the EOC formula is

$$\text{EOC} = \frac{1}{\ln(2)} \ln\left(\frac{E_{\text{I}}}{E_{2\text{I}}}\right), \tag{4.53}$$

where E_{I} is the discrete error norm using I number of mesh points, i.e., $E_{\text{I}} = \|N_E - N_{\text{I}}\|$, where N_E and N_I are the total number of particles generated analytically and numerically, respectively. Moreover, in order to observe the EOC of the FVS in the absence of analytical results, the following double mesh relation is used:

$$\text{EOC} = \ln\left(\frac{\|N_{\text{I}} - N_{2\text{I}}\|}{\|N_{2\text{I}} - N_{4\text{I}}\|}\right) / \ln(2). \tag{4.54}$$

Here, N_{I} denotes the total number of particles generated by the FVS (4.10) with a mesh of I number of cells.

Test Case 1: Consider $K(y,z) = yz$ and $b(x,y,z) = \frac{(\aleph+2)x^\aleph}{(y)^{\aleph+1}}, -1 < \aleph \leq 0$. The computation is exhibited only for $\aleph = 0$, where we have analytical result, see [23]. The

exponential decay initial condition (e^{-x}) supports this problem. The computational domain is divided into uniform subintervals of 30, 60, 120, and 240 number of cells. The analytical concentration function is given as $c(t,x) = e^{-(1+t)x}(1+t)^2$. Table 4.1 represents the numerical errors and the EOC examined through Eq.(4.53). It is observed that the scheme provides the error in decreasing pattern as grid gets refined and it is of first-order convergence, as predicted by the theoretical results in Section 4.3. It is interesting to mention here that $\aleph = 0$ leads to the breakage function which is having singularity near the origin, a case for which theoretical result is not discussed. However, the FVS still maintains the first order accuracy on uniform meshes. Therefore, a probable task in the future is to study the analysis such that classes of singular kernels can be included.

Cells	Error	EOC
30	0.4879×10^{-4}	-
60	0.2196×10^{-4}	1.1515
120	0.1032×10^{-4}	1.0901
240	0.0498×10^{-4}	1.0497

Table 4.1: Test Case 1

Test Cases 2-3: For the second and third examples, assume $K(y,z) = yz$ and $K(y,z) = y + z$, respectively, along with breakage function $b(x,y,z) = \delta(x - 0.4y) + \delta(x - 0.6y)$. As analytical concentration functions are unavailable in the literature, the error and the EOC are calculated via Eq.(4.54) for uniform cells with 30, 60, 120, 240, and 480 degrees of freedom. The computational volume domain and execution time are identical to the preceding test case. Again, according to Tables 4.2 and 4.3, the EOC of the FVS for these cases are comparable to the first case, i.e., the first-order convergence is noticed.

Cells	Error	EOC
30	-	-
60	0.4271×10^{-4}	-
120	0.2006×10^{-4}	1.0899
240	0.0973×10^{-4}	1.0449
480	0.0479×10^{-4}	1.0224

Table 4.2: Test Case 2

Cells	Error	EOC
30	-	-
60	0.4309×10^{-4}	-
120	0.2023×10^{-4}	1.0905
240	0.0981×10^{-4}	1.0452
480	0.0483×10^{-4}	1.0226

Table 4.3: Test Case 3

Chapter 5

Analytic Approximate Solution and Error Estimates for Non-linear Collision-Induced Breakage Equation

---

According to the literature survey [68, 72, 95], VIM and ODM are more suitable and efficient for solving non-linear ODEs/PDEs and integro PDEs including aggregation and breakage equations. As per our knowledge, there is no literature on semi-analytical techniques for non-linear CBE (1.8-1.9). For the first time, in this chapter, these methods are introduced for Eqs.(1.8-1.9) that provide the solutions in series form. The focus of the work is to deal with the theoretical convergence analysis for a particular class of kernels and the error estimation. Further, for the numerical validation, three examples are selected to demonstrate the superiority of VIM over ODM.

This chapter is framed as follows: Section 5.1 contains information on the preliminary steps for VIM and ODM, as well as their applications on CBE (1.8-1.9). The theoretical results on convergence and error analysis are presented in Section 5.2. Section 5.3 yields the numerical implementation and comparison between ODM, VIM, and exact solutions by providing the error graphs and tables.

5.1 Semi-analytical Approaches

5.1.1 Variational iteration method

VIM [96] is used to solve variety of non-linear ODEs/PDEs without linearization and small perturbations. This approach is feasible and effective for dealing with the non-linear problems. To understand the general idea of the VIM for any ODEs/PDEs, let us consider

$$\mathcal{L}(c(t,x)) + M(c(t,x)) = 0, \tag{5.1}$$

where $\mathcal{L} = \frac{\partial}{\partial t}$ (linear) and M (non-linear) are operators. According to VIM, we get the correction functional for Eq.(5.1) as

$$c_{k+1}(t,x) = c_k(t,x) + \int_0^t \Big[\lambda\Big(\mathcal{L}(c_k(\tau,x)) + M(\tilde{c}_k(\tau,x))\Big)\Big]\, d\tau. \tag{5.2}$$

Eq.(5.2) has a Lagrange multiplier $\lambda = -1$ that can be found optimally via variational theory, and $\tilde{c}_k$ is a restricted variation which means $\delta\tilde{c}_k = 0$, see [96] for more details. This provides the following iteration formula

$$c_{k+1}(t,x) = c_k(t,x) - \int_0^t \Big[\Big(\mathcal{L}(c_k(\tau,x)) + M(c_k(\tau,x))\Big)\Big]\, d\tau. \tag{5.3}$$

Let us construct the operator $A[c]$ as follows:

$$A[c] = \int_0^t \Big[-\Big(\mathcal{L}c(\tau,x) + Mc(\tau,x)\Big)\Big]\, d\tau, \tag{5.4}$$

then the solution of problem (5.1) is written in series form as $c(t,x) = \sum_{k=0}^{\infty} c_k(t,x)$ where the components $c_k(t,x)$ for $k = 0, 1, 2, ...$, are defined as

$$\left.\begin{aligned} c_0(t,x) &= c^{in}(x), \\ c_1(t,x) &= A[c_0(t,x)], \\ c_{k+1}(t,x) &= A[c_0(t,x) + c_1(t,x) + ... + c_k(t,x)],\ k \geq 1. \end{aligned}\right\} \tag{5.5}$$

An nth order truncated series solution of the result $c(t,x)$ is considered as $\varphi_n(t,x)$ and is denoted by

$$\varphi_n(t,x) := \sum_{k=0}^{n} c_k(t,x). \tag{5.6}$$

In the following, the general formulation for the n-term series solution for the CBE (1.8-1.9) is described.

VIM for CBE: Define the non-linear operator M as follows

$$Mc(t,x) = -\left(\int_0^\infty \int_x^\infty K(y,z)b(x,y,z)c(t,y)c(t,z)\,dy\,dz - \int_0^\infty K(x,y)c(t,x)c(t,y)\,dy\right). \tag{5.7}$$

Using the Eqs.(5.3), (5.7) and $\lambda = -1$, we get the following iteration formula to compute the number density function

$$\begin{aligned} c_{k+1}(t,x) =& c_k(t,x) + \int_0^t \left(-\frac{\partial c_k(\tau,x)}{\partial \tau} + \int_0^\infty \int_x^\infty K(y,z)b(x,y,z)c_k(\tau,y)c_k(\tau,z)\,dy\,dz \right. \\ & \left. - \int_0^\infty K(x,y)c_k(\tau,x)c_k(\tau,y)\,dy\right)d\tau \\ =& c_k(t,x) + A[c]. \end{aligned} \tag{5.8}$$

Using the above, the solution components are derived from the Eq.(5.5) and hence, an approximate series solution of nth-order is formed using n+1 components. We will simplify the details for various specific kernels in the numerical section.

5.1.2 Optimized decomposition method

This section contains a detailed explanation of ODM [95] for analytically solving Eqs.(1.8-1.9). Before going into this, let us address the essential concept of the proposed strategy for solving the following non-linear PDE

$$\frac{\partial}{\partial t}c(t,x) = M[c(t,x)], \tag{5.9}$$

where M is a non-linear operator and $\mathcal{L} = \frac{\partial}{\partial t}$. Applying inverse operator of $\mathcal{L}$ on (5.9) leads to

$$c(t,x) = c^{in}(x) + \mathcal{L}^{-1}\{M[c(t,x)]\}. \tag{5.10}$$

The fundamental concept of ODM lies in the linear approximation of non-linear term by a first-order Taylor series expansion at $t = 0$. Thus, the obtained approximation is

$$\frac{\partial}{\partial t}c(t,x) - M[c(t,x)] \approx \frac{\partial}{\partial t}c(t,x) - C(x)c, \tag{5.11}$$

where

$$C(x) = \left.\frac{\partial M}{\partial c}\right|_{t=0}. \tag{5.12}$$

The approximation mentioned above yields, a linear operator T specified by

$$T[c(t,x)] = M[c(t,x)] - C(x)c(t,x). \tag{5.13}$$

The solution is now constructed as an infinite series, by following [95], and is given by

$$c(t,x) = \sum_{k=0}^{\infty} c_k(t,x), \tag{5.14}$$

where the components are listed below

$$\left.\begin{aligned} c_0(t,x) &= c^{in}(x), \\ c_1(t,x) &= \mathcal{L}^{-1}[Q_0(t,x)], \\ c_2(t,x) &= \mathcal{L}^{-1}[Q_1(t,x) - C(x)c_1(t,x)], \\ c_{k+1}(t,x) &= \mathcal{L}^{-1}[Q_k(t,x) - C(x)(c_k(t,x) - c_{k-1}(t,x))],\ k \geq 2, \end{aligned}\right\} \tag{5.15}$$

with

$$Q_k(t,x) = \frac{1}{k!}\frac{d^k}{d\theta^k}\left[M\Big(\sum_{i=0}^{k}\theta^i c_i(t,x)\Big)\right]\Bigg|_{\theta=0}, \tag{5.16}$$

and

$$M\Big(\sum_{k=0}^{\infty} c_k(t,x)\Big) = \sum_{k=0}^{\infty} Q_k(t,x). \tag{5.17}$$

ODM for CBE: To obtain a ODM formulation for Eqs.(1.8-1.9), consider the non-linear operator $M[c(t,x)]$ as

$$M[c(t,x)] = \int_0^{\infty}\int_x^{\infty} K(y,z)b(x,y,z)c(t,y)c(t,z)\,dy\,dz - \int_0^{\infty} K(x,y)c(t,x)c(t,y)\,dy, \tag{5.18}$$

and differentiating it with respect to $c(t,x)$, we have at $t = 0$,

$$C(x) = -\int_0^{\infty} K(x,y)c(0,y)\,dy. \tag{5.19}$$

The linear operator T in Eq.(5.13) expresses the following equation after utilizing the Eqs.(5.18) and (5.19)

$$T[c(t,x)] = \int_0^\infty \int_x^\infty K(y,z)b(x,y,z)c(t,y)c(t,z)\,dy\,dz - \int_0^\infty K(x,y)c(t,x)c(t,y)\,dy + c(t,x)\int_0^\infty K(x,y)c(0,y)\,dy. \tag{5.20}$$

Using Eq.(5.18) and setting $k=0$ in Eq.(5.16), the term Q_0 is expressed as

$$Q_0(t,x) = \int_0^\infty \int_x^\infty K(y,z)b(x,y,z)c_0(t,y)c_0(t,z)\,dy\,dz - \int_0^\infty K(x,y)c_0(t,x)c_0(t,y)\,dy,$$

therefore,

$$c_1(t,x) = \mathcal{L}^{-1}\Big(\int_0^\infty \int_x^\infty K(y,z)b(x,y,z)c_0(t,y)c_0(t,z)\,dy\,dz - \int_0^\infty K(x,y)c_0(t,x)c_0(t,y)\,dy\Big). \tag{5.21}$$

For $k=1$, Eqs.(5.16) and (5.18) yield

$$Q_1(t,x) = \int_0^\infty \int_x^\infty K(y,z)b(x,y,z)\Big(c_0(t,y)c_1(t,z) + c_1(t,y)c_0(t,z)\Big)\,dy\,dz - \int_0^\infty K(x,y)\Big(c_0(t,x)c_1(t,y) + c_1(t,x)c_0(t,y)\Big)\,dy,$$

and hence, with assistance of Eq.(5.19), it provides

$$\begin{aligned} c_2(t,x) =& \mathcal{L}^{-1}\Bigg(\int_0^\infty \int_x^\infty K(y,z)b(x,y,z)\Big(c_0(t,y)c_1(t,z) + c_1(t,y)c_0(t,z)\Big)\,dy\,dz \\ &- \int_0^\infty K(x,y)\Big(c_0(t,x)c_1(t,y) + c_1(t,x)c_0(t,y)\Big)\,dy \\ &+ c_1(t,x)\int_0^\infty K(x,y)c(0,y)\,dy\Bigg). \end{aligned} \tag{5.22}$$

For $k \geq 2$ and only when $i+j=k$, we have

$$Q_k(t,x) = \int_0^\infty \int_x^\infty K(y,z)b(x,y,z)\Big(\sum_{i=0}^{k} c_i(t,y)\sum_{j=0}^{k} c_j(t,z)\Big)\,dy\,dz - \int_0^\infty K(x,y)\Big(\sum_{i=0}^{k} c_i(t,x)\sum_{j=0}^{k} c_j(t,y)\Big)\,dy,$$

and

$$c_{k+1}(t,x) = \mathcal{L}^{-1}\Big(\int_0^\infty \int_x^\infty K(y,z)b(x,y,z)\Big(\sum_{i=0}^{k} c_i(t,y)\sum_{j=0}^{k} c_j(t,z)\Big)\,dy\,dz - \int_0^\infty K(x,y)\Big(\sum_{i=0}^{k} c_i(t,x)\sum_{j=0}^{k} c_j(t,y)\Big)\,dy - C(x)[c_k(t,x) - c_{k-1}(t,x)]\Big). \tag{5.23}$$

Hence, Eq.(5.15) leads to the n-term series solution of Eqs.(1.8-1.9) as

$$\begin{aligned}\psi_n(t,x) := \sum_{k=0}^{n} c_k(t,x) &= c^{in}(x) + \mathcal{L}^{-1}\Big(\sum_{k=1}^{n} Q_{k-1}(t,x) - C(x)c_{n-1}(t,x)\Big) \\ &= c^{in}(x) + \mathcal{L}^{-1}\Big(M(\psi_{n-1}(t,x)) - C(x)c_{n-1}(t,x)\Big). \end{aligned} \tag{5.24}$$

5.2 Convergence Analysis

This section has discussion about the convergence of VIM and ODM solutions towards the precise ones including the error estimates for the finite term approximated solutions. The following results guarantee the convergence of VIM and provide the worst upper bound for error considering n-term series solution.

Theorem 5.2.1. Let the operator $A[c]$, mentioned in (5.4), be defined on a Hilbert space D to D. The series solution $c(t,x) = \sum_{k=0}^{\infty} c_k(t,x)$ converges, if

$$\|A[c_0(t,x) + c_1(t,x) + \cdots + c_{k+1}(t,x)]\| \le \alpha\|A[c_0(t,x) + c_1(t,x) + \cdots + c_k(t,x)]\|,$$

i.e., $\|c_{k+1}(t,x)\| \le \alpha\|c_k(t,x)\|$, where $0 < \alpha < 1$ and $\forall k \in \{0\} \cup \mathbb{N}$.

Proof. The proof of this result is explained by Z.M. Odibat in [96][see, Theorem 5.2.1]. □

Theorem 5.2.2. Let the series solution $\sum_{k=0}^{\infty} c_k(t,x)$ converges to the analytical solution $c(t,x)$, then the truncated solution φ_n of $c(t,x)$ has the maximum error bound

$$\|c - \varphi_n\| \le \frac{1}{1-\alpha}\alpha^{1+n}\|c^{in}\|, \quad \text{with } 0 < \alpha < 1. \tag{5.25}$$

Proof. The details of the result is provided in [96]. □

It is clear from Theorems 5.2.1 and 5.2.2 and by following the idea of [96] that $\forall i \in \{0\} \cup \mathbb{N}$, the parameters,

$$\gamma_i = \begin{cases} \frac{\|c_{i+1}\|}{\|c_i\|}, & \text{if } \|c_i\| \neq 0 \\ 0, & \text{if } \|c_i\| = 0, \end{cases} \tag{5.26}$$

provide the assurance of series convergence, when $0 \leq \gamma_i < 1$. Thus, our main aim for the convergence in VIM is to compute the values of γ_i and show that $0 \leq \gamma_i < 1$ holds for all i.

Let us begin with the convergence analysis for ODM solution. For this, assume a Banach space $\mathbb{Y} = \big(\mathcal{C}\big([0,\Gamma] : L^1((0,\infty), xdx)\big), c \geq 0, \|\cdot\|\big)$ (see, [36]) with the following enduced norm

$$\|c\| = \sup_{t\in[0,\Gamma]} \int_0^\infty x|c(t,x)|dx < \infty. \tag{5.27}$$

Eq.(1.8) provides the new form by using the Eqs.(5.10) and (5.18), that is

$$c = \mathcal{S}c, \tag{5.28}$$

where $\mathcal{S} : \mathbb{Y} \to \mathbb{Y}$ is a non-linear operator given as

$$\mathcal{S}c = c^{in}(x) + \mathcal{L}^{-1}\Big[\int_0^\infty \int_x^\infty K(y,z)b(x,y,z)c(t,y)c(t,z)\,dy\,dz - \int_0^\infty K(x,y)c(t,x)c(t,y)\,dy\Big]. \tag{5.29}$$

To establish the convergence result, let's first prove that the operator $\mathcal{S}$ is contractive. To do so, develop an equivalent form

$$\frac{\partial}{\partial t}[c(t,x)\exp[G(t,x,c)]] = \exp[G(t,x,c)] \int_0^\infty \int_x^\infty K(y,z)b(x,y,z)c(t,y)c(t,z)\,dy\,dz,$$

where,

$$G(t,x,c) = \int_0^t \int_0^\infty K(x,y)c(\nu,y)\,dy\,d\nu.$$

Hence, the equivalent operator of $\mathcal{S}$ is expressed by $\tilde{\mathcal{S}}$ as

$$\tilde{\mathcal{S}}c = c^{in}(x)\exp[-G(t,x,c)]$$

$$+\int_0^t \exp[G(\nu,x,c)-G(t,x,c)]\int_0^\infty\int_x^\infty K(y,z)b(x,y,z)c(\nu,y)c(\nu,z)\,dy\,dz\,d\nu. \tag{5.30}$$

In general, it is not easy to demonstrate the contractive nature of $\tilde{\mathcal{S}}$ due to the model's complexity. However, for a specific set of kernels, in the following theorem, the self-mapping and contraction results are proved under some additional hypotheses.

Theorem 5.2.3. Assume that the non-linear operator $\tilde{\mathcal{S}}$ is defined in (5.30) and the set $\mathbb{D}$ is introduced as $\mathbb{D}=\{c\in\mathbb{Y}:\ \|c\|\le L\}$. If the following hypotheses

(a) $K(x,y)=xy,\quad b(x,y,z)=\frac{2}{y},\quad$ and $\quad c^{in}(x)=\exp(-x)\ \forall\, x,y,z\in(0,\infty)$,

(b) $\eta:=\frac{1}{e}+\frac{3}{e}\mu_2(0)Lt_1<1$, and $\max(\|c^{in}\|,\mu_2(0))(1+Lt_0)\le L$ for $t_0,t_1\in[0,\Gamma]$

hold, then the operator $\tilde{\mathcal{S}}:\mathbb{D}\to\mathbb{D}$ and has contractive nature, i.e., $\|\tilde{\mathcal{S}}c_1-\tilde{\mathcal{S}}c_2\|\le\eta\|c_1-c_2\|,\forall\,(c_1,c_2)\in\mathbb{D}\times\mathbb{D}$.

Proof. Let us begin with the proof of $\tilde{\mathcal{S}}:\mathbb{D}\to\mathbb{D}$. For this, multiplying Eq.(5.30) with x and integrating over the domain of x provide

$$\begin{aligned}\|\tilde{\mathcal{S}}\|&\le\|c^{in}\|+\int_0^t\int_0^\infty\exp[G(\nu,x,c)-G(t,x,c)]\int_0^\infty\int_x^\infty 2xzc(\nu,y)c(\nu,z)\,dy\,dz\,dx\,d\nu\\&\le\|c^{in}\|+\int_0^t\int_0^\infty\exp\Big[-\int_\nu^t\int_0^\infty xyc(\xi,y)\,dy\,d\xi\Big]\int_0^\infty\int_x^\infty 2xzc(\nu,y)c(\nu,z)\,dy\,dz\,dx\,d\nu\\&\le\|c^{in}\|+\int_0^t\int_0^\infty\int_0^\infty\int_x^\infty 2xzc(\nu,y)c(\nu,z)\,dy\,dz\,dx\,d\nu.\end{aligned}$$

After changing the order of integration, we received

$$\begin{aligned}\|\tilde{\mathcal{S}}\|&\le\|c^{in}\|+\int_0^t\int_0^\infty\int_0^\infty\int_0^y 2xzc(\nu,y)c(\nu,z)\,dx\,dy\,dz\,d\nu\\&\le\|c^{in}\|+\mu_2(0)Lt.\end{aligned}$$

Hence, $\|\tilde{\mathcal{S}}\|\le L$ holds if $\max(\|c^{in}\|,\mu_2(0))(1+Lt_0)\le L$ is considered, for a suitable parameter $t_0\in(0,\Gamma)$.

Now, choose $c_1,c_2\in\mathbb{D}$. The expression of $\tilde{\mathcal{S}}c_1-\tilde{\mathcal{S}}c_2$ is given by

$$\tilde{\mathcal{S}}c_1-\tilde{\mathcal{S}}c_2=c^{in}(x)F(0,t,x)+\int_0^t F(\nu,t,x)\int_0^\infty\int_x^\infty k(y,z)b(x,y,z)c_1(\nu,y)c_1(\nu,z)\,dy\,dz\,d\nu$$

$$
\begin{aligned}
&+\int_0^t F(\nu,t,x)\int_0^\infty\int_x^\infty k(y,z)b(x,y,z)c_2(\nu,y)c_2(\nu,z)\,dy\,dz\,d\nu\\
&+\int_0^t \exp[G(\nu,x,c_2)-G(t,x,c_2)]\int_0^\infty\int_x^\infty K(y,z)b(x,y,z)c_1(\nu,y)c_1(\nu,z)\,dy\,dz\,d\nu\\
&-\int_0^t \exp[G(\nu,x,c_1)-G(t,x,c_1)]\int_0^\infty\int_x^\infty K(y,z)b(x,y,z)c_2(\nu,y)c_2(\nu,z)\,dy\,dz\,d\nu,
\end{aligned}
\tag{5.31}
$$

where,

$$F(\nu,t,x)=\exp[G(\nu,x,c_1)-G(t,x,c_1)]-\exp[G(\nu,x,c_2)-G(t,x,c_2)].$$

It should be mentioned here that the considered set of kernels, provide the mass conservation [76], i.e., $\mu_1(t)=\mu_1(0)=1$. An upper bound of F can be obtained by using $e^{-x}-e^{-y}\le -e^{-x}(x-y)$ and $xe^{-x}\le\frac{1}{e}$ for all $x,y\in[0,\infty)$, as

$$
\begin{aligned}
|F(\nu,t,x)| &= \left|\exp\Big[-\int_\nu^t\int_0^\infty xyc_1(\xi,y)\,dy\,d\xi\Big]-\exp\Big[-\int_\nu^t\int_0^\infty xyc_2(\xi,y)\,dy\,d\xi\Big]\right|\\
&\le \exp\Big[-\int_\nu^t\int_0^\infty xyc_1(\xi,y)\,dy\,d\xi\Big]x(t-\nu)\|c_1-c_2\|\\
&= x(t-\nu)\exp[-x(t-\nu)\|c_1\|]\|c_1-c_2\|\\
&= x(t-\nu)\|c_1\|\exp[-x(t-\nu)\|c_1\|]\,\|c_1-c_2\|\le\frac{1}{e}\|c_1-c_2\|.
\end{aligned}
\tag{5.32}
$$

To display the contractive map of $\tilde{\mathcal{S}}:\mathbb{D}\to\mathbb{D}$, employ the norm on Eq.(5.31) and utilizing the values of K,b, and Eq.(5.32), we have

$$
\begin{aligned}
\|\tilde{\mathcal{S}}c_1-\tilde{\mathcal{S}}c_2\|\le&\frac{1}{e}\|c_1-c_2\|\|c^{in}\|\\
&+\frac{2}{e}\|c_1-c_2\|\int_0^t\int_0^\infty\int_0^\infty\int_0^y xz\{c_1(\nu,y)c_1(\nu,z)+c_2(\nu,y)c_2(\nu,z)\}\,dx\,dy\,dz\,d\nu\\
&+2\Bigg[\int_0^t\exp[G(\nu,x,c_1)-G(t,x,c_1)]\int_0^\infty\int_0^\infty\int_0^y xzc_2(\nu,y)c_2(\nu,z)\,dx\,dy\,dz\,d\nu\\
&-\int_0^t\exp[G(\nu,x,c_2)-G(t,x,c_2)]\int_0^\infty\int_0^\infty\int_0^y xzc_1(\nu,y)c_1(\nu,z)\,dx\,dy\,dz\,d\nu\Bigg].
\end{aligned}
$$

It is known from [76] that the second moment of Eqs.(1.8-1.9) is $\mu_2(t)=\frac{2}{1+t}$ which is clearly bounded by $\mu_2(0)$. Using this fact and Eq.(5.32) as well as some further simplifi-

cations, the above inequality becomes

$$\begin{aligned}\|\tilde{\mathcal{S}}c_1 - \tilde{\mathcal{S}}c_2\| \leq & \frac{1}{e}\|c_1 - c_2\|\|c^{in}\| + \frac{1}{e}\|c_1 - c_2\|\mu_2(0)t\{\|c_1\| + \|c_2\|\} \\ & + \int_0^t \exp[G(\nu, x, c_1) - G(t, x, c_1)]\mu_2(0)\|c_2\|\, d\nu \\ & - \int_0^t \exp[G(\nu, x, c_2) - G(t, x, c_2)]\mu_2(0)\|c_1\|\, d\nu \\ \leq & \frac{1}{e}\|c_1 - c_2\| + \frac{2}{e}\|c_1 - c_2\|L\mu_2(0)t + L\mu_2(0)\int_0^t F(\nu, t, x)\, d\nu \\ \leq & \Big(\frac{1}{e} + \frac{3}{e}\mu_2(0)Lt\Big)\|c_1 - c_2\|. \end{aligned} \tag{5.33}$$

Hence, the operator $\tilde{\mathcal{S}}$ holds contractive property under the condition that $\eta := \frac{1}{e} + \frac{3}{e}\mu_2(0)Lt_1 < 1$, for the selective parameter t_1. Consequently, an invariant ball of radius L exists for a small parameter $t = \min(t_0, t_1)$, and $\tilde{\mathcal{S}}$ is contractive within this ball. □

Theorem 5.2.4. Let the series solution $\sum_{k=0}^{\infty} c_k(t, x)$ converges to the analytical solution $c(t, x)$ and the truncated solution ψ_n of $c(t, x)$ has the maximum error bound

$$\|c - \psi_m\| \leq \frac{\eta^m}{1 - \eta}\|c_1\|, \tag{5.34}$$

if the following assumptions satisfy

(A) $\eta := \frac{1}{e} + \frac{3}{e}\mu_2(0)Lt_0 < 1$, where $L = \mu_1(1 + \Gamma)$ with $\Gamma \in (0, t)$ and $\|c_1\| < \infty$.

(B) for any $0 \leq l \leq m - 1$, $\|c_{m-l} - c_{m-(l+1)}\| < \epsilon$, where $\epsilon = \frac{1}{n^p}$ such that $p > 1$.

Proof. Initially, with assistance of Eqs.(5.18), (5.24) and (6.40), n-term truncated solution develops into

$$\psi_n(t, x) = \tilde{\mathcal{S}}\psi_{n-1}(t, x) - \int_0^t C(x)c_{n-1}(\nu, x)d\nu. \tag{5.35}$$

Consider the term $\|\psi_n(t, x) - \psi_m(t, x)\|$. Applying the triangle inequality for $n \geq m$ provides

$$\|\psi_n(t, x) - \psi_m(t, x)\| \leq \|\tilde{\mathcal{S}}\psi_{n-1} - \tilde{\mathcal{S}}\psi_{m-1}\| + \|\int_0^t C(x)\big(c_{n-1}(\nu, x) - c_{m-1}(\nu, x)\big)d\nu\|. \tag{5.36}$$

Imposing the result of Theorem 5.2.3 and hypothesis (**B**) lead to

$$\|\psi_n(t,x) - \psi_m(t,x)\| \leq \eta\|\psi_{n-1} - \psi_{m-1}\| + \epsilon\, t.$$

The overhead inequality is converted into the following one after setting $n = m+1$, Eq.(5.36) and doing some further simplifications

$$\begin{aligned}
\|\psi_{m+1}(t,x) - \psi_m(t,x)\| \leq& \eta\|\psi_m - \psi_{m-1}\| + \epsilon t \\
\leq& \eta\Big(\|\tilde{\mathcal{S}}\psi_{m-1} - \tilde{\mathcal{S}}\psi_{m-2}\| + \|\int_0^t C(x)\big(c_{m-1}(\nu,x) - c_{m-2}(\nu,x)\big)d\nu\|\Big) \\
&+ \epsilon t \\
\leq& \eta(\eta\|\psi_{m-1} - \psi_{m-2}\| + \epsilon\, t) + \epsilon\, t \\
&\vdots \\
\leq& \eta^m\|\psi_1 - \psi_0\| + \epsilon\, t(1 + \eta + \eta^2 + \cdots + \eta^{m-1}).
\end{aligned}$$

Hence, the triangle inequality helps to attain the following result

$$\begin{aligned}
\|\psi_n(t,x) - \psi_m(t,x)\| \leq& \|\psi_n(t,x) - \psi_{n-1}(t,x)\| + \|\psi_{n-1}(t,x) - \psi_{n-2}(t,x)\| \\
&+ \cdots + \|\psi_{m+1}(t,x) - \psi_m(t,x)\| \\
\leq& \big[\eta^{n-1}\|\psi_1 - \psi_0\| + \epsilon\, t(1 + \eta + \eta^2 + \cdots + \eta^{n-2})\big] \\
&+ \big[\eta^{n-2}\|\psi_1 - \psi_0\| + \epsilon\, t(1 + \eta + \eta^2 + \cdots + \eta^{n-3})\big] + ... \\
&+ \big[\eta^{m}\|\psi_1 - \psi_0\| + \epsilon\, t(1 + \eta + \eta^2 + \cdots + \eta^{m-1})\big] \\
=& (\eta^{n-1} + \eta^{n-2} + \cdots + \eta^m)\|\psi_1 - \psi_0\| + \epsilon\, t[(1 + \eta + \eta^2 + \cdots + \eta^{n-2}) \\
&+ (1 + \eta + \eta^2 + \cdots + \eta^{n-3}) + \cdots + (1 + \eta + \eta^2 + \cdots + \eta^{m-1})].
\end{aligned}$$

Further, simplifying the above equation, the assumption $(\mathbf{A})$ and a desirable t_0 give us

$$\begin{aligned}
\|\psi_n(t,x) - \psi_m(t,x)\| =& \frac{\eta^m(1-\eta)^{n-m}}{1-\eta}\|\psi_1 - \psi_0\| \\
&+ \epsilon t\Big[\frac{(1-\eta)^{n-1}}{1-\eta} + \frac{(1-\eta)^{n-2}}{1-\eta} + \cdots + \frac{(1-\eta)^{m}}{1-\eta}\Big] \\
\leq& \frac{\eta^m}{1-\eta}\|c_1\| + \frac{\epsilon t_0}{1-\eta}(n-m). \qquad (5.37)
\end{aligned}$$

Thanks to the assumption (**B**) and $\frac{1}{m^p} > \frac{1}{n^p}$, Eq.(5.37) converges to zero as $m \to \infty$. It indicates that $\lim_{n\to\infty} \psi_n(t,x) = \psi(t,x)$, therefore, $c(t,x) = \sum_{k=0}^{\infty} c_k(t,x) = \lim_{n\to\infty} \psi_n(t,x) = \psi(t,x)$, which is the exact solution of (5.28). Hence, the maximum error bound (5.34) is attained through the Eq.(5.37), for a fixed m and letting $n \to \infty$. □

5.3 Numerical Discussion

This section portrays the implementation of VIM and ODM on CBE with three test cases. MATHEMATICA software displays all the computations, results, and graphs for the concentration and moments of the problems. To see the efficiency and accuracy of our proposed methods, analytical solutions for number density and moments are compared with the finite term VIM and ODM results. In the absence of a precise solution, the difference between successive series terms is provided to justify the convergence of the method.

Example 5.3.1. Assuming Eqs.(1.8-1.9) with $K(x,y) = xy$, $b(x,y,z) = \frac{2}{y}$ and $c^{in}(x) = \exp(-x)$ for which the corresponding exact solution is $c(t,x) = (1+t)^2 \exp(-x(1+t))$ described in [76].

The VIM approach is employed for this example and we get the operator A with the help of Eq.(5.8)

$$A[c] = \int_0^t \left(-\frac{\partial c_k(\tau,x)}{\partial \tau} + \int_0^\infty \int_x^\infty 2z c_k(\tau,y) c_k(\tau,z)\, dy\, dz - \int_0^\infty xy c_k(\tau,x) c_k(\tau,y)\, dy \right) d\tau,$$

and Eq.(5.5) assist for providing the following series terms

$$\begin{aligned}
c_0(t,x) =& e^{-x}, \quad c_1(t,x) = t(2e^{-x} - e^{-x}x), \quad c_2(t,x) = e^{-x}t^2 - 2e^{-x}t^2x + \frac{1}{2}e^{-x}t^2x^2,\\
c_3(t,x) =& -e^{-x}t^3x + e^{-x}t^3x^2 - \frac{1}{6}e^{-x}t^3x^3, \quad c_4(t,x) = \frac{1}{2}e^{-x}t^4x^2 - \frac{1}{3}e^{-x}t^4x^3 + \frac{1}{24}e^{-x}t^4x^4,\\
c_5(t,x) =& -\frac{1}{6}e^{-x}t^5x^3 + \frac{1}{12}e^{-x}t^5x^4 - \frac{1}{120}e^{-x}t^5x^5
\end{aligned}$$

and so on. The further terms can be computed using Eq.(5.5) and the series solution of n-terms, $\varphi_n(t,x) = \sum_{k=0}^{n} c_k(t,x)$, may be readily shown to be represented as

$$\varphi_n(t,x) = c_0(t,x) + c_1(t,x) + \sum_{k=2}^{n} \left(\frac{(-1)^k x^{k-2}}{(k-2)!} + \frac{2(-1)^{k-1}x^{k-1}}{(k-1)!} + \frac{(-1)^k x^k}{(k)!} \right) e^{-x}t^k. \tag{5.38}$$

Taking the limit $n \to \infty$, (5.38) reduces to

$$\lim_{n\to\infty} \varphi_n(t,x) = \sum_{k=0}^{\infty} \varphi_n(t,x) = (1+t)^2 \exp(-x(1+t)),$$

which is exactly the precise solution. Now, for the ODM approach, Eqs.(5.18), (5.19) and (5.21-5.23) helped us to get the first few series terms with $C(x) = -x$, as

$$\begin{aligned}
c_0(t,x) =& e^{-x},\ c_1(t,x) = t(2e^{-x} - e^{-x}x),\\
c_2(t,x) =& \frac{1}{2}t^2(-2e^{-x}(-1+x) + e^{-x}(-2+x)x + x(2e^{-x} - e^{-x}x)),\\
c_3(t,x) =& \frac{1}{6}e^{-x}t^2(3(-2+x)x - 2t(2+x)),\\
c_4(t,x) =& -\frac{1}{12}e^{-x}t^3(-8(1-x+x^2) + t(20-14x+3x^2)),
\end{aligned}$$

and

$$c_5(t,x) = -\frac{1}{30}e^{-x}t^3(5(-2+x)x^2 - 5t(17-8x+4x^2) + t^2(38-63x+17x^2)).$$

Thanks to MATHEMATICA, the higher terms can be determined using (5.23) and hence, an approximate solution by taking fixed number of series terms can be taken. Fig.5.1 demonstrates the comparison of exact solution with n =4, 6, 8, 10 terms series solutions obtained via VIM and ODM at time $t = 1.5$ and $t = 0.6$, respectively. From these graphs, it is clear that as the number of terms increases, the series solution tends to the precise one using both methods, and in fact, there's a great deal of agreement between the exact and the 10-term estimate. In case of ODM, it is observed that, as time increases, one needs a large number of series terms to get better accuracy, whereas VIM is consistently performing well. As expected, due to the collision event, the decreasing behaviour of the number density function is noticed as time progresses in Fig.5.1. Further, to see the excellency of our algorithms, the 3D display of the number density function is visualized in Figs.5.2(a) and 5.2(b) for $n = 10$ at time 0.6 by VIM and ODM, respectively. These plots are almost identical to the exact number density function given in Fig.5.2(c). However, as time increases to 1, the ODM solution does not have better precision with the analytical solution as compared to the VIM result, see Fig.5.3. The noticeable dissimilarity can

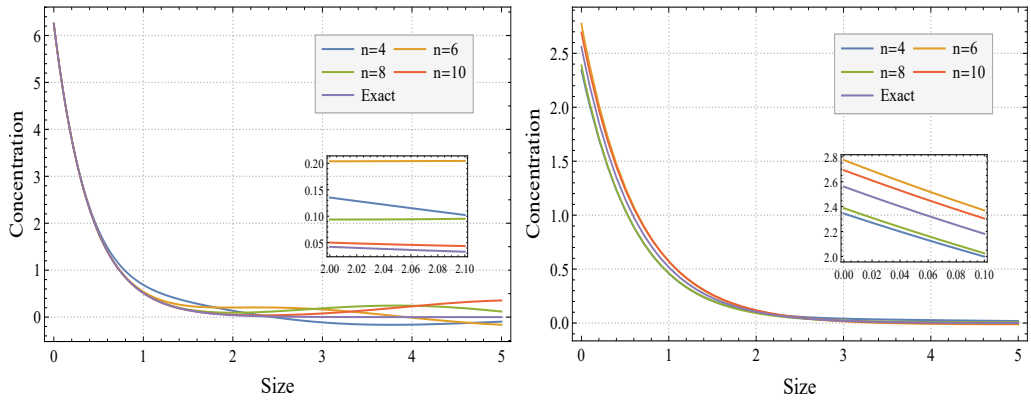

(a) VIM at time 1.5 (b) ODM at time 0.6

Figure 5.1: Series solutions of VIM, ODM and exact solution

visualize through the error plots of series and precise solutions.

Fig.5.4(a) portrays a minor error in approximate solution by VIM than the ODM outcome in Fig.5.4(b). The same information is also conveyed through the absolute error distribution provided in Table 5.1 for various values of n and time. The error computations are derived by dividing the size variable domain [0, 5] into subintervals $[x_{i-1/2}, x_{i+1/2}]$, where $i = 1, 2, \ldots, 1000$. The representative of the i^{th} cell is denoted by the mid-point $x_i = \frac{x_{i-1/2}+x_{i+1/2}}{2}$. Assuming step size $h_i = x_{i+1/2} - x_{i-1/2}$, the following rule is operated to estimate the error in VIM and ODM, respectively,

$$\text{Error} = \sum_{i=1}^{1000} |\varphi_n^i - c_i| h_i, \qquad \text{Error} = \sum_{i=1}^{1000} |\psi_n^i - c_i| h_i,$$

where $\varphi_n^i = \varphi_n(t, x_i)$, $\psi_n^i = \psi_n(t, x_i)$ and $c_i = c(t, x_i)$. As expected, the error reduces with the number of terms being increased at a particular time in each case. Moreover, the VIM solution has less error by taking a fixed number of terms at each time, i.e., VIM produces a better approximate solution than the ODM. Finally, Eq.(5.26) permits to attain the values of γ_i for $i = 5, 6, \ldots, 9$ and it is marked from Table 5.2 that all $\gamma_i < 1$ which is the required condition of series convergence in VIM. Proceeding further, the method's efficacy is also affirmed through the comparison between approximated

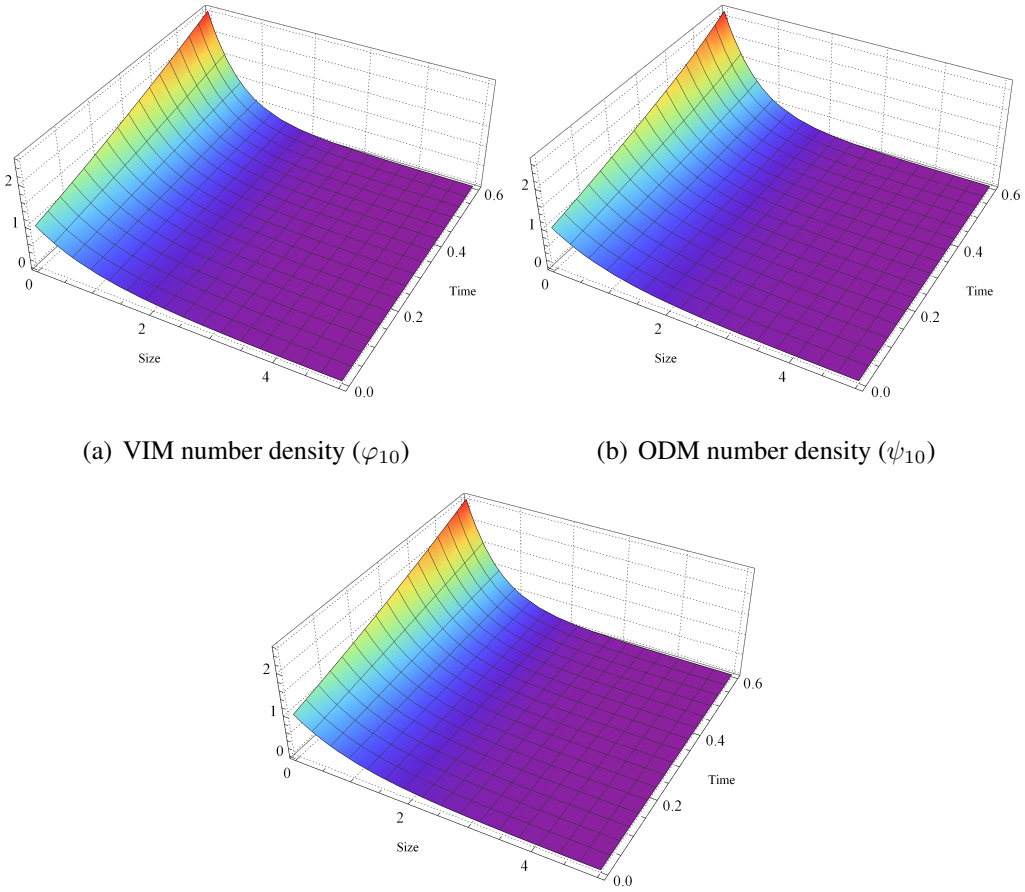

(a) VIM number density (φ_{10})

(b) ODM number density (ψ_{10})

(c) Exact number density

Figure 5.2: Number density plots at time t= 0.6

moments of VIM and ODM with the exact moments. Fig.5.5(a) represents the zeroth moment of the approximated solutions φ_{10} and ψ_{10} along with the exact zeroth moment. It authenticates that the total number of particles increases as time progresses and the ODM moment commences to slip away from VIM and precise ones around $t = 0.5$. In addition, the first and second moments in Figs.5.5(b) and 5.5(c) are shown and these graphs display that moments using 10-term ODM solutions are not sufficient enough to predict the exact ones in either case as it starts deviating soon after the simulation begins. Notice that a 10-term ODM solution was good to approximate the number denity function function for time 0.6 in Fig.5.2. So, it is not obvious that if a method delivers good accuracy with solutions, it can also provide similar behaviour with the moments.

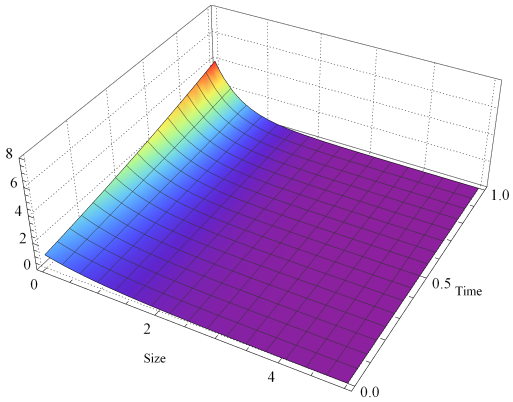

(a) VIM number density (φ_{10})

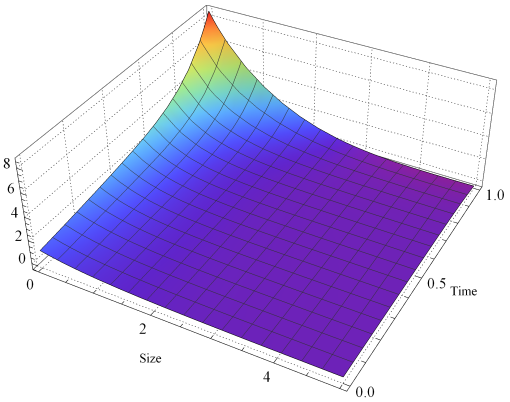

(b) ODM number density (ψ_{10})

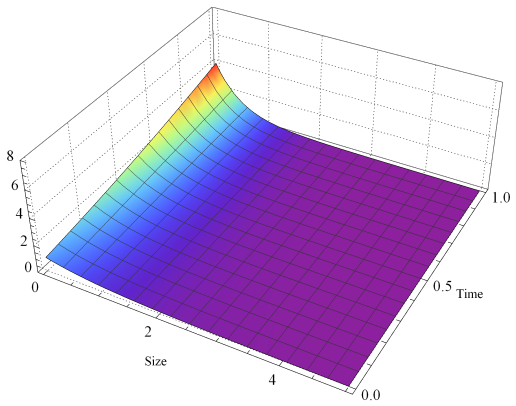

(c) Exact number density

Figure 5.3: Number density plots at time t= 1

From these figures, it is certain that VIM moments using φ_{10} have better approximation with the exact. The extraction of the above results lies in the significance of VIM over ODM in solving the CBE.

Example 5.3.2. Let us consider Eqs.(1.8-1.9) with kernels $K(x,y) = \frac{xy}{20}$, $b(x,y,z) = \frac{2}{y}$ and initial data $c^{in}(x) = x^2\exp(-x)$. The analytical solution for the number density function is hard to compute, however the precise formulations for the zeroth and the first moments are $\mu_0(t) = 2+\frac{9t}{5}$ and $\mu_1(t) = 6$, respectively. These moments can be generated by multiplying Eq.(1.8) by 1 and x as well as integrating from 0 to ∞ over x. Substituting these kernel parameters and initial condition in Eq.(5.8), we have

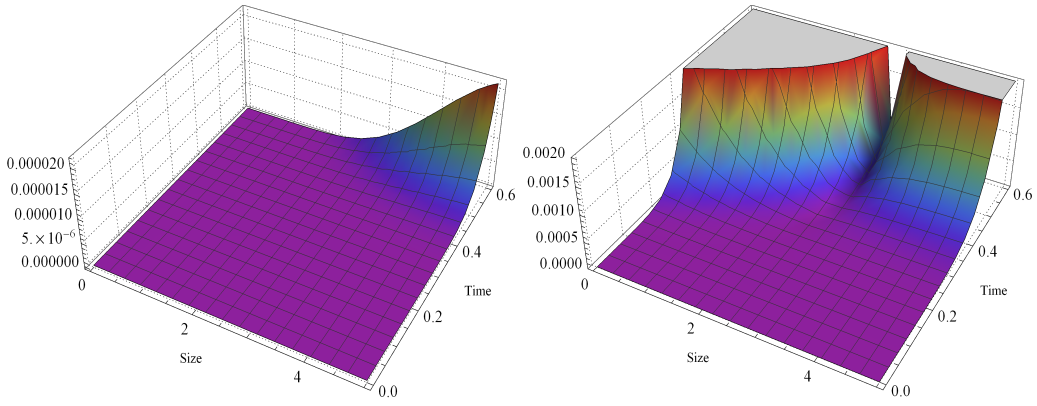

(a) VIM error (b) ODM error

Figure 5.4: Absolute error between exact solution and φ_{10} as well as ψ_{10}

$$A[c] = \int_0^t \left(-\frac{\partial c_k(\tau,x)}{\partial \tau} + \int_0^\infty \int_x^\infty \frac{z}{10} c_k(\tau,y) c_k(\tau,z)\, dy\, dz - \int_0^\infty \frac{xy}{20} c_k(\tau,x) c_k(\tau,y)\, dy \right) d\tau,$$

for the VIM, and so, the following first few terms of the series solution are computed using Eq.(5.5)

$$\begin{aligned}
c_0(t,x) =& x^2 e^{-x}, \quad c_1(t,x) = \frac{3}{10} e^{-x} t (4 + x(4 - (-2+x)x)),\\
c_2(t,x) =& \frac{9}{200} e^{-x} t^2 (12 + x^2(-6 + (-4+x)x)),\\
c_3(t,x) =& -\frac{9 e^{-x} t^3 x (36 + x(12 + x(-6 + (-6+x)x)))}{2000},\\
c_4(t,x) =& \frac{27 e^{-x} t^4 x^2 (72 + (-8+x)(-2+x)x(2+x))}{80000},
\end{aligned}$$

and

$$c_5(t,x) = -\frac{81 e^{-x} t^5 x^3 (120 + 60x - 10x^3 + x^4)}{4000000}.$$

The subsequent terms may be calculated using Eq.(5.5) and with the help of MATHEMATICA. For the numerical comparison, we have taken the results up to 10-terms solution.

Furthermore, the ODM technique is being applied to this example to get $C(x) = -\frac{3x}{10}$

t	Methods	Number of terms			
		4	6	8	10
0.1	VIM	1.8076×10^{-6}	1.1147×10^{-8}	7.6098×10^{-11}	4.0914×10^{-13}
	ODM	5.7102×10^{-4}	6.5328×10^{-5}	6.8206×10^{-6}	6.6708×10^{-7}
0.2	VIM	5.4645×10^{-5}	1.3350×10^{-6}	3.6569×10^{-8}	7.9085×10^{-10}
	ODM	5.3592×10^{-3}	1.2903×10^{-3}	2.7836×10^{-4}	5.7827×10^{-5}
0.3	VIM	3.9284×10^{-4}	2.1424×10^{-5}	1.3232×10^{-6}	6.4741×10^{-8}
	ODM	2.0709×10^{-2}	7.8754×10^{-3}	2.7180×10^{-3}	9.4369×10^{-4}
0.4	VIM	1.5704×10^{-3}	1.5126×10^{-4}	1.6630×10^{-5}	1.4540×10^{-6}
	ODM	5.5200×10^{-2}	2.9454×10^{-2}	1.4597×10^{-2}	7.5082×10^{-3}
0.5	VIM	4.5555×10^{-3}	6.8176×10^{-4}	1.1722×10^{-4}	1.6092×10^{-5}
	ODM	1.1958×10^{-1}	8.3816×10^{-2}	5.5852×10^{-2}	3.9088×10^{-2}
0.6	VIM	1.0795×10^{-2}	2.3154×10^{-3}	5.7361×10^{-4}	1.1389×10^{-4}
	ODM	2.2671×10^{-1}	2.0006×10^{-1}	1.7113×10^{-1}	1.5330×10^{-1}

Table 5.1: Distribution of errors of VIM and ODM with different series terms and times

γ_5	γ_6	γ_7	γ_8	γ_9
0.4513	0.4631	0.4299	0.5625	0.4142

Table 5.2: Different values of γ_i

and using Eq.(5.18), Eq.(5.19) as well as Eqs.(5.21-5.23), the following series terms are obtained

$$c_0(t,x) = e^{-x}, \quad c_1(t,x) = \frac{3}{10}te^{-x}(x(4-(x-2)x)+4),$$
$$c_2(t,x) = -\frac{9}{100}t^2e^{-x}\left(x\left(x^2+x-2\right)-6\right),$$
$$c_3(t,x) = \frac{1}{1000}((3e^{-x}t^2(4t(-10+x(-19+(-11+x)x))+15x(-4+x(-4+(-2+x)x))))),$$
$$c_4(t,x) = \frac{1}{20000}(e^{-x}\left(60t^3(x(x(x(6x-1)+20)+22)+40)-9t^4(x(x(x(15x-94)+2)+260))\right)).$$

Thanks to MATHEMATICA, it is possible to calculate the additional higher terms of the

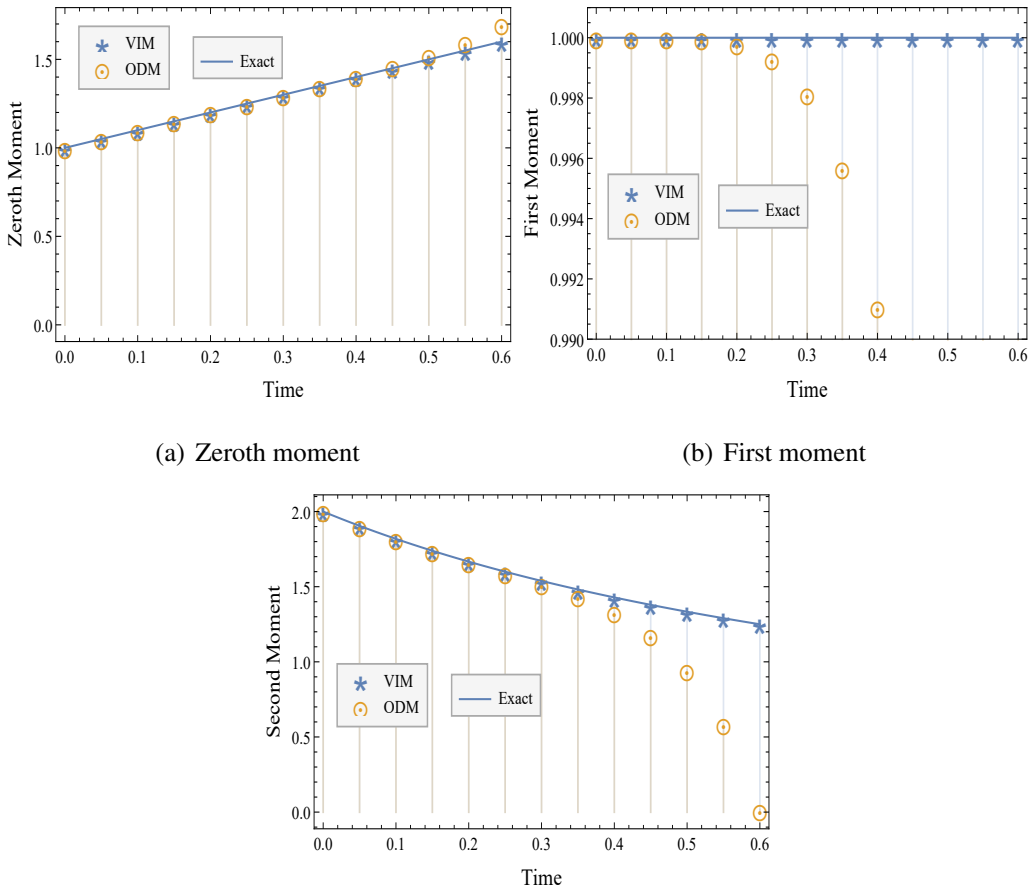

(a) Zeroth moment

(b) First moment

(c) Second moment

Figure 5.5: Moments comparision: VIM, ODM and exact

series solution (ψ_{14}). As the precise number density function is not there, Fig.5.6, plots of the absolute difference of consecutive iteration terms at time $t = 1$ are summarized for VIM and ODM. It can be observed that the behaviour of the differences is diminishing and $|c_{10} - c_9|$ is near to zero in VIM while $|c_{14} - c_{13}|$ in ODM is still higher than this. Therefore, the series solution is truncated to 10-term (φ_{10}) in case of VIM and a 14-term series solution is taken in ODM to anticipate more favourable outcomes. The estimated number density functions derived by VIM (φ_{10}) and ODM (ψ_{14}) for time 1.5 are shown in Fig.5.7, and they are comparable. The convergence of the VIM solution (φ_{10}) is further validated by providing the values of γ_i parameters at time 1.5 in Table 5.3. Further, to justify the novelty of proposed schemes, approximated moments using φ_{10} and ψ_{14}

γ_5	γ_6	γ_7	γ_8	γ_9
0.4212	0.4317	0.4381	0.4323	0.3525

Table 5.3: Different values of γ_i at time 1.5

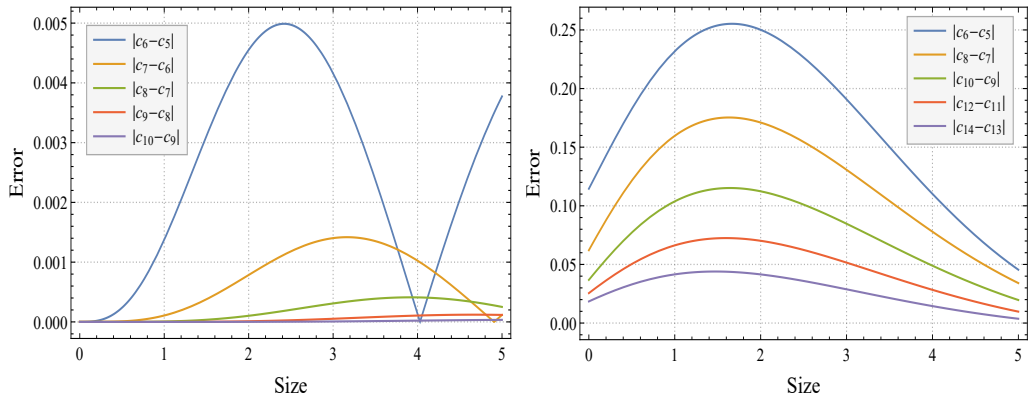

(a) VIM coefficients

(b) ODM coefficients

Figure 5.6: Absolute difference of series coefficients at time 1.0

are plotted against the exact ones in Fig.5.8. The zeroth and the first moments of VIM using φ_{10} and ODM using ψ_{15} are plotted against the analytical moments in Fiq.5.8. It is observed that the VIM results exactly overlap with the exact moments, whereas the ODM results start over-predicting and lower-predicting around time $t = 1.2$. Observably, VIM yields findings that resemble analytic solutions. Therefore, one can expect the accurate result for the second moment by VIM, which is given in Fig.5.8(c). The second moment of ODM missteps away from VIM around $t = 1.2$. The overall results authenticate that the VIM technique supplies better estimations than ODM.

Example 5.3.3. Consider Eqs.(1.8-1.9) with $K(x, y) = 1$, $b(x, y, z) = \delta(x - 0.4y) + \delta(x - 0.6y)$ and $c^{in}(x) = \exp(-x)$, its exact solution does not exist in the literature, but exact moments are $\mu_0(t) = \frac{1}{1-t}$, $\mu_1(t) = 1$ and $\mu_2(t) = 2(1-t)^{0.48}$, where the second moment is computed by multiplying Eq.(1.8) by x^2 and integrating from 0 to ∞ over x. So exclusively an approximate solution, find out using the VIM and ODM. The VIM approach (Eqs.(5.8) and (5.5)) offers the operator A

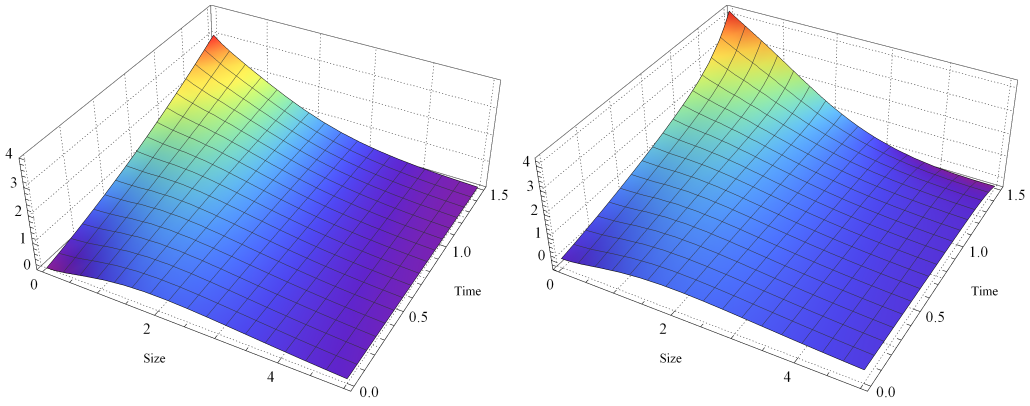

(a) VIM solution (b) ODM solution

Figure 5.7: Plots of series solution with φ_{10} and ψ_{14} at time 1.5

$$A[c] = \int_0^t \Bigg(-\frac{\partial c_k(\tau,x)}{\partial \tau} + \int_0^\infty \int_x^\infty \big(\delta(x-0.4y) + \delta(x-0.6y)\big) c_k(\tau,y) c_k(\tau,z)\, dy\, dz - \int_0^\infty c_k(\tau,x) c_k(\tau,y)\, dy \Bigg) d\tau,$$

and the following series terms

$$c_0(t,x) = e^{-x},\ c_1(t,x) = x\Big(-e^{-t} + 1.66667 e^{-1.66667t}\theta(0.666667t) + 2.5 e^{-2.5t}\theta(1.5t)\Big),$$
$$c_2(t,x) = -0.5 e^{-14.1944t} x^2 \Big(e^{13.1944t} + \theta(0.666667t)(-2.77778 e^{11.4167t}\theta(1.11111t) - 4.16667 e^{10.0278t}\theta(2.5t)) + \theta(1.5t)(-4.16667 e^{10.0278t}\theta(1.66667t) - 6.25 e^{7.94444t}\theta(3.75t))\Big),$$

where δ and θ are Dirac's delta and Heaviside step functions, respectively.

For the implementation of ODM, having $C(x) = -1$, for this case, the following series terms are obtained using Eqs.(5.19) and (5.21-5.23)

$$c_0(t,x) = e^{-x},\ c_1(t,x) = t(-e^{-x} + 1.6667 e^{-1.66667x}\theta[0.666667x] + 2.5 e^{-2.5x}\theta[1.5x]),$$
$$c_2(t,x) = -0.5 e^{-14.1944x} t^2 \Big(e^{13.1944x} + \theta[0.666667x]\Big(-2.77778 e^{11.4167x}\theta[1.11111x] - 4.1667 e^{10.0278x}\theta[2.5x]\Big) + \theta[1.5x]\Big(-4.1667 e^{10.0278x}\theta[1.66667x] - 6.25 e^{7.94444x}\theta[3.75x]\Big)\Big).$$

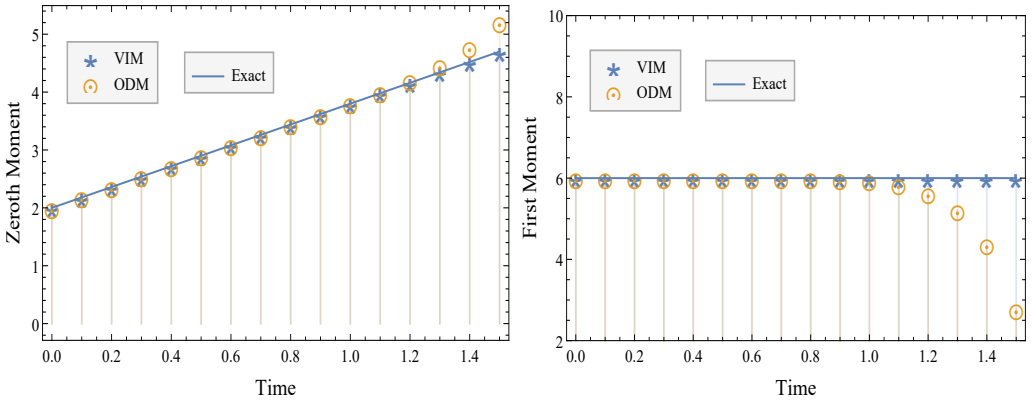

(a) Zeroth moment (b) First moment

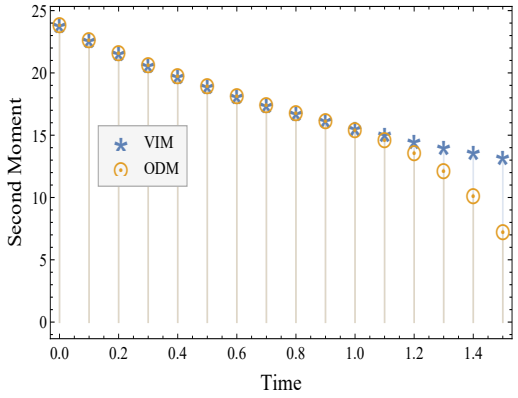

(c) Second moment

Figure 5.8: Moments comparision: VIM (φ_{10}), ODM (ψ_{14}) and exact at time 1.5

The third term is not easy to write due to lengthy expressions in both situations, and in fact, it is difficult to compute the higher series terms by MATHEMATICA due to the complexity of the model and kernels. It consumes a significant amount of time; therefore, consider φ_3 and ψ_3 as approximate solutions for numerical validation.

These provide the optimal solution to this problem, as shown by several parameter graphs. Since, analytical solution is not available for the number density function, absolute differences between successive series terms are made up to 3-terms, see Fig.5.9. Initially, the differences have minor gap but as size increases it is going to zero. In Fig.5.10, series solutions φ_3 and ψ_3 are almost identical at time 0.2. The comparison of approximated and analytical moments supplies information about the method which one is better than

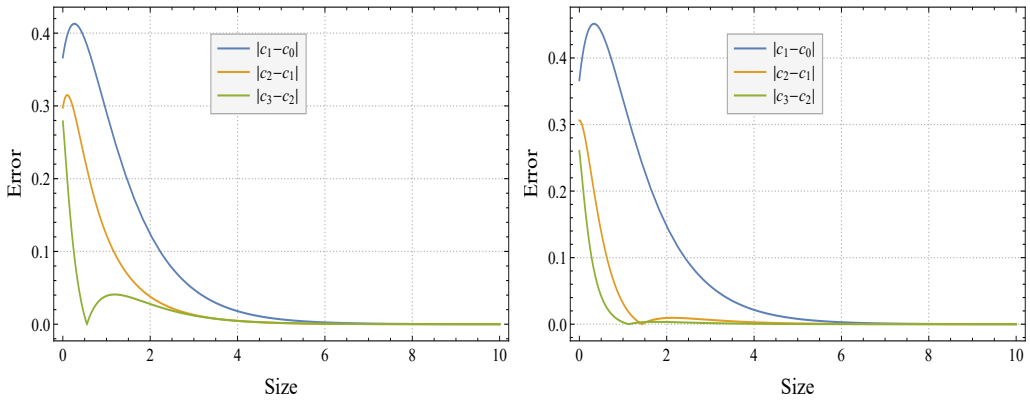

(a) VIM coefficients (b) ODM coefficients

Figure 5.9: Absolute difference of series coefficients at time 0.2

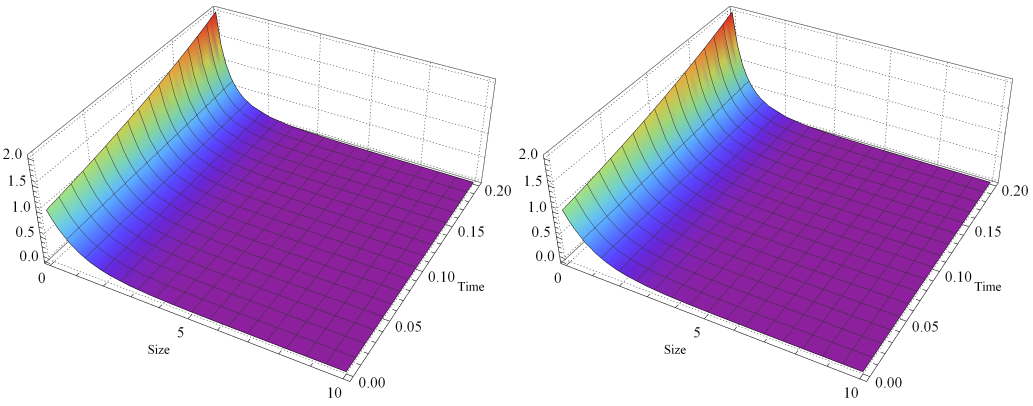

(a) VIM solution (b) ODM solution

Figure 5.10: Plots of series solution with φ_3 and ψ_3

the other.

In Fig.5.11(a), the zeroth moment of φ_3 and ψ_3 are presented with the exact zeroth moment at t=0.6. The ODM moment does not agree with the exact one after $t = 0.5$. In contrast, VIM provides better accuracy at this time. VIM and ODM first moment have suitable precision with exact at $t = 0.6$ in Fig.5.11(b). However, Fig.5.11(c) depicts the second moments of VIM (φ_3) and ODM (ψ_3), with VIM outperforming ODM in estimation. It is evident that the VIM moment is closest to the actual one.

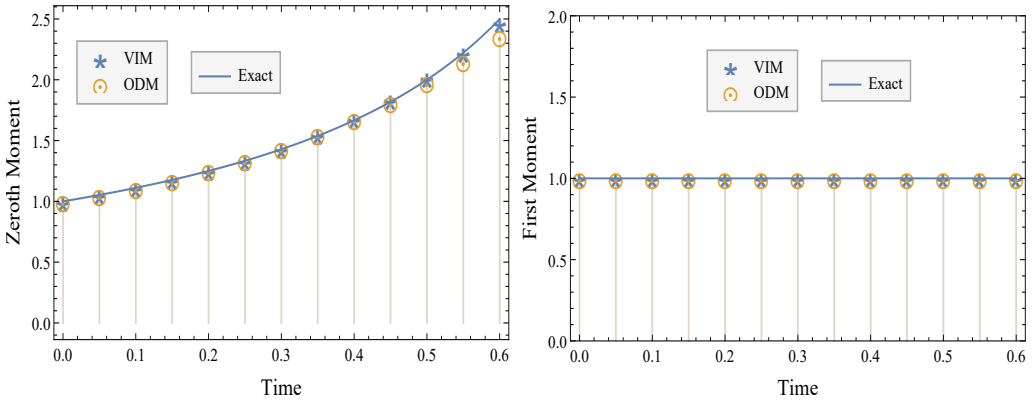

(a) Zeroth moment (b) First moment

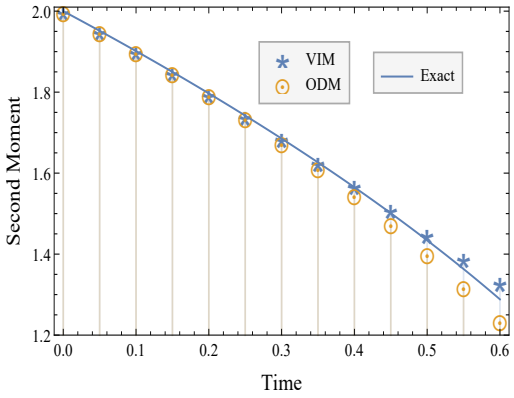

(c) Second moment

Figure 5.11: Moments comparision: VIM (φ_3), ODM (ψ_3) and exact at time 0.6

Chapter 6

Non-linear Collision-Induced Breakage Equation: Finite Volume and Semi-analytical Methods

---

The CBE (1.8) is the most unexplored area of PBEs to acquire new analytical results. In this chapter, we examine two different series solutions provided by HAM and AHPM for solving such equation. The convergence of the approximated series solutions along with the upper bound estimations of the errors are studied under some physical assumptions on kernels. Further, to show the novelty of our proposed schemes, results for the number density function and moments calculated via HAM and AHPM are compared with the findings of FVM and analytical solutions. Three different numerical examples are considered to support the scheme's reliability.

The chapter's structure is as follows: Section 6.1 provides the discretization scheme of FVM for CBE (1.8). Section 6.2 contributes to the semi-analytical methodologies of HAM, AHPM, and the coefficient form of the series solutions for CBE. In Section 6.3, convergence and error analysis are exhibited. Further, in Section 6.4, approximate solutions of HAM, AHPM and FVM are reported graphically for the density function and

moments. The effectiveness of the results is confirmed by comparing them to the analytical outcomes.

6.1 Finite Volume Method

FVM for the non-linear CBE is described in Section 4.1. Based on the idea of FVM [54], particle density is approximated over a grid cell instead of point mass, i.e., $\hat{c}_i \approx c_i$ in the i^{th} cell. The semi-discrete equation due to FVM is as follows

$$\frac{d\hat{c}_i(t)}{dt} = \frac{1}{\Delta x_i} \sum_{l=1}^{\mathrm{I}} \sum_{j=i}^{\mathrm{I}} K_{j,l} \hat{c}_j(t) \hat{c}_l(t) \Delta x_j \Delta x_l \int_{x_{i-1/2}}^{\lambda_j^i} b(x, x_j, x_l)\, dx - \sum_{j=1}^{\mathrm{I}} K_{i,j} \hat{c}_i(t) \hat{c}_j(t) \Delta x_j, \tag{6.1}$$

where the term λ_j^i is expressed by

$$\lambda_j^i = \begin{cases} x_i, & \text{if } j = i, \\ x_{i+1/2}, & j \neq i. \end{cases} \tag{6.2}$$

For solving the semi-discrete equation (6.1), any higher order numerical scheme (ode45) can be used to obtain the approximation results for particular cases of parameters K and b. Note that, our motive here is to validate the series solutions using FVM and exact solutions, so a detailed convergence analysis is not explained here. Now, series approximation methods HAM and AHPM are discussed below for the CBE (1.8).

6.2 Semi-analytical Methods

These are mathematical techniques that incorporate analytical and numerical approaches to solve complex problems. They reduce computational complexity by employing analytical expressions for specific problem components, resulting in faster calculations and fewer computational resources. If problems are solvable, semi-analytical method provides either the closed form solution which is actually the exact solution or the finite term series solution which is an approximate solution. By providing approximate solutions with known precision, these methods permit researchers to compare the performance and

accuracy of various numerical methods, thereby determining their efficacy. This section goes into details about the HAM and AHPM, which are well-established schemes.

6.2.1 Homotopy analysis method

The basic preliminaries and applicability of HAM to general form of different equations are discussed in [97]. We first examine the HAM and then expand it to construct an approximate series solution to CBE (1.8). Examine the generic differential equation

$$N[c(t,x)] = 0, \tag{6.3}$$

where N is a non-linear operator and c is an unknown function. Proceeding further, by following the idea of HAM, let us construct the zero-order deformation equation as

$$(1-p)L[\phi(t,x;p) - c^{in}(x)] = p\alpha N[\phi(t,x;p)], \tag{6.4}$$

where, significant roles are played by the embedding parameter $p \in [0,1]$, the non-zero convergence-control parameter α, and the auxiliary linear operator L with $L(0) = 0$ to modify and manage the convergence domain of series solution [97]. The term $\phi(t,x;p)$ is an unknown function and $c^{in}(x)$ is an initial guess. Eq.(6.4) provides $\phi(t,x;0) = c^{in}(x)$ and $\phi(t,x;1) = c(t,x)$, when $p = 0$ and $p = 1$, respectively. This means that that the initial guess $c^{in}(x)$ converts into the solution $c(t,x)$ as p varies from 0 to 1. Moreover, the Taylor series expansion of $\phi(t,x;p)$ with respect to p yields

$$\phi(t,x;p) = c^{in}(x) + \sum_{m=1}^{\infty} c_m(t,x)p^m, \tag{6.5}$$

where

$$c_m(t,x) = \frac{1}{m!}\frac{\partial^m \phi(t,x;p)}{\partial p^m}\bigg|_{p=0}. \tag{6.6}$$

The series solution is obtained by the power series (6.5) that is convergent at $p = 1$ and for a suitable convergence-control parameter α, i.e.,

$$c(t,x) = c^{in}(x) + \sum_{m=1}^{\infty} c_m(t,x). \tag{6.7}$$

The unknown terms $c_m(t,x)$ are computed with the assistance of high order deformation outlined below. Consider the vector $\vec{c}_m = \{c_0, c_1, \ldots, c_m\}$. Differentiating Eq.(6.4) m times with respect to p, dividing it by $m!$ with $p = 0$ provide the mth-order deformation equation as

$$L[c_m - \Pi_m c_{m-1}] = \alpha \Gamma_m(\vec{c}_{m-1}), \tag{6.8}$$

where

$$\Gamma_m(\vec{c}_{m-1}) = \frac{1}{(m-1)!} \frac{\partial^{m-1} N[\phi(t,x;p)]}{\partial p^{m-1}}\bigg|_{p=0}, \tag{6.9}$$

and

$$\Pi_m = \begin{cases} 0, & \text{if } m \leq 1, \\ 1, & m > 1. \end{cases} \tag{6.10}$$

Liao [98] explains that the so-called generalized Taylor series supplies a way to regulate and adjust the convergence region via an auxiliary parameter, enabling the HAM particularly well-suited for problems with strong non-linearity. Note that the convergence-control parameter α in Eq.(6.8) can be evaluated using the discrete averaged residual error formula [66], which is written at the end of this part.

Proceeding further, the development of mathematical formulation of CBE (1.8) using HAM is explained now. Integrating (1.8) from 0 to t over t with $c(0,x) = c^{in}(x)$, we obtain the integral form as

$$\begin{aligned} N[c(t,x)] =& c(t,x) - c^{in}(x) - \int_0^t \int_0^\infty \int_x^\infty K(y,z) b(x,y,z) c(t,y) c(t,z)\, dy\, dz\, dt \\ &+ \int_0^t \int_0^\infty K(x,y) c(t,x) c(t,y)\, dy\, dt. \end{aligned} \tag{6.11}$$

The zero-order deformation equation of (6.11) is

$$(1-p)[\phi(t,x;p) - c^{in}(x)] = p\alpha N[\phi(t,x;p)], \quad p \in [0,1], \tag{6.12}$$

where $\phi(t,x;p)$ is an unknown function and $N[\phi(t,x;p)]$ is constructed as

$$N[\phi(t,x;p)] = \phi(t,x;p) - c^{in}(x) - \int_0^t \int_0^\infty \int_x^\infty K(y,z) b(x,y,z) \phi(t,y;p) \phi(t,z;p)\, dy\, dz\, dt$$

$$+\int_0^t\int_0^\infty K(x,y)\phi(t,x;p)\phi(t,y;p)\,dy\,dt=0. \tag{6.13}$$

As we have noticed from Eqs.(6.5-6.6) for $p=1$, the series solution is

$$\phi(t,x;1)=c(t,x)=c^{in}(x)+\sum_{m=1}^{\infty}c_m(t,x). \tag{6.14}$$

Next, define the mth-order deformation equation as

$$c_m-\Pi_m c_{m-1}=\alpha\Gamma_m(\vec{c}_{m-1}), \tag{6.15}$$

where

$$\Gamma_m(\vec{c}_{m-1})=\frac{1}{(m-1)!}\frac{\partial^{m-1}N[\phi(t,x;p)]}{\partial p^{m-1}}\bigg|_{p=0}=\frac{1}{(m-1)!}\frac{\partial^{m-1}N\big[\sum_{k=1}^{\infty}c_k(t,x)p^k\big]}{\partial p^{m-1}}\bigg|_{p=0}.$$

After simplifying the above term, we have

$$\begin{aligned}\Gamma_m(\vec{c}_{m-1})=&c_{m-1}(t,x)-(1-\Pi_m)c^{in}(x)-\int_0^t\int_0^\infty\int_x^\infty K(y,z)b(x,y,z)\Omega^1_{m-1}\,dy\,dz\,dt\\&+\int_0^t\int_0^\infty K(x,y)\Omega^2_{m-1}\,dy\,dt,\end{aligned} \tag{6.16}$$

where

$$\Omega^1_{m-1}=\frac{1}{(m-1)!}\frac{\partial^{m-1}}{\partial p^{m-1}}\bigg(\sum_{r=1}^{\infty}\sum_{k=0}^{r-1}c_k(t,y)c_{r-k-1}(t,z)p^k\bigg)\bigg|_{p=0}, \tag{6.17}$$

and

$$\Omega^2_{m-1}=\frac{1}{(m-1)!}\frac{\partial^{m-1}}{\partial p^{m-1}}\bigg(\sum_{r=1}^{\infty}\sum_{k=0}^{r-1}c_k(t,x)c_{r-k-1}(t,y)p^k\bigg)\bigg|_{p=0}. \tag{6.18}$$

The simplified mth-order deformation equation (6.15) is attained via applying the Eqs.(6.16-6.18), that is

$$\begin{aligned}c_m=&\Pi_m c_{m-1}+\alpha\bigg[c_{m-1}-(1-\Pi_m)c^{in}(x)-\int_0^t\int_0^\infty\int_x^\infty K(y,z)b(x,y,z)\Omega^1_{m-1}\,dy\,dz\,dt\\&+\int_0^t\int_0^\infty K(x,y)\Omega^2_{m-1}\,dy\,dt\bigg],\quad m=1,2,3,\cdots.\end{aligned} \tag{6.19}$$

Hence, the series solution components are derived by (6.19) with initial condition $c_0(t,x,\alpha) = c^{in}(x)$, and are listed below

$$\left.\begin{aligned} c_0(t,x,\alpha) =& c^{in}(x), \\ c_1(t,x,\alpha) =& \alpha\Big[-\int_0^t\int_0^\infty\int_x^\infty K(y,z)b(x,y,z)\Omega_0^1\,dy\,dz\,dt + \int_0^t\int_0^\infty K(x,y)\Omega_0^2\,dy\,dt\Big], \\ c_m(t,x,\alpha) =& (1+\alpha)c_{m-1} + \alpha\Big[-\int_0^t\int_0^\infty\int_x^\infty K(y,z)b(x,y,z)\Omega_{m-1}^1\,dy\,dz\,dt \\ &+ \int_0^t\int_0^\infty K(x,y)\Omega_{m-1}^2\,dy\,dt\Big], \quad m>1. \end{aligned}\right\} \tag{6.20}$$

For the numerical simulations, let us denote the approximated solution of nth-order for CBE (1.8) by

$$\Theta_n(t,x,\alpha) := \sum_{i=0}^{n} c_i(t,x,\alpha). \tag{6.21}$$

The optimal value of α, for the best approximated series solution of CBE, is computed by minimizing the following function, i.e.,

$$\min_{\alpha\in R} A(\alpha), \quad A(\alpha) = \frac{1}{n^2}\sum_{m=1}^{n}\sum_{r=1}^{n}[N(\Theta_n(t_m,x_r,\alpha))]^2, \tag{6.22}$$

where $A(\alpha)$ is the averaged residual error of the nth-order approximation for CBE problem and (t_m, x_r) belongs to the operational domain. This concept's specifics can be extracted from [66]. The symbolic computation software MATHEMATICA has a command "Minimize" to compute the optimal value of α explicitly.

6.2.2 Accelerated homotopy perturbation method

In HPM [99], He's polynomial is equivalently taken as Adomain polynomial introduced in [100]. The author in [101] generates a new class of accelerated polynomials which after incorporating into HPM yields a new scheme called AHPM that provides better accuracy to examine non-linear differential equations. To explain AHPM, consider a general functional form as

$$\psi(t,x) - N[\psi(t,x)] = g(x), \tag{6.23}$$

where ψ is an unknown function and g is a given function. Also, N is the non-linear operator. Subsequently, rewrite Eq.(6.23) with solution $c(t,x) = \psi(t,x)$ into the following form

$$\mathrm{L}(c(t,x)) = c(t,x) - g(x) - N[c(t,x)]. \tag{6.24}$$

Further, construct a homotopy $H(c,p)$ having the properties $H(c,0) = T(c)$, $H(c,1) = \mathrm{L}(c(t,x))$ and

$$H(c,p) = (1-p)T(c) + p\mathrm{L}(c) = 0, \tag{6.25}$$

where $T(c)$ is an operator with solution c_0. The embedding parameter p is crucial for continuously deforming Eq.(6.25) from $H(c_0,0) = T(c_0) = 0$ to $H(\psi,1) = \mathrm{L}(c) = 0$ as p increases from 0 to 1. The semi-analytical solution $c(t,x) = \sum_{n=0}^{\infty} p^n c_n(t,x)$ and exact solution $\psi(t,x)$ have a relation as

$$\psi(t,x) = \sum_{n=0}^{\infty} c_n(t,x) = \lim_{p\to 1} c(t,x). \tag{6.26}$$

For further use, let us suppose $T(c) = c(t,x) - g(x)$. Substituting this and $\mathrm{L}(c)$ from Eq.(6.24) into Eq.(6.25) yields a form

$$H(c,p) = c - g - pN(c) = 0. \tag{6.27}$$

The non-linear term $N(c)$ can be written in the form of accelerated polynomials ($\hat{H}_n$) that is explained in [101], as

$$N(c) = \sum_{n=0}^{\infty} p^n \hat{H}_n(c_0, c_1, \cdots, c_n), \tag{6.28}$$

where $\hat{H}_n$ has mathematical structure as

$$\hat{H}_n(c_0, c_1, \cdots, c_n) = N(S_n) - \sum_{i=0}^{n-1} \hat{H}_i, \quad n \geq 1, \tag{6.29}$$

with $S_n = \sum_{i=0}^{n} c_i(t,x)$ and $\hat{H}_0 = N(c_0)$. The series iterative terms are obtained by substituting $c(t,x) = \sum_{n=0}^{\infty} p^n c_n(t,x)$ and (6.28) into Eq.(6.27) and then by comparing

the powers of p,

$$\left.\begin{aligned} c_0(t,x) =& c^{in}(x) = g(x), \\ c_n(t,x) =& \hat{H}_{n-1}, \quad n \geq 1. \end{aligned}\right\} \tag{6.30}$$

Next, to find the mathematical formulation for CBE (1.8) by AHPM, the above idea follows. Therefore, integrating Eq.(1.8) over time variable t provides

$$\begin{aligned} \mathrm{L}(c(t,x)) =& c(t,x) - c^{in}(x) - \int_0^t \int_0^\infty \int_x^\infty K(y,z)b(x,y,z)c(t,y)c(t,z)\,dy\,dz\,dt \\ &+ \int_0^t \int_0^\infty K(x,y)c(t,x)c(t,y)\,dy\,dt, \end{aligned} \tag{6.31}$$

where

$$\begin{aligned} N[c(t,x)] =& \int_0^t \int_0^\infty \int_x^\infty K(y,z)b(x,y,z)c(t,y)c(t,z)\,dy\,dz\,dt \\ &- \int_0^t \int_0^\infty K(x,y)c(t,x)c(t,y)\,dy\,dt. \end{aligned} \tag{6.32}$$

Now, supersede $c(t,x) = \sum_{n=0}^{\infty} p^n c_n(t,x)$ and (6.28) into (6.27), yield a homotopy. Proceeding further to equate the terms with identical powers of p lead to get the iterative components, i.e.,

$$\sum_{n=0}^{\infty} p^n c_n(t,x) - c^{in}(x) - p\hat{H}_n(c_0, c_1, \cdots, c_n) = 0, \tag{6.33}$$

where for $n = 0$, it provides the first term

$$c_0(t,x) = c^{in}(x), \tag{6.34}$$

for $n = 1$

$$\begin{aligned} c_1(t,x) =& \int_0^t \int_0^\infty \int_x^\infty K(y,z)b(x,y,z)c_0(t,y)c_0(t,z)\,dy\,dz\,dt \\ &- \int_0^t \int_0^\infty K(x,y)c_0(t,x)c_0(t,y)\,dy\,dt, \end{aligned} \tag{6.35}$$

and for $n \geq 2$, the general term is

$$c_n(t,x) = \int_0^t \int_0^\infty \int_x^\infty K(y,z)b(x,y,z) \left(\sum_{i=0}^{n-1} c_i(t,y)\right) \left(\sum_{i=0}^{n-1} c_i(t,z)\right) dy\,dz\,dt$$

$$-\int_0^t \int_0^\infty K(x,y)\left(\sum_{i=0}^{n-1} c_i(t,x)\right)\left(\sum_{i=0}^{n-1} c_i(t,y)\right) dy\, dt - \left(\sum_{i=1}^{n-1} c_i(t,x)\right). \tag{6.36}$$

The truncated AHPM series solution of nth-order is expressed by the term $\Upsilon_n(t,x)$, i.e.,

$$\Upsilon_n(t,x) := \sum_{i=0}^{n} c_i(t,x). \tag{6.37}$$

6.3 Convergence Analysis

This section describes the reliability and efficiency of the methods with the given framework. It enables the development of theoretical guarantees concerning the algorithm's behavior. Here, convergence analysis of the HAM and AHPM solutions shall be illustrated for a set of assumptions on collisional kernels. For that, consider the set $\mathcal{W} = \{(t,x) : 0 \le t \le T, 0 < x < \infty\}$ for a fix T and assume a space of all continuous function c, say $\mathbb{Y}_{r,s}(T)$ with the following induced norm

$$\|c\| = \sup_{t\in[0,T]} \int_0^\infty \Big(x^r + \frac{1}{x^{2s}}\Big)|c(t,x)|dx, \quad r \ge 1, s \ge 0. \tag{6.38}$$

Eq.(6.11) provides the new operator form as

$$c = \mathcal{S}c, \tag{6.39}$$

where $\mathcal{S} : \mathbb{Y}_{r,s}(T) \to \mathbb{Y}_{r,s}(T)$ is a non-linear operator given as

$$\mathcal{S}c = c^{in}(x) + \mathcal{L}^{-1}\Big[\int_0^\infty \int_x^\infty K(y,z)b(x,y,z)c(t,y)c(t,z)\, dy\, dz - \int_0^\infty K(x,y)c(t,x)c(t,y)\, dy\Big], \tag{6.40}$$

with $\mathcal{L}^{-1} = \int_0^t(\cdot)dt$. Firstly, for the existence of the solution in $\mathbb{Y}^+_{r,s}(t)$ (set of non-negative functions from $\mathbb{Y}_{r,s}(T)$), operator $\mathcal{S}$ has to fulfill the contractive property under some hypotheses using the following theorem.

Theorem 6.3.1. Assume that the non-linear operator $\mathcal{S}$ is defined in (6.40). If the following hypotheses;

(a) $K(x,y)$ is non-negative and continuous function with compact support $\mathcal{K}_1$ $= \sup_{\frac{s}{R}\leq x,y\leq R} K(x,y)$, $(x,y)\in[0,R]\times[0,R]$,

(b) $b(x,y,z)$ is non-negative, continuous function satisfying the condition

$$\int_0^\infty x^{-\theta s} b(x,y,z)dx \leq \eta y^{-\theta s}, \quad \theta,\eta>0,$$

(c) L_0 is a fix constant for a small $t>0$ such that

$$\|c\|_t = \sup_{t\in[0,t]} \int_0^\infty \Big(x^r + \frac{1}{x^{2s}}\Big)|c(t,x)|dx \leq L_0, \tag{6.41}$$

hold, then the operator $\mathcal{S}$ has contractive nature, i.e., $\|\mathcal{S}c - \mathcal{S}c^\star\| \leq \xi\|c_- c^\star\|, \forall\,(c,c^\star)\in \mathbb{Y}^+_{r,s}(t)\times\mathbb{Y}^+_{r,s}(t)$, where $\xi = 2t\mathcal{K}_1(\mu+1)L_0 < 1$ with $\mu = \max\{\bar{N},\eta\}$.

Proof. The detailed proof of this theorem had been investigated in [[102], Theorem 1]. □

Theorem 6.3.2. Let all the assumptions of Theorem 6.3.1 hold. If $\Theta_m = \sum_{i=0}^m c_i$ is the mth-order HAM truncated solution obtained using (6.20-6.21) for the CBE (1.8), then Θ_m converges to the exact solution $c(t,x)$ having following error bound

$$\|c-\Theta_m\| \leq \frac{\nabla^m}{1-\nabla}\|c_1\|, \tag{6.42}$$

where $\nabla = \xi|\alpha| + |1+\alpha| < 1$ and $\|c_1\| < \infty$.

Proof. From Eqs.(6.20-6.21), we have

$$\begin{aligned}
\Theta_m = \sum_{i=0}^m c_i =& c^{in}(x) - \alpha\sum_{j=1}^m \mathcal{L}^{-1}\Big[\int_0^\infty\int_x^\infty K(y,z)b(x,y,z)\Omega^1_{j-1}\,dy\,dz \\
&- \int_0^\infty K(x,y)\Omega^2_{j-1}\,dy\Big] + (1+\alpha)\sum_{j=1}^{m-1} c_j \\
=& c^{in}(x) - \alpha\mathcal{L}^{-1}\Big[\int_0^\infty\int_x^\infty K(y,z)b(x,y,z)\Big(\sum_{j=1}^m \Omega^1_{j-1}\Big)\,dy\,dz \\
&- \int_0^\infty K(x,y)\Big(\sum_{j=1}^m \Omega^2_{j-1}\Big)\,dy\Big] + (1+\alpha)\sum_{j=1}^{m-1} c_j.
\end{aligned} \tag{6.43}$$

Adding and subtracting the term $(1+\alpha)c^{in}(x)$ reduce the Eq.(6.43) into the following one

$$\begin{aligned}\Theta_m =& -\alpha\Bigg[c^{in}(x)\\ &+\mathcal{L}^{-1}\Bigg[\underbrace{\int_0^\infty\int_x^\infty K(y,z)b(x,y,z)\Big(\sum_{j=1}^{m}\Omega_{j-1}^1\Big)\,dy\,dz-\int_0^\infty K(x,y)\Big(\sum_{j=1}^{m}\Omega_{j-1}^2\Big)\,dy}_{\Omega(m)}\Bigg]\Bigg]\\ &+(1+\alpha)\Theta_{m-1}\\ =&-\alpha[c^{in}(t)+\mathcal{L}^{-1}[\Omega(m)]]+(1+\alpha)\Theta_{m-1}. \end{aligned}\tag{6.44}$$

For all $n,m\in\mathbb{N}$ and $n>m$, it is certain that

$$\|\Theta_n-\Theta_m\|\le|\alpha|\|\big[c^{in}(t)+\mathcal{L}^{-1}[\Omega(n)]-c^{in}(t)-\mathcal{L}^{-1}[\Omega(m)]\big]\|+|1+\alpha|\|\Theta_{n-1}-\Theta_{m-1}\|.$$

Article [103] suggested that $\sum_{i=1}^{n}\Omega_{i-1}^1\le c(\Theta_{n-1}(y))c(\Theta_{n-1}(z))$ and $\sum_{i=1}^{n}\Omega_{i-1}^2\le c(\Theta_{n-1}(x))c(\Theta_{n-1}(y))$, imply that

$$\begin{aligned}\|\Theta_n-\Theta_m\|\le&|\alpha|\|\big[c^{in}(t)+\mathcal{L}^{-1}[\Theta_{n-1}]-c^{in}(t)-\mathcal{L}^{-1}[\Theta_{m-1}]\big]\|+|1+\alpha|\|\Theta_{n-1}-\Theta_{m-1}\|\\ =&|\alpha|\|\big[\mathcal{S}\Theta_{n-1}-\mathcal{S}\Theta_{m-1}\big]\|+|1+\alpha|\|\Theta_{n-1}-\Theta_{m-1}\|.\end{aligned}$$

Using the contractive result of $\mathcal{S}$ in the aforementioned equation leads to

$$\begin{aligned}\|\Theta_n-\Theta_m\|\le&\xi|\alpha|\|\Theta_{n-1}-\Theta_{m-1}\|+|1+\alpha|\|\Theta_{n-1}-\Theta_{m-1}\|\\ =&\nabla\|\Theta_{n-1}-\Theta_{m-1}\|,\end{aligned}$$

for $\nabla=\xi|\alpha|+|1+\alpha|$. After substituting $n=m+1$, the above inequality converted into

$$\|\Theta_{m+1}-\Theta_m\|\le\nabla\|\Theta_m-\Theta_{m-1}\|\le\nabla^2\|\Theta_{m-1}-\Theta_{m-2}\|\le\cdots\le\nabla^m\|\Theta_1-\Theta_0\|.\tag{6.45}$$

Eq.(6.45) assists in finding the bound of $\|\Theta_n-\Theta_m\|$ having triangle inequality, as

$$\begin{aligned}\|\Theta_n-\Theta_m\|\le&\|\Theta_{m+1}-\Theta_m\|+\|\Theta_{m+2}-\Theta_{m+1}\|+\cdots+\|\Theta_{n-1}-\Theta_{n-2}\|+\|\Theta_n-\Theta_{n-1}\|\\ \le&\nabla^m\big(1+\nabla+\nabla^2+\cdots+\nabla^{n-m-1}\big)\|\Theta_1-\Theta_0\|=\nabla^m\left(\frac{1-\nabla^{n-m}}{1-\nabla}\right)\|c_1\|.\end{aligned}$$

If $\nabla < 1$, then $(1 - \nabla^{n-m}) < 1$ and $\|c_1\| < \infty$, thus we get

$$\|\Theta_n - \Theta_m\| \leq \frac{\nabla^m}{1-\nabla}\|c_1\|, \tag{6.46}$$

which converges to zero as $m \to \infty$. Therefore, a function Θ exists such that $\lim_{n\to\infty} \Theta_n = \Theta$. Hence, $c = \sum_{i=0}^{\infty} c_i = \lim_{n\to\infty} \Theta_n = \Theta$, which is the exact solution of (1.8). For a fixed m and taking $n \to \infty$, the error bound is derived as

$$\|c - \Theta_m\| \leq \frac{\nabla^m}{1-\nabla}\|c_1\|,$$

where c_1 is given in (6.20). □

Remark 6.3.3. The value of α is considered such that $\nabla < 1$, for that

$$\xi|\alpha| + |1+\alpha| < 1 \implies \xi < \frac{1-|1+\alpha|}{|\alpha|},\ \alpha \neq 0.$$

Hence, to ensure that $\nabla < 1$, α should be chosen from [-1, 0).

The following theorem equips the convergence and error results for the CBE's approximated nth-order AHPM solutions.

Theorem 6.3.4. Let us assume that all the assumptions of Theorem 6.3.1 hold. Consider $\Upsilon_m = \sum_{i=0}^{m} c_i$ is the mth-order AHPM series solution obtained using (6.30) for the CBE (1.8). Then Υ_m converges to the exact solution $c(t,x)$ with the following error bound

$$\|c - \Upsilon_m\| \leq \frac{\xi^m}{1-\xi}\|c_1\|, \tag{6.47}$$

where $\xi = 2t\mathcal{K}_1(\mu+1)L_0 < 1$ and $\|c_1\| < \infty$.

Proof. From the Eqs.(6.29) and (6.30), mth-order approximated solution is

$$\Upsilon_m = \sum_{i=0}^{m} c_i = c^{in} + \hat{H}_0 + \hat{H}_1 + \cdots + \hat{H}_{m-1} \tag{6.48}$$

where

$$\hat{H}_0 = N(c_0), \quad \hat{H}_1 = N(c_0 + c_1) - N(c_0),$$

$$\begin{aligned}\hat{H}_2 =& N(c_0 + c_1 + c_2) - N(c_0 + c_1),\\ \hat{H}_{m-1} =& N(c_0 + c_1 + \cdots + c_{m-1}) - N(c_0 + c_1 + \cdots + c_{m-2}).\end{aligned}$$

Substitute all the values of $\hat{H}_m$ into (6.48), the new form of Υ_m is obtained as

$$\Upsilon_m = c^{in} + N(c_0 + c_1 + \cdots + c_{m-1}) = c^{in} + N(\Upsilon_{m-1}) = \mathcal{S}\Upsilon_{m-1}. \tag{6.49}$$

By Theorem 6.3.1, we have

$$\|\Upsilon_{m+1} - \Upsilon_m\| \leq \xi\|\Upsilon_m - \Upsilon_{m-1}\|, \tag{6.50}$$

implies that

$$\|\Upsilon_{m+1} - \Upsilon_m\| \leq \xi\|\Upsilon_m - \Upsilon_{m-1}\| \leq \xi^2\|\Upsilon_{m-1} - \Upsilon_{m-2}\| \leq \cdots \leq \xi^m\|\Upsilon_1 - \Upsilon_0\|. \tag{6.51}$$

Next, the triangle inequality helps us to get the bound of $\|\Upsilon_n - \Upsilon_m\|$ for all $n, m \in \mathbb{N}$ with $n > m$, as

$$\begin{aligned}\|\Upsilon_n - \Upsilon_m\| \leq& \|\Upsilon_{m+1} - \Upsilon_m\| + \|\Upsilon_{m+2} - \Upsilon_{m+1}\| + \cdots + \|\Upsilon_{n-1} - \Upsilon_{n-2}\| + \|\Upsilon_n - \Upsilon_{n-1}\|\\ \leq& \xi^m\big(1 + \xi + \xi^2 + \cdots + \xi^{n-m-1}\big)\|\Upsilon_1 - \Upsilon_0\| = \xi^m\left(\frac{1 - \xi^{n-m}}{1 - \nabla}\right)\|c_1\|.\end{aligned} \tag{6.52}$$

Again, the term $\xi < 1$ provides the following

$$\|\Upsilon_n - \Upsilon_m\| \leq \frac{\xi^m}{1 - \xi}\|c_1\|, \tag{6.53}$$

that converges to zero as $m \to \infty$. Therefore, a function Υ exists such that $\Upsilon_n \to \Upsilon$, as $n \to \infty$ and so $c = \sum_{i=0}^{\infty} c_i = \lim_{n\to\infty} \Upsilon_n = \Upsilon$, which is the exact solution of (1.8). Further, for a fixed m and letting $n \to \infty$, the error bound (6.47) is accomplished. □

6.4 Numerical Results and Discussion

This section analyses the accuracy, verification, and visual representation of the numerical and semi-analytical methods and their results. It contains the findings of CBE (1.8) by

implementing the FVM, HAM, and AHPM for various collisional kernels. The discussion regarding the density function and the integral property of density (moments) is supported by the approximate solutions provided by three different schemes for an appropriate time scale. Graphs display all the results simulated by MATLAB and MATHEMATICA software.

Example 6.4.1. Assuming Eq.(1.8) with $K(x,y) = xy$, $b(x,y,z) = \frac{2}{y}$ and $c^{in}(x) = \exp(-x)$ for which the corresponding exact solution is $c(t,x) = (1+t)^2 \exp(-x(1+t))$ described in [76].

Eq.(6.20) provides the series solution terms, thanks to HAM as

$$\begin{aligned}
c_0(t,x,\alpha) =& e^{-x}, \quad c_1(t,x,\alpha) = \alpha t \left(e^{-x}x - 2e^{-x}\right), \\
c_2(t,x,\alpha) =& \frac{1}{2}\alpha t e^{-x}\left(2\alpha(t-2) + \alpha t x^2 + x(\alpha(2-4t)+2) - 4\right), \\
c_3(t,x,\alpha) =& \frac{1}{6}\alpha t e^{-x}\big(\alpha^2 t^2 x^3 + 6x\big(\alpha^2\big(t^2-4t+1\big)+\alpha(2-4t)+1\big) \\
&+ 12(\alpha+1)(\alpha(t-1)-1) + 6\alpha t x^2(\alpha+\alpha(-t)+1)\big).
\end{aligned}$$

While, the computation of series terms of approximated AHPM solution is derived by Eqs.(6.34-6.36) as

$$\begin{aligned}
c_0(t,x) =& e^{-x}, \quad c_1(t,x) = t\left(2e^{-x} - e^{-x}x\right), \quad c_2(t,x) = \frac{1}{2}t^2 e^{-x}((x-4)x+2), \\
c_3(t,x) =& -\frac{1}{6}t^3 e^{-x}x^3 + t^3 e^{-x}x^2 - t^3 e^{-x}x, \\
c_4(t,x) =& \frac{1}{24}t^4 e^{-x}x^4 - \frac{1}{3}t^4 e^{-x}x^3 + \frac{1}{2}t^4 e^{-x}x^2, \\
c_5(t,x) =& -\frac{1}{120}t^5 e^{-x}x^3((x-10)x+20).
\end{aligned}$$

Continuing in this manner, one can compute the higher order terms of the series solution using MATHEMATICA. The 5th-order series approximated solutions, i.e., Θ_5 of HAM and Υ_5 of AHPM, are considered for evaluation and the results are compared with finite volume and exact solutions. The corresponding optimal value of $\alpha = -0.826$, up to 3 significant digit (SD) with rounding, is generated by applying the formula (6.22) for the truncated solution of HAM.

The illustrations of the number density functions obtained via three methods are visualized along with the analytical solution for various volumes in Fig.6.1. As anticipated, the density function exhibits decreasing behaviour as size increases. At a particular time $t = 1$, small-sized particles are abundant and large-sized particles are scarce. We observe that FVM results demonstrate excellent chemistry with the analytical solution for particles of any sizes, whereas HAM (Θ_5) and AHPM (Υ_5) show acceptable precision for particles of small sizes but fail to maintain the accuracy for large sizes particles. Error plots in Fig.6.2 are graphical representations that assess the accuracy and quality of predicated FVM, HAM and AHPM solutions. The maximum error bounds of HAM, AHPM and FVM emerge for small size particles at considerable time and are almost identical to zero. This indicates the novelty of our proposed schemes. Now, we expressed the concept of the experimental order of convergence (EOC) for the approximated methods to quantify how quickly the error decreases. The formula to find the EOC for FVM, HAM and AHPM is written as follows

$$\text{EOC} = \frac{1}{\ln(2)} \ln\left(\frac{E_{\text{I}}}{E_{2\text{I}}}\right), \tag{6.54}$$

where E_{I} is the discrete error norm for I number of mesh points, i.e., $E_{\text{I}} = \|N_E - N_{\text{I}}\|$, where $N_E = \sum_{i=1}^{\text{I}} c_i \Delta x_i$ and $N_I = \sum_{i=1}^{\text{I}} \hat{c}_i \Delta x_i$ are the total number of particles generated analytically and numerically via FVM (6.1), respectively. Similarly, for HAM $N_I = \sum_{i=1}^{\text{I}} \Theta_n^i \Delta x_i$ and for AHPM $N_I = \sum_{i=1}^{\text{I}} \Upsilon_n^i \Delta x_i$, where $\Theta_n^i = \Theta_n(t, x_i)$ and $\Upsilon_n^i = \Upsilon_n(t, x_i)$. Table 6.1 reveals that the EOC of all the techniques is one which implies that they are first order accurate. Furhter, to justify the approximated solutions, integral properties like moments are also computed by Eq.(2.2) and compared with the analytical moments. Fig.6.3 provides information regarding the comparison of HAM, AHPM, FVM moments with the exact ones at time $t = 1$. The zeroth moment, in Fig.6.3(a) can be visualized with an increasing pattern as time increases. All the results of approximated moment overlap to each other and demonstrate excellent accuracy with the exact one. As expected, in Fig.6.3(b), the approximated first moments obtained by HAM, AHPM and FVM are constant and identical to the analytic moment, that is 1. It shows the conserva-

Cells (I)	FVM	HAM	AHPM
30	-	-	-
60	1.1515	0.9808	0.9981
120	1.0901	0.9906	0.9990
240	1.0497	0.9953	0.9994

Table 6.1: EOC using FVM, HAM and AHPM at time $t = 1$ for Example 6.4.1

tion of mass during the particulate process in the system for a set of kernels considered in Example 6.4.1. The approximated second moments using Θ_5, Υ_5 and FVM have decreased behaviour along with the exact moment as time progresses, see Fig.6.3(c). HAM and FVM moments have affirmed satisfactory agreement to the precised one, whereas AHPM results deviate after time $t = 0.5$.

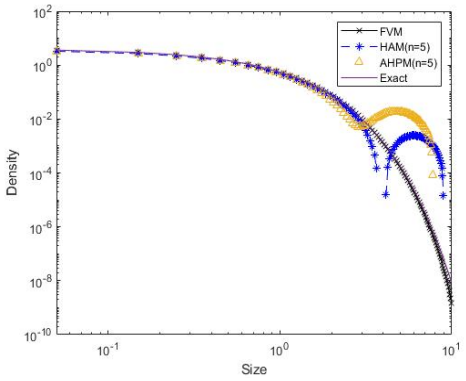

Figure 6.1: Log-log plots of density functions at time 1

Example 6.4.2. Let us consider Eq.(1.8) with kernels $K(x, y) = \frac{xy}{20}$, $b(x, y, z) = \frac{2}{y}$ and initial data $c^{in}(x) = x\exp(-x)$. The analytical solution for the density function is hard to compute, however the precise formulations for the zeroth and first moments are $\mu_0(t) = 1 + \frac{t}{5}$ and $\mu_1(t) = 2$, respectively.

Substituting these kernel parameters and initial condition in Eq.(6.20), we get the series terms due to HAM as

$$c_0(t, x, \alpha) = xe^{-x}, \quad c_1(t, x, \alpha) = \frac{1}{10}\alpha t e^{-x}((x - 2)x - 2),$$

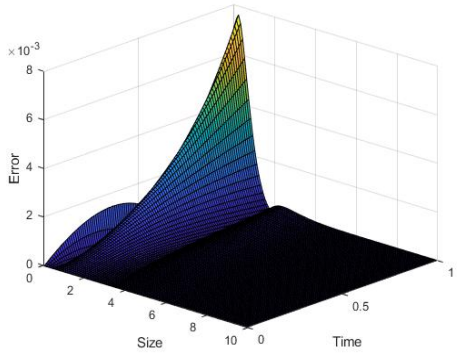

(a) FVM error

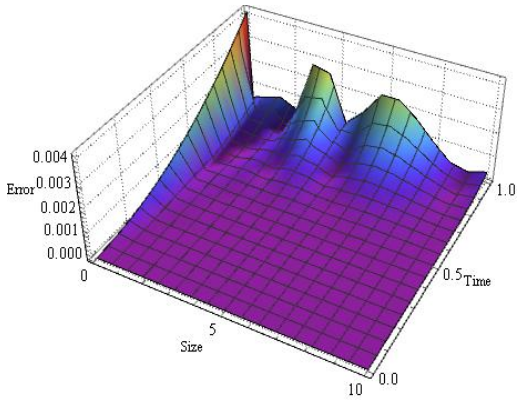

(b) HAM error

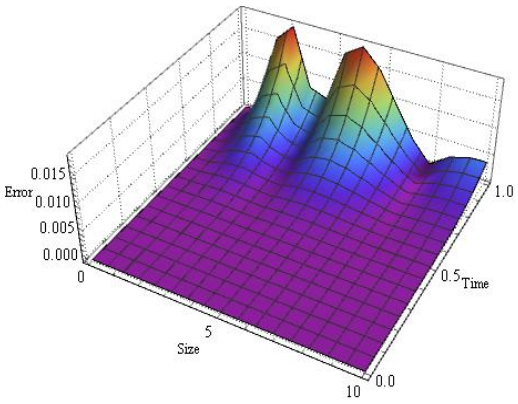

(c) AHPM error

Figure 6.2: Absolute error plots

$$c_2(t,x,\alpha) = \frac{1}{200}\alpha t e^{-x}(\alpha(tx((x-4)x-2)+4t+20(x-2)x-40)+20((x-2)x-2)),$$

$$\begin{aligned} c_3(t,x,\alpha) =& \frac{\alpha^2 t^2 e^{-x}\left(\alpha t x\left((x-6)x^2+12\right)+30(\alpha+1)(x((x-4)x-2)+4)\right)}{6000} \\ &+ (\alpha+1)\Big(\frac{1}{2}\alpha t^2\Big(\frac{1}{100}\alpha e^{-x}x\big(x^2-2x-2\big)-\frac{1}{50}\alpha e^{-x}\big(x^2-2\big)\Big) \\ &+ \alpha(\alpha+1)t\Big(\frac{1}{10}e^{-x}x^2-\frac{1}{5}e^{-x}(x+1)\Big)\Big). \end{aligned}$$

For $\alpha = -0.969$ taken up to 3 SD with rounding, we have considered 5th-order HAM (Θ_5) truncated series solution for numerical verification. The higher terms could not be obtained due to the complexity of the model and parameters.

Further, AHPM (6.34-6.36) is also applied for this case to compute the first few series

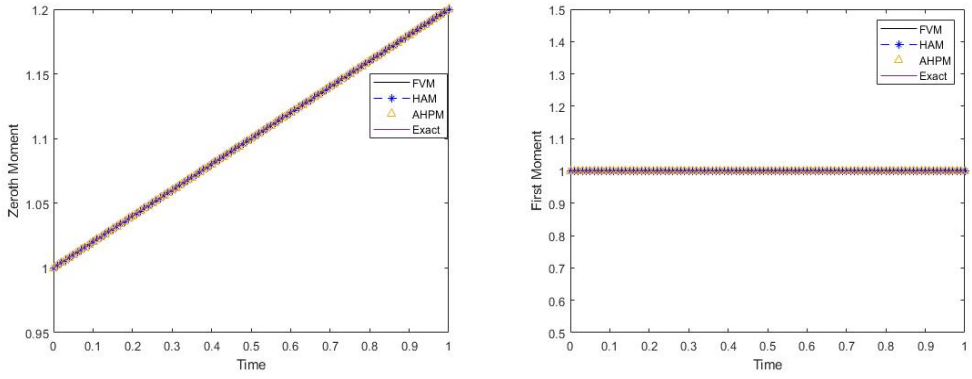

(a) Zeroth moment

(b) First moment

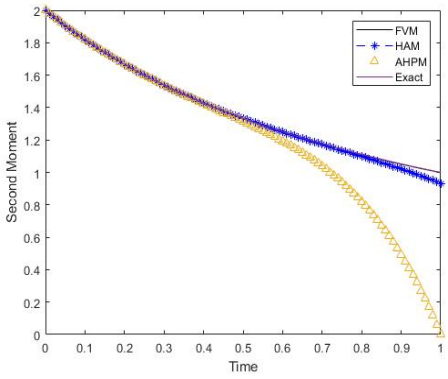

(c) Second moment

Figure 6.3: Moments comparison at time 1: FVM, HAM, AHPM and exact

terms for the approximated solution. The terms are listed below

$$
\begin{aligned}
c_0(t,x) =& xe^{-x}, \quad c_1(t,x) = \frac{1}{10}te^{-x}(2-(x-2)x),\\
c_2(t,x) =& \frac{1}{200}t^2e^{-x}(x((x-4)x-2)+4),\\
c_3(t,x) =& -\frac{t^3e^{-x}x^4}{6000} + \frac{t^3e^{-x}x^3}{1000} - \frac{1}{500}t^3e^{-x}x,\\
c_4(t,x) =& \frac{t^4e^{-x}x^5}{240000} - \frac{t^4e^{-x}x^4}{30000} + \frac{t^4e^{-x}x^3}{60000} + \frac{t^4e^{-x}x^2}{10000}.
\end{aligned}
$$

In the absence of an exact solution of density function, the difference between consecutive terms of series solutions is plotted in Fig.6.4(b) to see the precision of semi-analytical algorithms. Graph shows that the difference between 4 and 5 terms solutions is negligible

for each schemes and hence, it is certain that the approximated solutions converge to the exact one. Further, to validate the results, 5th-order truncated solutions via HAM (Θ_5) and AHPM (Υ_5) are also compared with the FVM solution in Fig.6.4(a) at time $t = 1$. The figure elaborates that HAM and AHPM results have little disturbance to FVM solution for small size particles, however, all results exhibit similar behaviour as particle size increases. The approximated density function plots display an increasing pattern till the size $x = 1$, which decreases further as particle size progresses.

Since, expressions for analytical moments are available, to justify the approximated solutions, we resemble the approximated moments of HAM using Θ_5, AHPM via Υ_5 and FVM to the corresponding analytical moments in Fig.6.5 for different time distributions. In Figs.6.5(a), 6.5(b), zeroth and first moments of HAM, AHPM and FVM show remarkable accuracy with the exact ones for various time scales. Therefore, we can consider our approximated solutions to predict better results for different particle sizes and times. In the unavailability of the exact second moment, series (HAM, AHPM) and FVM moments are compared at a time scale of 0 to 1 in Fig.6.5(c). The figure indicates that all approximated moments follow same pattern where HAM and AHPM moments exactly coincide with each other.

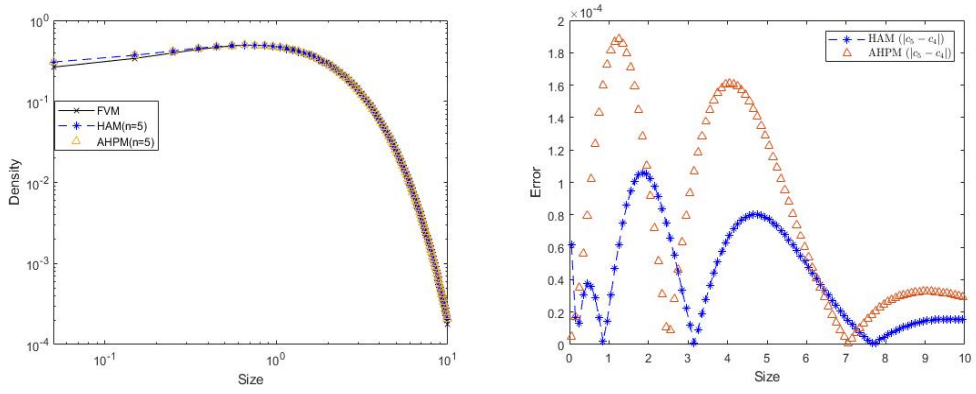

(a) Log-log plots of density functions at time 1

(b) Terms error

Figure 6.4: Density and consecutive terms error plots

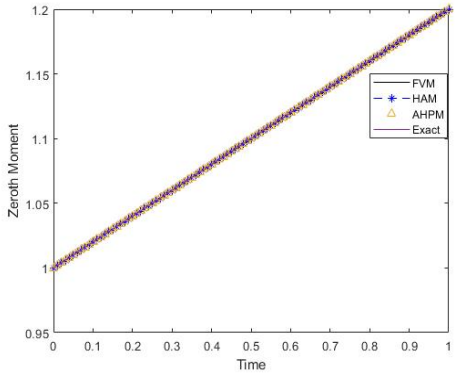

(a) Zeroth moment

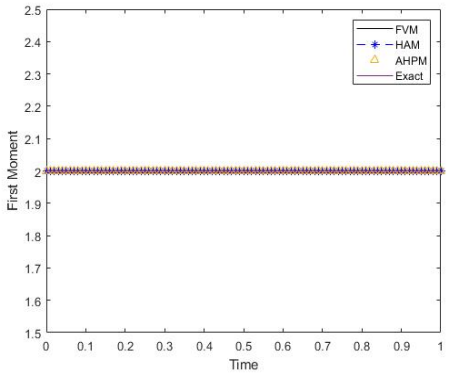

(b) First moment

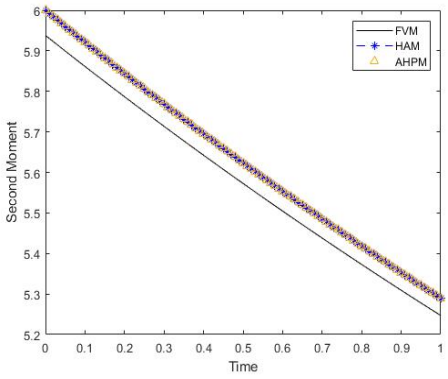

(c) Second moment

Figure 6.5: Moments comparison at time 1: FVM, HAM, AHPM and exact

Example 6.4.3. Consider Eq.(1.8) with $K(x,y) = 1$, $b(x,y,z) = \delta(x - 0.4y) + \delta(x - 0.6y)$ and $c^{in}(x) = \exp(-x)$. In this case, the exact solution for the density function is not available in the literature. However, exact moments (zeroth, first and second) can be calculated analytically as $\mu_0(t) = \frac{1}{1-t}, \quad \mu_1(t) = 1$ and $\mu_2(t) = 2(1-t)^{0.48}$. The second moment is computed by multiplying Eq.(1.8) by x^2 and integrating from 0 to ∞ over x.

Implement the HAM, AHPM and FVM to determine a solely approximative solutions. The HAM (6.20) is applied for these set of kernels to get the following series terms

$$c_0(t,x,\alpha) = e^{-x}, \quad c_1(t,x,\alpha) = \alpha t\left(-1.67e^{-1.67x}\theta(0.67x) - 2.5e^{-2.5x}\theta(1.5x) + e^{-x}\right),$$
$$c_2(t,x,\alpha) = \alpha t e^{-18.36x}\Big(\theta(0.67x)\big(1.39\alpha t e^{15.58x}\theta(1.11x) + 2.08\alpha t e^{14.19x}\theta(2.5x)$$

$$+ e^{16.69x}(-1.67\alpha - 0.83\alpha t - 1.67)\big)+\theta(1.5x)\big(\alpha t\big(2.08e^{14.19x}\theta(1.67x)$$
$$+ 3.13e^{12.11x}\theta(3.75x)\big)+e^{15.86x}(-2.5\alpha - 1.25\alpha t - 2.5)\big)+(\alpha+1)e^{17.36x}\big).$$

We continue this procedure to compute the next term to estimate the $3rd$-order approximate solution (Θ_3) by MATHEMATICA. The optimal value of α is taken as -0.829, again using only 3 SD with rounding, by operating Eq.(6.22). Moving further, the second semi-analytical method AHPM executes the first few terms of the series solution as

$$c_0(t,x) = e^{-x}, \quad c_1(t,x) = t\left(1.67e^{-1.67x}\theta(0.67x) + 2.5e^{-2.5x}\theta(1.5x) - e^{-x}\right),$$
$$c_2(t,x) = te^{-22.53x}\big(\theta(1.5x)\big(te^{18.36x}((2.08\ -1.39t)\theta(1.67x) + 2.78t\theta(x))$$
$$+ te^{16.28x}((3.12\ -2.08t)\theta(3.75x) + 4.17t\theta(x)) + e^{20.03x}\big(2.5\ -0.83t^2\big)$$
$$+ ((-0.83t - 1.25)t - 2.5)e^{20.03x}\big)+t\theta(0.67x)\big(e^{19.75x}((1.39\ -0.93t)\theta(1.11x)$$
$$+ 1.85t\theta(x)) + e^{18.36x}((2.08\ -1.39t)\theta(2.5x) + 2.78t\theta(x)) + (-1.11t$$
$$- 0.83)e^{20.86x}\big)+0.33t^2e^{21.53x}\big).$$

An approximated truncated solution of order 3 (Υ_3) is considered to see the results of density function and moments for a range of particle sizes. Due to the lack of an exact density function, only approximate solutions of HAM (Θ_3), AHPM (Υ_3) and FVM are presented graphically in Fig.6.6 for time $t = 0.5$ over a range of particle sizes. Interestingly, FVM and HAM results are almost identical up to size 10, but AHPM does not show the same behaviour as HAM/FVM for large size particles. Similar to the previous case, it is noticed that the difference between consecutive terms of the series solutions decreases and tends to zero, ensuring the convergence of the algorithms. Thus, plot is omitted here. The approximated moments computed via FVM and series solution methods are compared with the analytical moments in Fig.6.7 to justify the novelty of schemes. In Fig.6.7(a), zeroth moments using AHPM 3-term solution (Υ_3) and FVM are exactly matching with the exact number of particles. However, HAM (Θ_3) moment starts slipping away from the accuracy after time 0.25. In addition, Fig.6.7(c) also justifies a slight disturbance in the second moment of HAM. As expected, the total mass is conserved and all the approximated methods provide the excellent accuracy with it, see Fig.6.7(b). In

conclusion, we can visualize from these figures that AHPM and FVM results are nearest to the exact ones as compared to the HAM.

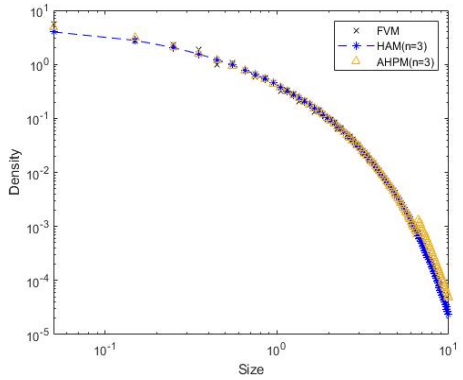

Figure 6.6: Log-log plots of density functions at time 0.5

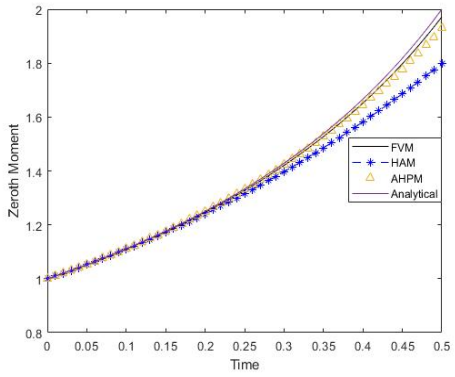

(a) Zeroth moment

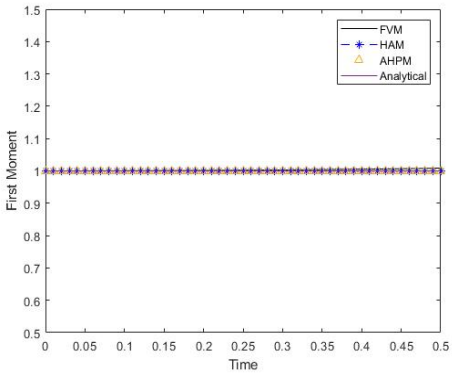

(b) First moment

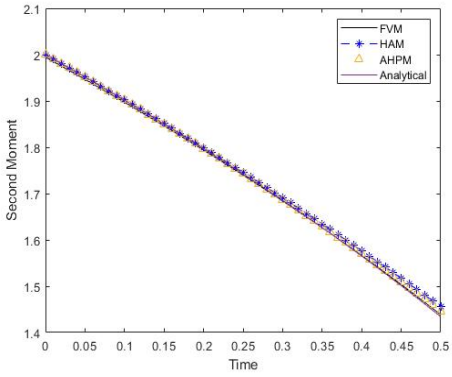

(c) Second moment

Figure 6.7: Moments comparison at time 0.5: FVM, HAM, AHPM and exact

Chapter 7

Conclusions and Future Directions

Conclusions

This chapter serves as a summary of the findings presented in this dissertation. Here, the theoretical, numerical and semi-analytical results were discussed for the CMBE and CBE. Additionally, we explored potential ways for extending the research and identify areas with promising prospects for future investigations in this field.

In Chapter 2, we have examined the convergence analysis of a weighted FVS for solving coagulation and multiple breakage models in weighted L^1 space by using weak compactness arugment. Dunford-Pettis and La Vall$\acute{e}$e Poussin theorems were used to establish the convergence of numerically approximated solutions towards a weak solution of continuous problem with locally bounded coagulation and singular breakage functions. Further, error analysis was also explored considering a uniform mesh with kinetic parameters in $W^{1,\infty}_{loc}$ space. Furthermore, four different test cases of numerical examples have been used to validate the first order theoretical error observations.

Further, for the Chapter 3, we considered the divergence form of the continuous CMBE. After that, FVS was implemented to get the fully discrete system using the explicit Euler method for the time variable. Then, analysis of the weak convergence was

completed in L^1 space, and error estimation of first order in $W^{1,\infty}_{loc}$ space for uniform mesh. This observation was justified numerically by considering four different practical examples of coupled coagulation and breakage equations.

Chapter 4 proposed a theoretical convergence analysis of FVS for solving the collisional breakage equation for the non-uniform mesh. It yielded a non-conservative scheme, for which a weak convergence analysis has been executed with unbounded collision and breakage distribution kernels. The result was accomplished in the presence of weak L^1 compactness method. In addition, explicit error estimation of the method was also explored for the locally bounded kernels. It has been demonstrated that the FVS is first-order accurate for uniform meshes which was further validated by taking various numerical examples of model.

In Chapter 5, semi-analytical VIM and ODM techniques were implemented on the non-linear collision-induced breakage equation. These methods provided a recursive algorithm for calculating the closed form of exact solution or approximate solutions. The convergence result for VIM was taken from [96]. In ODM, we have used the contraction mapping theorem to show series convergence, which was reliable enough to estimate the maximum absolute truncated error. The applicability and accuracy of these methods were shown by comparing the approximated solutions and various moments against the analytical results for three different test cases. Interestingly, in the first case, we got the closed form solution via VIM which was also the exact solution. In each example, VIM's solution demonstrated superior long-term compliance with the analytical requirements, whereas ODM's solution failed to do so. Observations indicated that moment plots were more precise than concentration plots over extended time periods. In conclusion, it was observed as per the outcomes that VIM was superior to ODM.

Finally, in Chapter 6, HAM, AHPM and FVM were employed successfully for solving the non-linear collision-induced breakage equation with certain collision and breakage kernels. The approximate analytical solutions were obtained by truncating the infinite series form of the series solution which was proven to be the exact solution. These methods were easy to implement on such non-linear integro-partial differential equations for

various kernels and exponential decay initial functions. Convergence analysis was exhibited for the series solutions of HAM and AHPM and it was reliable enough to achieve the error estimations in each case. The approximated results of concentration function and moments by HAM, AHPM and FVM were compared to the exact ones for three test problems. All the graphs described the good precision and efficiency of considered techniques. The research aims to shed light on the inherent limitations associated with semi-analytical methods. Our investigations revealed that the terms generated using the HAM often exhibited significant complexity, rendering the derivation of closed-form solutions a challenging endeavor. Furthermore, determining higher-order components within the series solution was computationally expansive in both methods, particularly in case where the kernels were functions involving the Dirac delta function.

Future Directions

Based on the work done in this thesis, the possible future scopes are as follows:

1. To find weak convergence of the discretized solution towards the continuous solution of the non-linear collision-induced breakage equation with singular kernels.

2. To explore other numerical methods to solve collision-induced breakage equation and convergence analysis since only the finite volume method is implemented.

3. To prove the weak convergence for the finite volume solution of the coagulation and collision-induced breakage equation.

4. To implement the semi-analytical methods for coagulation and collision-induced breakage equation and convergence analysis.

Bibliography

[1] Suresh Pathi, Rajesh Kumar, and Vikranth Kumar Surasani. Investigation on agglomeration kinetics of acetaminophen using fluidized bed wet granulation. *Asia-Pacific Journal of Chemical Engineering*, 15(2):e2416, 2020.

[2] Yan Jin, Feiyong Chen, Bing Xu, Guangxiang Ma, Lijie Zhang, Zhigang Yang, Rupeng Liu, Cuizhen Sun, Xiaoxiang Cheng, Ning Guo, et al. Iron-based technology coupling moderate preoxidation with hybrid coagulation for highly effective removal and moderate growth inhibition of oscillatoria in drinking water treatment plants. *Journal of Environmental Chemical Engineering*, 10(3):107723, 2022.

[3] Dominic Samra, Ch Helling, and Tilman Birnstiel. Mineral snowflakes on exoplanets and brown dwarfs-coagulation and fragmentation of cloud particles with hylands. *Astronomy & Astrophysics*, 663:A47, 2022.

[4] Vincent Guillet, P Hennebelle, G Pineau Des Forêts, Alexandre Marcowith, B Commerçon, and P Marchand. Dust coagulation feedback on magnetohydrodynamic resistivities in protostellar collapse. *Astronomy & Astrophysics*, 643:A17, 2020.

[5] Mehakpreet Singh, Saeed Shirazian, Vivek Ranade, Gavin M Walker, and Ashish Kumar. Challenges and opportunities in modelling wet granulation in pharmaceutical industry–a critical review. *Powder Technology*, 403:117380, 2022.

[6] Shrenik Mehta, Heather Flores, Benjamin Walters, and Alavattam Sreedhara.

Metal ion interactions with mabs: Part 2. zinc-mediated aggregation of igg1 monoclonal antibodies. *Pharmaceutical Research*, 38(8):1387–1395, 2021.

[7] CA Biggs, C Sanders, AC Scott, AW Willemse, AC Hoffman, T Instone, AD Salman, and MJ Hounslow. Coupling granule properties and granulation rates in high-shear granulation. *Powder Technology*, 130(1-3):162–168, 2003.

[8] Primož Poredoš, Nada Petelin, Boris Vidrih, Tilen Žel, Qiuming Ma, Ruzhu Wang, and Andrej Kitanovski. Condensation of water vapor from humid air inside vertical channels formed by flat plates. *Iscience*, 25(1), 2022.

[9] Firnaaz Ahamed, Mehakpreet Singh, Hyun-Seob Song, Pankaj Doshi, Chien Wei Ooi, and Yong Kuen Ho. On the use of sectional techniques for the solution of depolymerization population balances: Results on a discrete-continuous mesh. *Advanced Powder Technology*, 31(7):2669–2679, 2020.

[10] Katelyn Breivik, Scott Coughlin, Michael Zevin, Carl L Rodriguez, Kyle Kremer, S Ye Claire, Jeff J Andrews, Michael Kurkowski, Matthew C Digman, Shane L Larson, et al. Cosmic variance in binary population synthesis. *The Astrophysical Journal*, 898(1):71, 2020.

[11] Nikolai Brilliantov, PL Krapivsky, Anna Bodrova, Frank Spahn, Hisao Hayakawa, Vladimir Stadnichuk, and Jürgen Schmidt. Size distribution of particles in saturn's rings from aggregation and fragmentation. *Proceedings of the National Academy of Sciences*, 112(31):9536–9541, 2015.

[12] Mingzhe Wei, Yiyang Zhang, Zhu Fang, Xinxin Wu, and Libin Sun. Graphite aerosol release to the containment in a water ingress accident of high temperature gas-cooled reactor (htgr). *Nuclear Engineering and Design*, 342:170–175, 2019.

[13] Sheng Chen and Shuiqing Li. Collision-induced breakage of agglomerates in homogenous isotropic turbulence laden with adhesive particles. *Journal of Fluid Mechanics*, 902:A28, 2020.

[14] M v Smoluchowski. Versuch einer mathematischen theorie der koagulationskinetik kolloider lösungen. *Zeitschrift für Physikalische Chemie*, 92(1):129–168, 1918.

[15] Hans Müller. Zur allgemeinen theorie ser raschen koagulation: Die koagulation von stäbchen-und blättchenkolloiden; die theorie beliebig polydisperser systeme und der strömungskoagulation. *Kolloidchemische Beihefte*, 27:223–250, 1928.

[16] Z. Melzak. A scalar transport equation. *Transactions of the American Mathematical Society*, 85(2):547–560, 1957.

[17] SK Friedlander. On the particle size spectrum of a condensing vapor. *The Physics of Fluids*, 3(5):693–696, 1960.

[18] Robert M Ziff. New solutions to the fragmentation equation. *Journal of Physics A: Mathematical and General*, 24(12):2821, 1991.

[19] PJ Blatz and AV Tobolsky. Note on the kinetics of systems manifesting simultaneous polymerization-depolymerization phenomena. *The journal of physical chemistry*, 49(2):77–80, 1945.

[20] R Dennis Vigil and Robert M Ziff. On the stability of coagulation—fragmentation population balances. *Journal of Colloid and Interface Science*, 133(1):257–264, 1989.

[21] Z Cheng and S Redner. Scaling theory of fragmentation. *Physical Review Letters*, 60(24):2450, 1988.

[22] Philippe Laurençot and Dariusz Wrzosek. The discrete coagulation equations with collisional breakage. *Journal of Statistical Physics*, 104:193–220, 2001.

[23] Matthieu H Ernst and Ignacio Pagonabarraga. The nonlinear fragmentation equation. *Journal of Physics A: Mathematical and Theoretical*, 40(17):F331, 2007.

[24] Z Alexander Melzak. The effect of coalescence in certain collision processes. *Quarterly of Applied Mathematics*, 11(2):231–234, 1953.

[25] Govind Menon and Robert L Pego. Approach to self-similarity in smoluchowski's coagulation equations. *Communications on Pure and Applied Mathematics: A Journal Issued by the Courant Institute of Mathematical Sciences*, 57(9):1197–1232, 2004.

[26] Philippe Laurençot. Uniqueness of mass-conserving self-similar solutions to smoluchowski's coagulation equation with inverse power law kernels. *Journal of Statistical Physics*, 171:484–492, 2018.

[27] F Leyvraz. Existence and properties of post-gel solutions for the kinetic equations of coagulation. *Journal of Physics A: Mathematical and General*, 16(12):2861, 1983.

[28] François Leyvraz. Scaling theory and exactly solved models in the kinetics of irreversible aggregation. *Physics Reports*, 383(2-3):95–212, 2003.

[29] François Leyvraz and Hans Rudolf Tschudi. Singularities in the kinetics of coagulation processes. *Journal of Physics A: Mathematical and General*, 14(12):3389, 1981.

[30] AF Filippov. On the distribution of the sizes of particles which undergo splitting. *Theory of Probability & Its Applications*, 6(3):275–294, 1961.

[31] ED McGrady and Robert M Ziff. "shattering"transition in fragmentation. *Physical Review Letters*, 58(9):892, 1987.

[32] Miguel Escobedo, Ph Laurençot, Stéphane Mischler, and Benoît Perthame. Gelation and mass conservation in coagulation-fragmentation models. *Journal of Differential Equations*, 195(1):143–174, 2003.

[33] Jacek Banasiak, Wilson Lamb, and Philippe Laurençot. Analytic methods for coagulation-fragmentation models, volume ii. In *Chapman and Hall/CRC Monographs and Research Notes in Mathematics*. CRC Press, 2019.

[34] Fernando Pestana da Costa. Existence and uniqueness of density conserving solutions to the coagulation-fragmentation equations with strong fragmentation. *Journal of Mathematical Analysis and Applications*, pages 892–914, 1995.

[35] Philippe Laurençot. Mass-conserving solutions to coagulation-fragmentation equations with non-integrable fragment distribution function. *arXiv preprint arXiv:1804.08861*, 2018.

[36] IW Stewart and E Meister. A global existence theorem for the general coagulation–fragmentation equation with unbounded kernels. *Mathematical Methods in the Applied Sciences*, 11(5):627–648, 1989.

[37] Philippe Laurençot. Mass-conserving solutions to coagulation-fragmentation equations with balanced growth. *arXiv preprint arXiv:1901.08313*, 2019.

[38] Vladimir N Piskunov. The asymptotic behavior and self-similar solutions for disperse systems with coagulation and fragmentation. *Journal of Physics A: Mathematical and Theoretical*, 45(23):235003, 2012.

[39] Philippe Laurençot. On a class of continuous coagulation-fragmentation equations. *Journal of Differential Equations*, 167(2):245–274, 2000.

[40] Philippe Laurençot. The discrete coagulation equations with multiple fragmentation. *Proceedings of the Edinburgh Mathematical Society*, 45(1):67–82, 2002.

[41] Ankik Kumar Giri, Jitendra Kumar, and Gerald Warnecke. The continuous coagulation equation with multiple fragmentation. *Journal of Mathematical Analysis and Applications*, 374(1):71–87, 2011.

[42] IW Stewart. A uniqueness theorem for the coagulation-fragmentation equation. In *Mathematical Proceedings of the Cambridge Philosophical Society*, volume 107, pages 573–578. Cambridge University Press, 1990.

[43] Ankik Kumar Giri, Philippe Laurençot, and Gerald Warnecke. Weak solutions to the continuous coagulation equation with multiple fragmentation. *Nonlinear Analysis: Theory, Methods & Applications*, 75(4):2199–2208, 2012.

[44] Doraiswami Ramkrishna. *Population balances: Theory and applications to particulate systems in engineering*. Elsevier, 2000.

[45] Akinola Falola, Antonia Borissova, and Xue Zhong Wang. Extended method of moment for general population balance models including size dependent growth rate, aggregation and breakage kernels. *Computers & Chemical Engineering*, 56: 1–11, 2013.

[46] Mohsen Shiea, Antonio Buffo, Marco Vanni, and Daniele Marchisio. Numerical methods for the solution of population balance equations coupled with computational fluid dynamics. *Annual Review of Chemical and Biomolecular Engineering*, 11:339–366, 2020.

[47] Stelios Rigopoulos and Alan G Jones. Finite-element scheme for solution of the dynamic population balance equation. *AIChE Journal*, 49(5):1127–1139, 2003.

[48] M Nicmanis and MJ Hounslow. Finite-element methods for steady-state population balance equations. *AIChE Journal*, 44(10):2258–2272, 1998.

[49] Francis Filbet and Philippe Laurençot. Numerical simulation of the smoluchowski coagulation equation. *SIAM Journal on Scientific Computing*, 25(6):2004–2028, 2004.

[50] Jean-Pierre Bourgade and Francis Filbet. Convergence of a finite volume scheme for coagulation-fragmentation equations. *Mathematics of Computation*, 77(262): 851–882, 2008.

[51] Rajesh Kumar, Jitendra Kumar, and Gerald Warnecke. Moment preserving finite volume schemes for solving population balance equations incorporating aggrega-

tion, breakage, growth and source terms. *Mathematical Models and Methods in Applied Sciences*, 23(07):1235–1273, 2013.

[52] Haibo Zhao, Chuguang Zheng, and Minghou Xu. Multi-monte carlo method for particle coagulation: description and validation. *Applied Mathematics and Computation*, 167(2):1383–1399, 2005.

[53] Gregor Kotalczyk, Jherna Devi, and Frank Einar Kruis. A time-driven constant-number monte carlo method for the gpu-simulation of particle breakage based on weighted simulation particles. *Powder Technology*, 317:417–429, 2017.

[54] Robert Eymard, Thierry Gallouët, and Raphaèle Herbin. Finite volume methods. *Handbook of Numerical Analysis*, 7:713–1018, 2000.

[55] Randall J LeVeque. *Finite volume methods for hyperbolic problems*, volume 31. Cambridge university press, 2002.

[56] RAJESH KUMAR and JITENDRA KUMAR. Finite volume scheme for multiple fragmentation equations. *IJNAM*, 3(3):270–284, 2012.

[57] Jitraj Saha and Jitendra Kumar. Development of a mass conserving discretization technique for breakage problems and its convergence analysis. *International Journal of Advances in Engineering Sciences and Applied Mathematics*, 7:51–61, 2015.

[58] Mehakpreet Singh, Jitendra Kumar, Andreas Bück, and Evangelos Tsotsas. A volume-consistent discrete formulation of aggregation population balance equations. *Mathematical Methods in the Applied Sciences*, 39(9):2275–2286, 2016.

[59] Louis Forestier-Coste and Simona Mancini. A finite volume preserving scheme on nonuniform meshes and for multidimensional coalescence. *SIAM Journal on Scientific Computing*, 34(6):B840–B860, 2012.

[60] Mojtaba Ranjbar, Hojatollah Adibi, and Mehrdad Lakestani. Numerical solution of homogeneous smoluchowski's coagulation equation. *International Journal of Computer Mathematics*, 87(9):2113–2122, 2010.

[61] J Manafianheris. Application of the modified laplace decomposition method for solving the homogeneous smoluchowski's equation. *World Applied Sciences Journal*, 14(12):1804–1815, 2011.

[62] Zakia Hammouch and Toufik Mekkaoui. A laplace-variational iteration method for solving the homogeneous smoluchowski coagulation equation. *Applied Mathematical Sciences*, 6(18):879–886, 2012.

[63] Sonali Kaushik, Saddam Hussain, and Rajesh Kumar. Laplace transform-based approximation methods for solving pure aggregation and breakage equations. *Mathematical Methods in the Applied Sciences*, 2023.

[64] Daniil Aleksandrovich Stefonishin, Sergei Aleksandrovich Matveev, Aleksandr Pavlovich Smirnov, and Eugene Evgen'evich Tyrtyshnikov. Tensor decompositions for solving the equations of mathematical models of aggregation with multiple collisions of particles. *Numerical Methods and Programming*, 19:390–404, 2018.

[65] Jafar Biazar, Zainab Ayati, and Mohammad Reza Yaghouti. Homotopy perturbation method for homogeneous smoluchowsk's equation. *Numerical Methods for Partial Differential Equations*, 26(5):1146–1153, 2010.

[66] Gurmeet Kaur, Randhir Singh, Mehakpreet Singh, Jitendra Kumar, and Themis Matsoukas. Analytical approach for solving population balances: a homotopy perturbation method. *Journal of Physics A: Mathematical and Theoretical*, 52 (38):385201, 2019.

[67] A Hasseine, Z Barhoum, M Attarakih, and H-J Bart. Analytical solutions of the

particle breakage equation by the adomian decomposition and the variational iteration methods. *Advanced Powder Technology*, 26(1):105–112, 2015.

[68] Abdelmalek Hasseine, Menwer Attarakih, Rafik Belarbi, and Hans Jörg Bart. On the semi-analytical solution of integro-partial differential equations. *Energy Procedia*, 139:358–366, 2017.

[69] Gourav Arora, Saddam Hussain, and Rajesh Kumar. Comparison of variational iteration and adomian decomposition methods to solve growth, aggregation and aggregation-breakage equations. *Journal of Computational Science*, 67:101973, 2023.

[70] Gurmeet Kaur, Randhir Singh, and Heiko Briesen. Approximate solutions of aggregation and breakage population balance equations. *Journal of Mathematical Analysis and Applications*, 512(2):126166, 2022.

[71] Randhir Singh, Jitraj Saha, and Jitendra Kumar. Adomian decomposition method for solving fragmentation and aggregation population balance equations. *Journal of Applied Mathematics and Computing*, 48:265–292, 2015.

[72] Sonali Kaushik and Rajesh Kumar. A novel optimized decomposition method for smoluchowski's aggregation equation. *Journal of Computational and Applied Mathematics*, 419:114710, 2023.

[73] IL EL-Kalla. An accelerated homotopy perturbation method for solving nonlinear equation. *J Fract Calc Appl*, 3:1–6, 2012.

[74] Z Cheng and S Redner. Kinetics of fragmentation. *Journal of Physics A: Mathematical and General*, 23(7):1233, 1990.

[75] PL Krapivsky and Eli Ben-Naim. Shattering transitions in collision-induced fragmentation. *Physical Review E*, 68(2):021102, 2003.

[76] Margaritis Kostoglou and AJ Karabelas. A study of the nonlinear breakage equation: analytical and asymptotic solutions. *Journal of Physics A: Mathematical and General*, 33(6):1221, 2000.

[77] Jayanta Paul and Jitendra Kumar. An existence-uniqueness result for the pure binary collisional breakage equation. *Mathematical Methods in the Applied Sciences*, 41(7):2715–2732, 2018.

[78] Prasanta Kumar Barik and Ankik Kumar Giri. Global classical solutions to the continuous coagulation equation with collisional breakage. *Zeitschrift für Angewandte Mathematik und Physik*, 71:1–23, 2020.

[79] Ankik Kumar Giri and Philippe Laurençot. Existence and nonexistence for the collision-induced breakage equation. *SIAM Journal on Mathematical Analysis*, 53 (4):4605–4636, 2021.

[80] Ankik Kumar Giri and Philippe Laurençot. Weak solutions to the collision-induced breakage equation with dominating coagulation. *Journal of Differential Equations*, 280:690–729, 2021.

[81] Ashok Das, Jitendra Kumar, Maksym Dosta, and Stefan Heinrich. On the approximate solution and modeling of the kernel of nonlinear breakage population balance equation. *SIAM Journal on Scientific Computing*, 42(6):B1570–B1598, 2020.

[82] Jayanta Paul, Ashok Das, and Jitendra Kumar. Moments preserving finite volume approximations for the non-linear collisional fragmentation model. *Applied Mathematics and Computation*, 436:127494, 2023.

[83] Prakrati Kushwah, Arijit Das, Jitraj Saha, and Andreas Bück. Population balance equation for collisional breakage: A new numerical solution scheme and its convergence. *Communications in Nonlinear Science and Numerical Simulation*, 121: 107244, 2023.

[84] Maxime Lombart, Mark Hutchison, and Yueh-Ning Lee. Fragmentation with discontinuous galerkin schemes: non-linear fragmentation. *Monthly Notices of the Royal Astronomical Society*, 517(2):2012–2027, 2022.

[85] Sanjiv Kumar Bariwal and Rajesh Kumar. Convergence and error estimation of weighted finite volume scheme for coagulation-fragmentation equation. *Numerical Methods for Partial Differential Equations*, 39(3):2561–2583, 2023.

[86] JF Steffensen. On a generalization of certain inequalities by tchebychef and jensen. *Scandinavian Actuarial Journal*, 1925(3-4):137–147, 1925.

[87] Walter Rudin. *Principles of mathematical analysis*. 1953.

[88] Haim Brezis and Haim Brézis. *Functional analysis, Sobolev spaces and partial differential equations*, volume 2. Springer, 2011.

[89] Bernard Beauzamy. *Introduction to Banach spaces and their geometry*. Elsevier, 2011.

[90] Philippe Laurençot. Weak compactness techniques and coagulation equations. In *Evolutionary Equations with Applications in Natural Sciences*, pages 199–253. Springer, 2014.

[91] Ch De La Vallée Poussin. Sur l'intégrale de lebesgue. *Transactions of the American Mathematical Society*, 16(4):435–501, 1915.

[92] Philippe Laurençot and Stéphane Mischler. The continuous coagulation-fragmentationśequations with diffusion. *Archive for Rational Mechanics and Analysis*, 162:45–99, 2002.

[93] Yuming Qin et al. *Analytic inequalities and their applications in PDEs*, volume 241. Springer, 2017.

[94] Thomas W Peterson. Similarity solutions for the population balance equation describing particle fragmentation. *Aerosol Science and Technology*, 5(1):93–101, 1986.

[95] Zaid Odibat. An optimized decomposition method for nonlinear ordinary and partial differential equations. *Physica A: Statistical Mechanics and its Applications*, 541:123323, 2020.

[96] Zaid M Odibat. A study on the convergence of variational iteration method. *Mathematical and Computer Modelling*, 51(9-10):1181–1192, 2010.

[97] Shijun Liao. On the homotopy analysis method for nonlinear problems. *Applied Mathematics and Computation*, 147(2):499–513, 2004.

[98] Shijun Liao. *Beyond perturbation: introduction to the homotopy analysis method*. CRC press, 2003.

[99] Ji-Huan He. Homotopy perturbation method: a new nonlinear analytical technique. *Applied Mathematics and Computation*, 135(1):73–79, 2003.

[100] George Adomian. *Solving frontier problems of physics: the decomposition method*, volume 60. Springer Science & Business Media, 2013.

[101] Ibrahim L El-Kalla. Error analysis of adomian series solution to a class of nonlinear differential equations. *Applied Mathematics E-Notes*, 7:214–221, 2007.

[102] Farel William Viret Kharchandy, Arijit Das, Vamsinadh Thota, Jitraj Saha, and Mehakpreet Singh. A note on the volume conserving solution to simultaneous aggregation and collisional breakage equation. *Axioms*, 12(2):181, 2023.

[103] Randolph C Rach. A new definition of the adomian polynomials. *Kybernetes*, 37 (7):910–955, 2008.

List of Publications, Conferences and Workshops

Journal Publications

1. **Sanjiv Kr. Bariwal**, Rajesh Kumar: "Convergence and error estimation of Weighted Finite Volume Scheme for Solving Coagulation-Fragmentation Equation,"**Numerical Methods for Partial Differential Equations (2022), no.39, 2561-2583**.

2. **Sanjiv Kr. Bariwal**, Prasanta Kr. Barik, Ankik Kr. Giri, Rajesh Kumar: "Finite volume scheme for coagulation-fragmentation equation with singular rates, "**Journal of Hyperbolic Differential Equations (2024), no. 20, 793-823**.

3. Saddam Hussain, **Sanjiv Kr. Bariwal**, Rajesh Kumar: "Collisional Breakage Population Balance Equation: An Analytical Approach," (Under minor revision).

4. **Sanjiv Kr. Bariwal**, Rajesh Kumar: "Convergence and error analysis for non-linear collisional-induced breakage equation," (Under review).

5. **Sanjiv Kr. Bariwal**, Rajesh Kumar: "Analytic approximate solution and error estimates for non-linear collision-induced breakage equation," (Under review).

6. **Sanjiv Kr. Bariwal**, Saddam Hussain, Rajesh Kumar: "A note on finite volume and semi-analytical methods for non-linear collision-induced breakage equation," (Under review).

7. **Sanjiv Kr. Bariwal**, Rajesh Kumar, "Semi-analytical solution of non-linear collision-induced breakage equation via Temimi and Ansari method," (Under review).

8. **Sanjiv Kr. Bariwal**, Rajesh Kumar,"Weak convergence analysis for non-linear collisional induced breakage equation with singular kernel," (Manuscript prepared)

Conference Publications

1. **Sanjiv Kr. Bariwal**, Gourav Arora, Rajesh Kumar: "Semi-analytical solutions for breakage and aggregation-breakage equations via Daftardar-Jafari method," **(Accepted in Springer Proceedings in Physics)**.

Conferences and Workshops

1. Attended the workshop on " **Asian and European Schools in Mathematics (AESIM-2023) School on Mathematics for Health Sciences**", organised by BITS Pilani, Pilani Campus, INDIA.

2. Presented a paper titled "**Semi-analytical solution of non-linear collision-induced breakage equation via Temimi and Ansari method**", International Conference on Differential Equations and Control Problems (ICDECP23), IIT Mandi, INDIA.

3. Presented a paper titled "**Semi-analytical solutions for breakage and aggregation-breakage equations via Daftardar-Jafari method**", International Conference on Dynamical Systems, Control and their Applications (ICDSCA-2022), IIT Rookee, INDIA.

4. Presented a paper with title "**Finite volume convergence analysis for coagulation-fragmentation equations with singular rates**", Advances in Mechanics, Modelling, Computing, and Statistics (ICAMMCS-2022)", BITS PILANI, Pilani campus.

5. An Workshop on "**Artificial Intelligence Application for Electro Optical Sensors (WAIAEOS-2022)**", BITS PILANI, Pilani campus, INDIA.

6. Presented a paper with title "**Convergence and error estimation of finite volume scheme for coagulation-fragmentation equations with unbounded rate**", in the 4th International Conference on Frontiers in Industrial and Applied Mathematics (FIAM 2021), SLIET, INDIA.

7. Attended the workshop on "**The International Workshop On Applied Modelling And Simulation (WAMS 2019)**", organised by IIT Roorkee, INDIA.

8. Attended "**International Conference and 22nd Annual Convention of Vij$\tilde{n}\bar{a}$na Parishad of India on Advances in Operations Research Statistics and Mathematics (AOSM 2019)**", organised by BITS PILANI, Pilani Campus.

9. Attended an International Webinar on "**Applications of Mathematics**", organised by Department of Mathematics, BITS Pilani, Pilani Campus, INDIA.

Biography of the Candidate

Sanjiv Kumar Bariwal did schooling in Alwar, Rajasthan, with outstanding scores in 10th and 12th. After that, he got an inspired scholarship for five years duration. Then, he completed B.Sc. (PCM) from Maharaja College, University of Rajasthan, in 2015 and M.Sc. (applied mathematics) from South Asian University, New Delhi in 2018. He cracked the CSIR, Net-JRF (Mathematics) examination with AIR 98 to pursue higher study. He got admitted in Ph.D in the Department of Mathematics, BITS PILANI, Pilani Campus, Rajasthan, under the supervision of Prof. Rajesh Kumar. His research interests include population balance equations, finite volume method, and semi-analytical methods. He has served as a teaching assistant for courses like calculus, complex analysis, and linear algebra. In his research journey, he has published two articles in peer-reviewed journals and presented his work at four national and international conferences. Moreover, he has attended three workshops.

Biography of the Supervisor

Rajesh Kumar is an accomplished Associate Professor in the Department of Mathematics at Birla Institute of Technology and Science Pilani, Pilani Campus, India. His academic journey includes a Bachelor's degree in Mathematics from Delhi University, an M.Sc. in Applied Mathematics from IIT Roorkee, and an Erasmus Mundus Fellowship, leading to a dual-degree M.Sc. in Industrial Maths and Scientific Computing from universities in Germany and Austria. He earned his Ph.D. from Otto-von-Guericke University Magdeburg, Germany. Throughout his career, he has held various academic and research positions, including a Postdoctoral Fellow at MOX, Politecnico di Milano, Italy; a scientific collaborator at EPFL, Switzerland and a research scientist at RICAM, Austria. His research contributions span differential equations, nonlinear analysis, population dynamics, numerical linear algebra, and more. Prof. Kumar has supervised numerous students, published research papers extensively in reputable journals, and actively participated in academic and research committees at BITS Pilani. He has organized several international workshops including GIAN, IFCAM workshop and CIMPA School. His expertise and interests encompass various mathematical topics, including partial-integro differential equations and hyperbolic conservation laws.